

Synthesis and Properties of Lyotropic Poly(amide-*block*-aramid) Copolymers

Synthesis and Properties of Lyotropic Poly(amide-*block*-aramid) Copolymers

Proefschrift

ter verkrijging van de graad van doctor
aan de Technische Universiteit Delft,
op gezag van Rector Magnificus Prof. Dr. Ir. J.T. Fokkema
voorzitter van het College van Promoties
in het openbaar te verdedigen op woensdag 13 september 2006 om 10:00 uur
door

Christiaan de Ruijter

Ingenieur in de Scheikundige Technologie
geboren te Vlaardingen

Dit proefschrift is goedgekeurd door de promotor:

Prof. Dr. S.J. Picken Technische Universiteit Delft

Samenstelling promotiecommissie:

Prof. Dr. S.J. Picken	Technische Universiteit Delft, promotor
Prof. Dr. D.J. Broer	Phillips Research Laboratories en Technische Universiteit Eindhoven
Prof. Dr. E.J.R. Südhofter	Universiteit Wageningen
Prof. Dr. Ir. R. Marissen	DSM-Dyneema en Technische Universiteit Delft
Dr. W.F. Jager	Technische Universiteit Delft
Dr. Ir. H. Boerstoel	Teijin Twaron
Prof. Dr. Ir. W.H. de Jeu	Fom Instituut voor Atoom- en Molecuulfysica (AMOLF) en Technische Universiteit Eindhoven

Reservelid:

Prof. Dr. L.D.A. Siebbeles Technische Universteit Delft

The research described in this thesis forms part of the research program of the FOM (Fundamentals of Advanced Materials), Project number 01EMM14

ISBN: 90-9020985-9

Copyright © 2006 by Christiaan de Ruijter

Contents

Chapter 1	Introduction	1
1.1	Liquid Crystalline Systems	2
1.2	Liquid Crystalline Polymers	7
1.3	Block Copolymers	11
1.4	Rod-Coil Block Copolymers	14
1.5	Scope of this Thesis	20
1.5.1	Incentive for this Work	20
1.5.2	Preview of the Following Chapters	22
1.6	References	23
Chapter 2	Synthesis and Characterization of PPTA-<i>block</i>-PA 6,6 Multiblock Copolymers	25
2.1	Introduction	26
2.2	Experimental	28
2.2.1	Materials	28
2.2.2	Measurements	29
2.2.3	General Procedure for the One-Pot Block Copolymer Polycondensation Reaction	29
2.3	Results and Discussion	31
2.3.1	Polymer Synthesis	31
2.3.2	Extraction and ¹ H-NMR Analyses of PPTA- <i>b</i> -PA 6,6 Block Copolymers	32
2.3.3	Molecular Mass Determination	35
2.3.4	TGA	40
2.4	Conclusions	41
2.5	References	43
Chapter 3	Phase Behaviour in Sulfuric Acid	45
3.1	Introduction	46
3.2	Experimental	47
3.2.1	Materials	47

3.2.2 Measurements	48
3.3 Results and Discussion	48
3.3.1 Phase Behaviour in Sulfuric Acid	48
3.3.2 Comparison of the Phase Behaviour with an Extended Maier-Saupe (EMS) Theory	51
3.4 Conclusions	54
3.5 References	56
Chapter 4 Structural Study in the Solid State	57
4.1 Introduction	58
4.2 Experimental	58
4.2.1 Materials	58
4.2.2 Measurements	59
4.3 Results and Discussion	59
4.3.1 Effect of Copolymer Composition on Thermal Behaviour using DSC	59
4.3.2 Microstructure of PPTA- <i>b</i> -PA 6,6 Copolymers using SAXS	61
4.4 Conclusions	65
4.5 References	67
Chapter 5 Orientational Order and Mechanical Properties PPTA-<i>b</i>-PA 6,6 Block Copolymer Films	69
5.1 Introduction	70
5.2 Experimental	71
5.2.1 Materials	71
5.2.2 Film Preparation	71
5.2.3 Measurements	72
5.3 Results and Discussion	73
5.3.1 WAXS Measurements	73
5.3.2 Mechanical Properties	79
5.4 Conclusion	84
5.5 References	86

Chapter 6	Orientational Order and Mechanical Properties of PPTA-<i>b</i>-PA 6,6 Block Copolymer Fibers	87
6.1	Introduction	88
6.2	Experimental	88
6.2.1	Materials	88
6.2.2	Fiber Spinning	88
6.2.3	Measurements	89
6.3	Results and Discussion	90
6.3.1	WAXS Measurements	90
6.3.2	Mechanical Properties	93
6.4	Conclusions	97
6.5	References	98
Chapter 7	Conclusions and Scientific Outlook	99
7.1	Conclusions	99
7.2	Scientific outlook	100
7.3	References	101
Summary		103
Samenvatting		105
Curriculum Vitae		107
Dankwoord		109

Chapter 1

Introduction

Self-organisation is an intriguing phenomenon which has been receiving an increasing amount of attention in (polymer) science. Self-organisation is a process where molecules or particles spontaneously form organised structures. Two important classes of materials that can readily undergo self-organisation are liquid crystals and block copolymers.

A liquid crystal is a material that combines characteristic properties of both crystalline solids and liquids. As in crystalline solids, liquid crystals display orientational ordering. The ordering phenomenon in liquid crystals is a result of the highly anisotropic shape of its components. Because in a liquid crystal the components display only partial positional ordering, liquid crystals have the ability to flow like liquids. The orientational order in a liquid crystal state is characterized by the tendency of the molecules to align along a common director, giving rise to highly anisotropic properties. Based on this principle liquid crystalline polymers (LCP's) have been synthesized that are very suitable for preparing fibers with impressive mechanical properties along the fiber axis. In this type of polymers the rigid (LC) moieties are incorporated in the polymer backbone and are generally called main-chain liquid crystalline polymers (MC-LCP's). However, LC moieties can also be attached onto the polymer backbone and as a result a side-chain liquid crystalline polymer (SC-LCP) is formed.

A block copolymer consists of at least two dissimilar polymers chains (blocks) that are connected by means of covalent bonds. Because these different blocks are usually highly incompatible a block copolymer often forms phase-separated structures. The covalent bonds between the blocks prevent the system to phase separate on a macroscopic scale. As a consequence organisation of the blocks occurs in nanometer size domains. The length scale can be controlled by the degree of polymerisation of the blocks and the morphology can be influenced by the volume ratio between the blocks.

Liquid crystalline (LC) block copolymers form a relatively new field of research combining the characteristics of both concepts, i.e. orientational order of liquid crystals and microphase separation of block copolymers. As a result morphologies

arise that are distinctly different than obtained for traditional block copolymers comprised of flexible coil components.

The objective in this thesis is to investigate LC block copolymers comprised of alternating flexible and rigid rod blocks for the purpose of preparing self-reinforcing materials. The incentive for this work was the expectation that the rigid segments would phase separate and form nematic domains causing an enhanced orientation of the flexible segments (coil stretching). Because of the induced orientation of the flexible coils, the mechanical properties of these flexible blocks are expected to be better than for the corresponding pure (i.e. non-stretched) flexible polymer.

Therefore the main focus of this introduction will be on the self-assembly of liquid crystal block copolymers with rod-like moieties incorporated in the main-chain. In order to better understand the phase behaviour of LC block copolymers first a general introduction will be given on liquid crystals, LCP's, and block copolymers, where the self-organisation concept is emphasized in order to subsequently highlight the phase behaviour of rod-coil LC block copolymers.

1.1 Liquid Crystalline Systems

In general materials can be classified into 3 states of matter, the solid state, which is often crystalline, the liquid state and the gaseous state. The main difference between the phases is the degree of order that is present. In crystalline solids the molecules possess orientational and 3-dimensional positional order. On the other hand in liquids and gasses the molecules are highly disordered. Upon increasing the temperature the interactions between the molecules will decrease and a material in general will show a phase transition from the solid to the liquid state and next from the liquid to the gaseous state. In the late 19th century Reinitzer¹ and Lehmann² discovered a state of matter in between the crystalline solid and the liquid state and called this the liquid crystal state³. Later for this state also the term mesogenic (= in between) phase was proposed. Characteristic for LC phases is that they combine aspects of solids and liquids, i.e. orientational order, reduced positional order and the ability to flow; liquid crystals can therefore also be seen as ordered liquids. A requirement for a material to display LC behaviour is a highly anisotropic (molecular) shape. This can be accomplished by the shape of the molecules themselves or by molecules that are able to organize into an anisotropic structure (e.g. worm-like micelles or dimers). Two of the most common anisotropic shapes are the rod- and the disc-shape and the

corresponding mesophases are called calamitic and discotic. In Figure 1.1 the chemical structures of a well known rod-shaped and disc-shaped liquid crystal, respectively 4-n-pentyl-4'-cyanobiphenyl (5CB) and hexa-alkoxy triphenylene (HAT6), are shown. More recently other shapes, like bent shaped⁴ and board shaped^{5,6} mesogens have been discovered, that give rise to respectively bananic and sanidic liquid crystal phases.

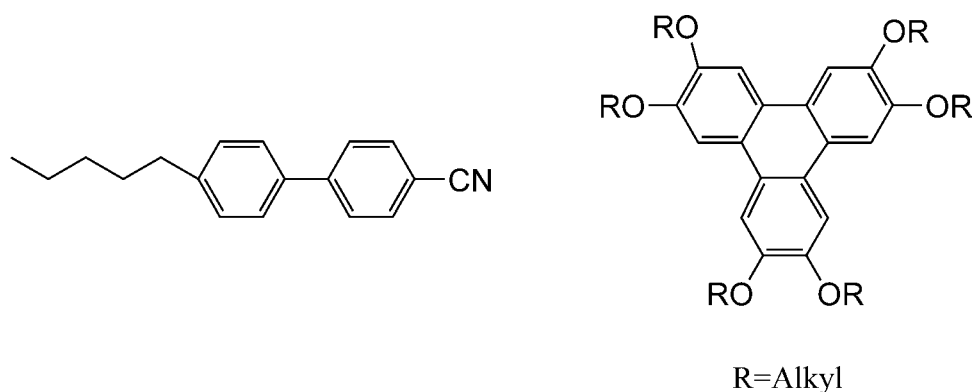


Figure 1.1: Examples of well-known LC mesogens: rod-shaped 5CB (left) and disc-shaped hexa-alkoxy triphenylene (right)

Materials may show LC behaviour upon heating, in a certain temperature regime. When the phase behaviour is governed by temperature only it is called thermotropic behaviour. Liquid crystallinity can also occur in solution as a function of concentration. This is called lyotropic behaviour. However it is often seen that LC behaviour in solution depends on both concentration and temperature.

Because liquid crystals combine order and mobility on a molecular level they form interesting materials with a wide variety of applications. Important applications of thermotropic liquid crystals are for example in electro-optical displays and in pressure and temperature sensors. DNA and cellulose are examples of lyotropic liquid crystals. Lyotropic liquid crystals have important applications in biomembranes, the cosmetics and soap industry, and in fiber spinning.

Liquid Crystal Phases

As mentioned above one of the characteristics of the LC state is the presence of orientational order. This order is expressed by the tendency of the molecules to align along a common axis called the director (\vec{n}). The axial symmetry implies that molecules have an equal chance to point “up” or “down” with an average alignment of the molecular axis along the director. Besides orientational order liquid crystals may

also display positional order. The mesophase where the molecules only show orientational order and no long-range positional order is called the nematic (N) phase. The nematic phase can be observed for both rod- and disc-like liquid crystals. The most important phases for rod-like mesogens that show both positional and orientational order are smectic (Sm) phases. The positional order of these phases is expressed by packing of the molecules in a layer like fashion. If the director is perpendicular to the layers the smectic A (SmA) phase is formed. Other smectic phases have been discovered which differ in the organisation within the layers. Besides rod-like molecules also disc-shaped molecules can give rise to liquid crystal phases. The simplest LC phase where the discs only show orientational order is called the nematic discotic (N_D) phase. The discs also may arrange themselves into stacks and the phases are called columnar phases. The columnar phases can be classified into the degree of order present between the discs within a column (ordered and disordered) and the order between the columns. The columns usually organize into 2D hexagonal (Col_h) or rectangular (Col_r) fashion. In Figure 1.2 a schematic representation of the most-common liquid crystal phases are shown.

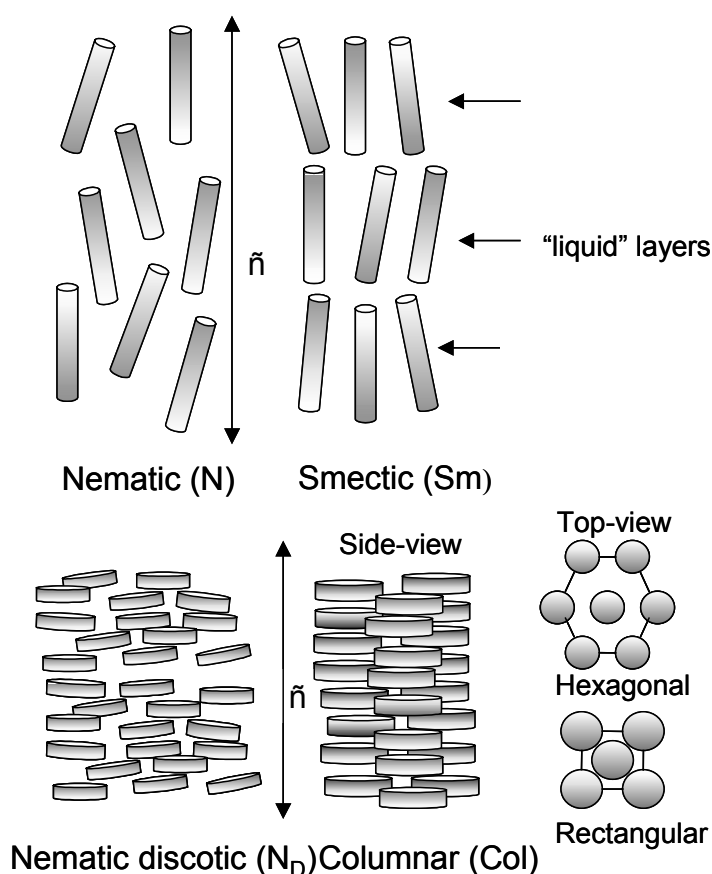


Figure 1.2: Schematic representation of nematic (N), smectic (SmA), nematic discotic (N_D) and a columnar (Col) phase

Orientalional Order

For molecules constituting a nematic domain the degree of orientation with respect to the director can be expressed by an orientational distribution function $f(\varphi)$. This function describes the chance to find a molecule at an angle φ with respect to the director and can be defined as:

$$N(\varphi)d\varphi = f(\varphi)\sin\varphi d\varphi \quad [1.1]$$

where $N(\varphi)d\varphi$ is the fraction of molecules at an angle between φ and $\varphi+d\varphi$. In Figure 1.3 the disorientation angle φ with respect to the director and the shape of the distribution function $f(\varphi)$ is shown.

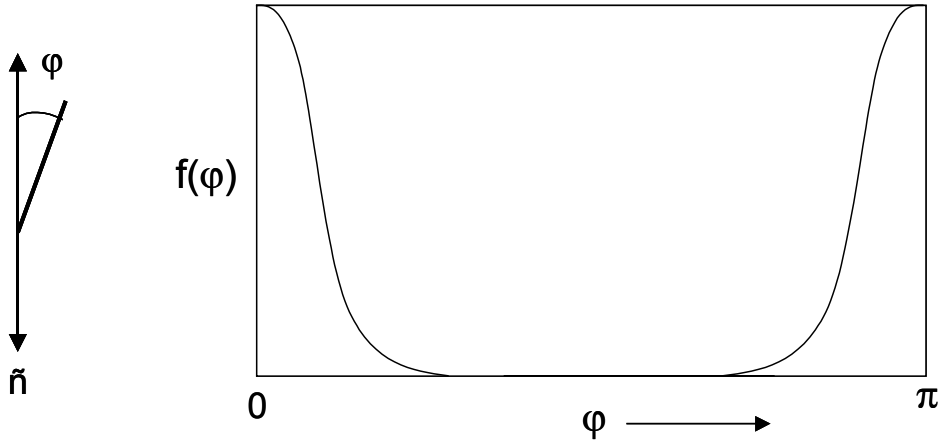


Figure 1.3: Representation of the disorientation angle φ with respect to the director (\hat{n}) (left) and the profile of the orientational distribution function (right)

The local order parameter $\langle P_2 \rangle$ can be defined as the average value, weighed by the orientational distribution function, of the second order Legendre polynomial P_2 of $\cos\varphi$ and is given by:

$$\langle P_2 \rangle = \int_{-1}^1 f(\varphi) P_2(\cos\varphi) d\cos\varphi \quad [1.2]$$

where the second order Legendre polynomial P_2 of $\cos(\varphi)$ is given by:

$$P_2(\cos\varphi) = \frac{1}{2}(3\cos^2\varphi - 1) \quad [1.3]$$

The $\langle P_2 \rangle$ order parameter describes the degree of anisotropy in a material. For an isotropic material the $\langle P_2 \rangle = 0$ whereas for a perfectly aligned sample the order parameter $\langle P_2 \rangle = 1$. The $\langle P_2 \rangle$ order parameter in a liquid crystal is usually between 0.3 and 0.9. Note that due to the axial symmetry the odd order parameters like $\langle P_1 \rangle = \langle \cos \varphi \rangle$ are zero.

To quantify the overall orientational order in a material the $\overline{\langle P_2 \rangle}$ order parameter is defined which is the product of the local molecular order $\langle P_2 \rangle$ and the macroscopic director order $\overline{P_2}$:

$$\overline{\langle P_2 \rangle} = \langle P_2 \rangle \overline{P_2} \quad [1.4]$$

As an illustration, Figure 1.4 shows a texture of a macroscopic director field (left). On the right hand side local ordering of rod-like molecules around a director \tilde{n} is shown.

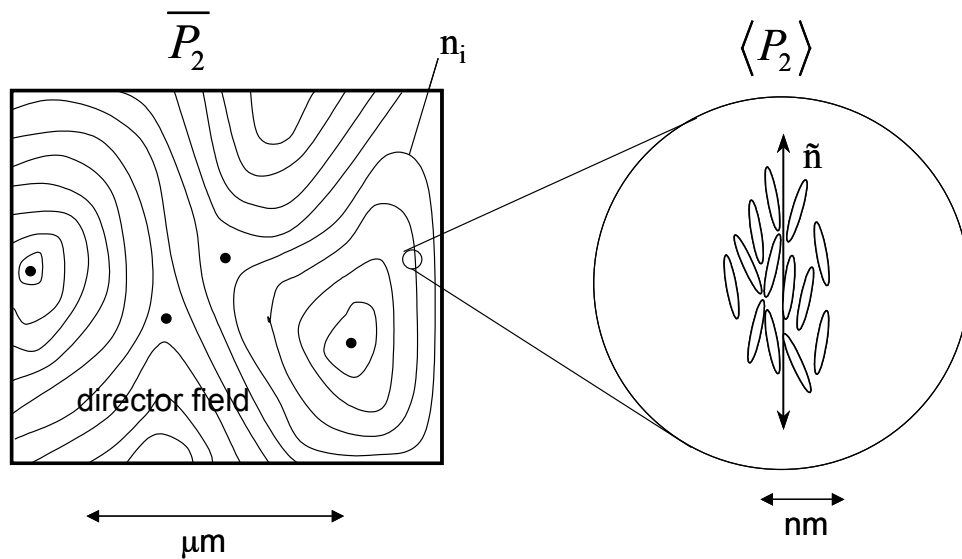


Figure 1.4: Texture of a liquid crystalline specimen (left), which indicates the orientation field of the director n_i and (right) the local molecular order along the director \tilde{n}

So for a material to display a high overall orientation, both the local molecular order and the director orientation must be high. This means that the directors of the different nematic regions in a material should be aligned, which can be accomplished by the use of external fields, such as electric, magnetic or flow-fields.

Molecular Models to Describe Liquid Crystalline Ordering

Many models have been proposed in order to describe liquid crystalline ordering of anisotropically shaped molecules. Although it is beyond the scope of this introduction to go into the details of these models there are two general approaches to describe the ordering of liquid crystal systems, which will be outlined next.

The first group of molecular theories considers the volume excluded from the center-of-mass of rigid cylindrical rods of length L with diameter D . This theory predicts the existence of a lyotropic liquid crystal phase based on steric reasons only. Upon increasing the concentration of rod shaped molecules in solution a phase transition occurs which can be explained because the decrease in orientational entropy due to parallel arrangements of the rods is compensated by an increase in positional entropy. This theory was originally described by Onsager⁷ and the phase transition from the isotropic to the nematic LC phase is described as function of the concentration and the aspect ratio (L/D) of the rods. A similar theory has been developed by Flory⁸ who used a lattice approach to predict lyotropic phase transitions. By extending the original Onsager^{9,10} and the Flory¹¹ theories also phase transition in solutions of semi-flexible polymer chains have been predicted.

The other group of molecular theories describing the occurrence of the nematic phase based on an orientation energy term. The occurrence of the nematic phase is described by an anisotropic potential between the rod-shaped molecules that stabilize parallel alignment. This theory was originally postulated by Maier and Saupe^{12,13} and has been successfully applied to describe thermotropic phase transitions in low MW liquid crystals. The Maier-Saupe model has been extended^{14,15} with the Kratky-Porod or worm-like chain model¹⁶ to take the flexibility of polymers into account. The Kratky-Porod model¹⁶ will be outlined into more detail in the next section. To describe the nematic ordering of polymers, as a function of both concentration and temperature, combinations the Maier-Saupe theory with the Onsager theory¹⁷ have been used.

1.2 Liquid Crystalline Polymers

In order for a polymer to display LC behaviour a sufficient number of mesogens should be incorporated in the polymer. In principle this can be done in two ways. Main chain liquid crystal polymers (MC-LCP's) are formed when the mesogens are incorporated in the polymer chain and side chain polymer liquid crystal polymers

(SC-LCP's) are formed when the mesogens are connected to the polymer backbone. Also combined polymers (MC/SC-LCP's) are possible. Another classification that was made for low MW liquid crystals can also be made for LCP's and that is whether LC behaviour is observed in the melt as a function of temperature (thermotropic LCP's) or in solution (lyotropic LCP's) as a function of concentration (and possibly temperature).

SC-LCP's are generally constructed from three structural components: the backbone, the mesogen and the spacer. The backbone is usually a flexible polymer with a low glass transition temperature such as polysiloxane, polyester, polyether or polyacrylates. The mesogens can in principle be both disc-like and rod-like and a spacer is used in order to decouple the polymer backbone from the mesogen. An example of a SC-LCP with a rod-like mesogen is shown in Figure 1.5. SC-LCP's are usually thermotropic. Possible applications of SC-LCP's are in the field of data storage, optical films in display technology and in optically non-linear devices.

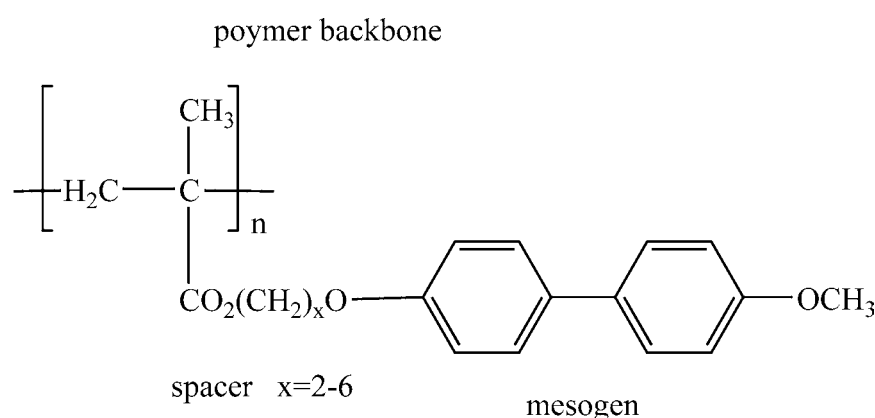


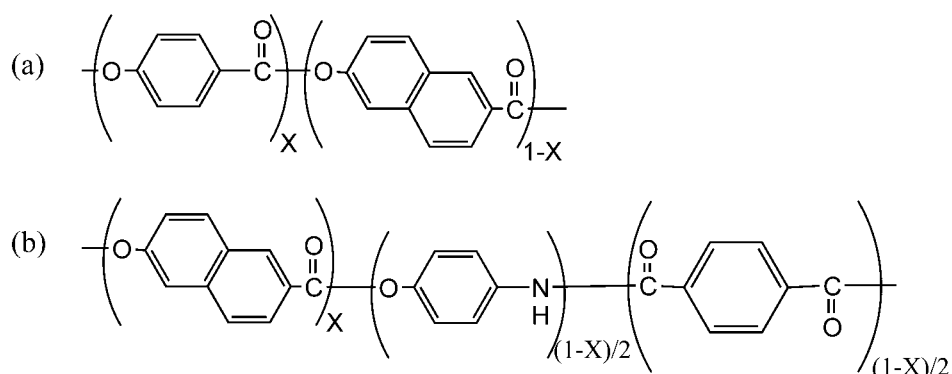
Figure 1.5: An example of a SC-LCP¹⁸

Worm-like Polymers

MC-LCP's are formed when sufficient rigid moieties are incorporated in the polymer backbone. These rigid mesogens may be separated by a short flexible spacer. Polyesters and polyamides comprising of alternating aromatic and aliphatic groups fall into this category. Usually these polymers are thermotropic. Another group of MC-LCP's is comprised of rigid moieties only and these polymers are known as worm-like polymers. An example of a polymer that falls into this category is Vectra[®] which is a thermotropic copolyester of 4-hydroxybenzoic acid (HBA) and 2-hydroxy-6-naphthoic

acid (HNA). Some well-known examples of lyotropic worm-like polymers are the fully aromatic aramids like eg. poly(*p*-phenylene terephthalamide) (PPTA) or polybenzamide (PBA), and aromatic heterocyclic polymers like eg. poly(*p*-phenylene-2,6-benzobisoxazole) (PBO) and poly(*p*-phenylene-2,6-benzimidazole) (PBI) and poly{2,6-diimidazo[4,5-*b*:4',5'-*e*]pyridinylene-1,4(2,5-dihydroxy)phenylene} (PIPD) commercially known as M5[®]. The polymers mentioned above are not thermotropic because they degrade before the melting point is reached. Therefore only processing from a solution is possible. In Figure 1.6 the chemical structures of some important worm-like polymers are shown.

Thermotropic wormlike polymers



Lyotropic wormlike polymers

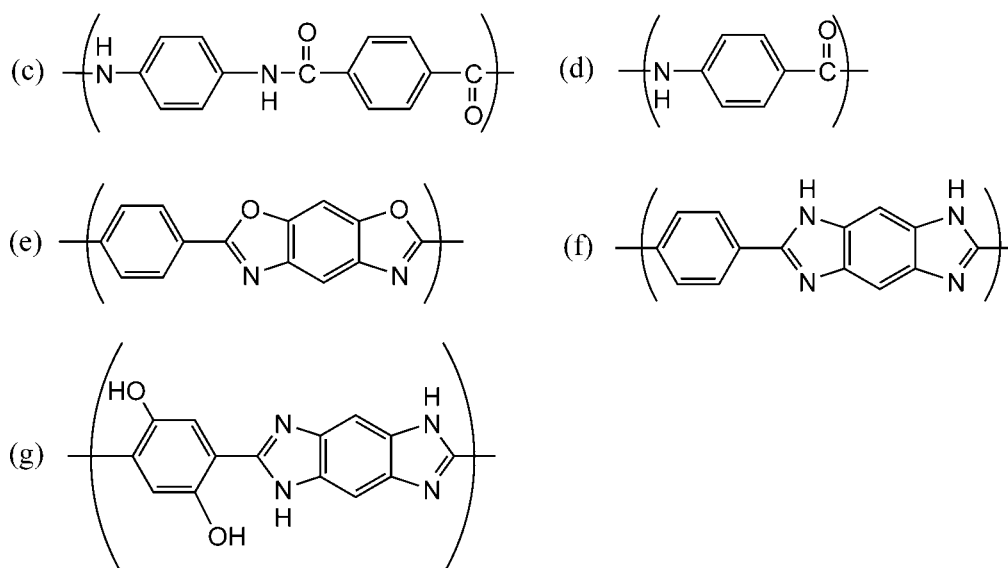


Figure 1.6 Examples of worm-like polymers: (a) thermotropic copolyester of HBA (hydroxybenzoic acid) and HNA (hydroxynaphthoic acid), (b) thermotropic polyester amide of HNA, APh (amino phenol) and TA (terephthalic acid), (c) PPTA, (d) PBA, (e) *cis*-PBO and (f) *cis*-PBI and (g) PIPD (M5[®])

The term worm-like polymer is used because the LCP's are not perfectly rigid; as a consequence the shape of these polymers is more worm-like than rod-like. The Karatky-Porod¹⁶ worm-like chain model is generally used to describe the conformational characteristics of such semi-flexible chains. Figure 1.7 shows a worm-like chain, which can be seen as a semi-flexible string of overall contour length L_c with a continuous curvature where s is the distance measured along the contour from one of the chain ends. The correlation between the tangential vectors $\mathbf{u}(s)$ and $\mathbf{u}(s')$ of unit length of two segments at s and s' is given by:

$$\langle \mathbf{u}(s) \cdot \mathbf{u}(s') \rangle = \langle \cos \theta \rangle_{ss'} = \exp\left(-\frac{|s-s'|}{L_p}\right) \quad [1.5]$$

where L_p is called the persistence length, which is a measure of the rigidity of a worm-like polymer.

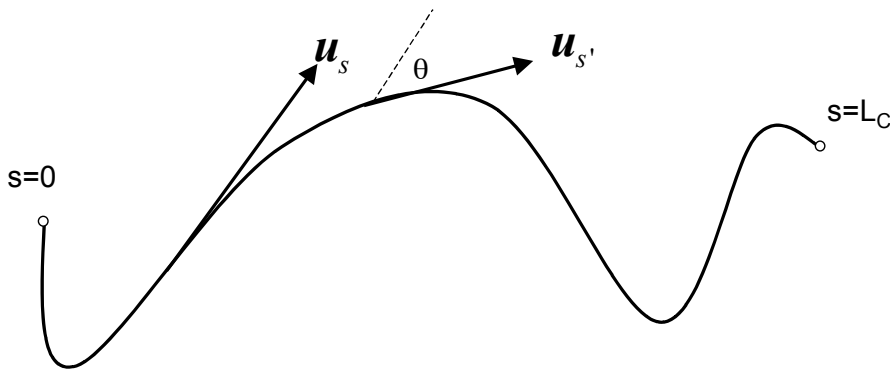


Figure 1.7: Illustration of a worm-like chain (parameters are described in the text)

The worm-like chain is described by two parameters, L_p and L_c , and the following expression can be derived for the average squared end-to-end distance of a worm-like chain:

$$\langle R^2 \rangle = 2L_c L_p + 2L_p^2 (\exp(-L_c / L_p) - 1) \quad [1.6]$$

Two interesting limiting cases are:

$$\langle R^2 \rangle = L_c^2 \quad \text{when } L_p \gg L_c \quad [1.7]$$

for low molecular weight chains, and

$$\langle R^2 \rangle = 2L_c L_p \quad \text{when } L_c \gg L_p \quad [1.8]$$

for very high molecular weight chains. Since $\langle R^2 \rangle \sim L_c$, this demonstrates that worm-like polymer chains behave as flexible coils if the molecular weight is high enough.

Because of the rigid structures and anisotropic properties in the LC state MC-LCP's have been successfully used in industry to make fibers displaying very high modulus and strength along the fiber direction.

1.3 Block Copolymers

As mentioned in the introduction a block copolymer is formed when at least two different polymer chains are linked together by means of a covalent bond. Because different polymers generally have repulsive interactions, which are expressed by a positive χ (Flory-Huggins) parameter, block copolymers in general have a strong tendency towards phase separation. The Flory-Huggins interaction parameter reflects the interaction energy between the different blocks and is inversely proportional to temperature. Due to the chemical connection between the two distinct blocks macroscopic phase separation cannot occur and phase separation is limited to the microscopic or nanometer scale. As a consequence spontaneous structural organisation of the blocks arises in domains with periodicities in the order of ~1-100 nm.

Block copolymers can be made with a wide range of architectures, which can be controlled by the procedure of synthesis. For example it is possible to prepare diblock, triblock, starblocks or multiblock copolymer. These block copolymers can show a wide range of morphologies. Parameters that allow the control of the microstructure of the block copolymer are the (volume) fraction of the blocks, the interactions between the blocks which are expressed by the χ -parameter, the overall molecular weight of the block copolymer and the block copolymer architecture (i.e. di-, tri- or multiblock). Because of the numerous possible microstructures block copolymers are widely used industrially and have a great number of applications like

for instance in surfactants, adhesives, thermoplastic elastomers, compatibilizers and in lithography.

Phase Behaviour of Flexible Coil Block Copolymers

The phase behaviour of block copolymers is governed by thermodynamics. The free energy of a block copolymer system is given by

$$F = U - TS \quad [1.9]$$

and its minimum determines the equilibrium state. The translational entropy is proportional to the number of molecules and consequently for a block copolymer irreversibly proportional to the degree of polymerisation N . The enthalpic contribution to the free energy is proportional to the interaction parameter χ , which is inversely proportional to temperature. Consequently the product χN expresses the balance between entropy and enthalpy and is the parameter that controls the phase behaviour as a function of the composition. The product χN determines the degree of microphase separation. Depending on χN three regimes can be distinguished¹⁹:

1. the weak-segregation limit (WSL) for $\chi N < 10$
2. the intermediate-segregation region (ISR) for $10 < \chi N < 100$
3. the strong-segregation limit (SSL) for $\chi N > 100$

At high temperatures the entropy dominates the free energy and the copolymer will be in the disordered state. On reducing the temperature the enthalpic interactions start to dominate and as a result χN increases. At a critical temperature called the ODT-temperature (order-disorder transition), phase separation occurs and an ordered microstructure is formed. Which structure is formed depends on the composition of the blocks and is a consequence of two opposing effects that compete during the minimization of the free energy, i.e. minimization of the interfacial area between the blocks and minimization of the stretching of the coils. In terms of free energy this is given by:

$$F = F_{\text{int}} + F_{\text{str}} \quad [1.10]$$

where F_{int} is the interfacial and F_{str} is the stretching contribution to the free energy. When minimizing the free energy, decreasing the interfacial free energy leads to a higher coil stretching while decreasing the stretching free energy leads to a larger

interfacial area. So as a function of the composition f , a structure will form which is a balance between these two opposing effects. For the simplest case a conformationally symmetric coil-coil diblock copolymer in the melt, the phase diagram as calculated using a self-consistent mean-field by Matsen and Schick^{20, 21} is shown in Figure 1.8. An illustration of the equilibrium morphologies is also shown in this figure. For symmetric ($f=0.5$) block copolymers, the stretching free energy of both blocks is equal. As a result the copolymers order into a morphology with a flat surface, i.e. the melt is ordered in a lamellar structure. If one block is made longer at the expense of the other it becomes energetically more favourable to form phases with curved interfaces and the morphology changes to hexagonal cylinders (for f about 0.3-0.4 and for $f=0.6-0.7$) and then to spheres (for $f<0.3$ and $f>0.7$). These morphologies represent equilibrium states with the lowest free energy. In the weak segregation region, additional complex morphologies such as the gyroid morphology and hexagonally perforated layers (HPL) have been found in a narrow range of χN and f (between the lamellar and columnar morphology).

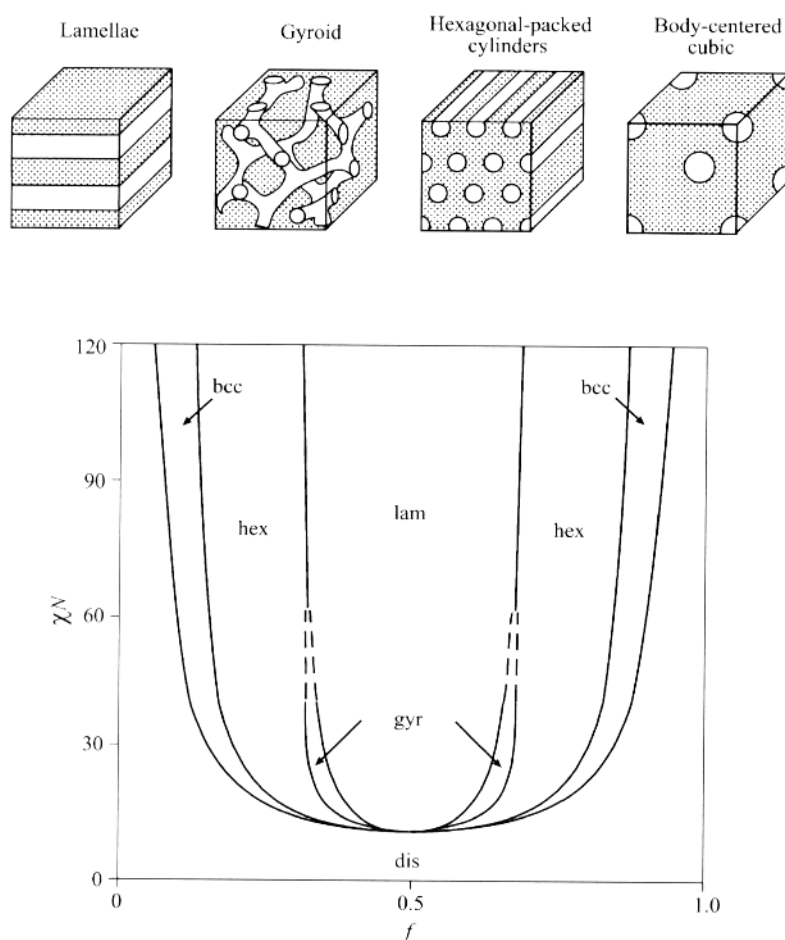


Figure 1.8: Phase diagram and illustration of equilibrium morphologies of a conformationally symmetric diblock copolymer melt, calculated by using a self-consistent mean field theory^{20, 21}

The phase diagrams for real, i.e. synthesized copolymers are usually more complex and less symmetric.

1.4 Rod-Coil Block Copolymers

As mentioned above, in case of a diblock copolymer that consists of two flexible coil blocks the incompatibility of the components results in microphase separation and possibly long-range ordering. But if one of the flexible blocks is replaced by a rigid block, the self-assembly is no longer determined by phase-separation alone. Liquid crystallinity and block copolymer microphase separation both compete during the minimization of the free energy. The result of this is that a large number of morphologies are possible which are different from the morphologies seen in coil-coil diblock copolymers. As a result, these new morphologies combine two different types of self-organisation: LC order at the molecular scale and phase separation on a nm scale. Since the early seventies the combination rigid blocks and flexible blocks received a great deal of attention of both chemists and physicists. Rod-coil diblock copolymers of small polydispersity have been synthesised via living polymerisation methods and served as model compounds in order to study the phase behaviour. The possibility to show both orientational order, and phase separation on an adjustable length scale offers numerous opportunities for designing nano-structured materials in a wide field of applications. In particular rod-coil block copolymers bearing a conjugated segment as the rod block received great interest and have been proposed for electro-optical and photonic devices.²²⁻²⁴ Recently, Lee *et al.*²⁵ have written a comprehensive review article dealing with supramolecular structures observed in rod-coil block copolymers. The main developments concerning ordering and phase behaviour for monodisperse rod-coil copolymers will be highlighted next.

Phase Behaviour of Rod-Coil Block Copolymers

Lamellar Phases

In contrast to flexible coil block copolymers, for which a theoretical description of the phase behaviour is more or less established, research on the phase behaviour of block copolymers containing rigid blocks is still in progress. However, over the last two decades a great deal of effort has been done to describe the phase behaviour of rod-coil block copolymers. Considering their relative simplicity monodisperse diblock

copolymers are most frequently studied. The diblock copolymer in these theories are represented by a rigid rod-like block of length L and diameter d ($L \gg d$), and a flexible block with N segments of length a and volume v . Theories on rod-coil multiblock copolymers or the influence of polydispersity on the phase behaviour are less well developed. Semenov and Vasilenko²⁶ were the first to study the phase behaviour of rod-coil block copolymers and predicted a homogeneous nematic and an SmA lamellar phase for a monodisperse rod-coil diblock copolymer melt. In later studies Semenov²⁷ and Halperin²⁸ included SmC phases where the rods are tilted by an angle relative to the lamellar normal. The theoretical approach of Semenov's work was based on minimization of the free energy of the diblock melt. This free energy term was constructed by four terms: ideal gas entropy of mixing, unfavourable rod-coil interactions, steric interaction among the rods and coil stretching. The steric (orientational) interactions of the rods were modelled using Flory lattice arguments⁸. The phase behaviour was described as a function of rod/coil immiscibility χN , the coil volume fraction f , and the ratio v of the characteristic coil to rod dimensions. According to this theory upon increasing incompatibility χ (decreasing temperature), an N to SmA transition occurs (if the volume fraction of rods is large enough). This smectic phase is an interdigitated lamellar phase (SmA₁). As the χ -parameter further increases a phase transition from the interdigitated smectic phase to a smectic bilayer (SmA₁ - SmA₂) occurs. In the SmA₁ phase rod-rich layers alternate with coil-rich layers; and in the SmA₂ phase rod-rich layers of twice the length, alternate with coil-rich layers, as shown in Figure 1.9. The SmA₁ phase has less coil stretching whereas the SmA₂ phase has a smaller interfacial area.

By increasing the coil fraction the theory predicts an SmA – SmC transition. In the SmC phase the tilt causes some extra interfacial area so that the degree of coil stretching is reduced. When comparing the interfacial and stretching free energy at high coil fractions the stretching penalty of the coils starts to dominate and the SmC morphology is the stable phase. In Figure 1.9 a schematic representation of the N, SmA₁, SmA₂, SmC₁, SmC₂, phases are shown.

Matsen and Barrett²⁹ have applied the self-consistent field technique to the Semenov-Vasilenko²⁶ model and constructed phase diagrams (χN vs. f) for fixed values of v . When $\chi N < 5$ the theory predicts a nematic phase in which the rods and coils are homogeneously mixed and at larger χN microphase separation occurs and a lamellar phase is formed. Because Matsen and Barrett²⁹ have performed the calculations in a 1D framework non-lamellar phases were not considered. In Figure 1.12 the 1D phase diagram is shown for $v=0.25$. Typical values for v for rod-coil

block copolymers are between $0 < \nu < 0.25$. With decreasing ν the fraction of the SmC phase in the phase diagram increases at the expense of the SmA phase. According to the 1D calculations bilayer phases were only stable at large values of χN and ν .

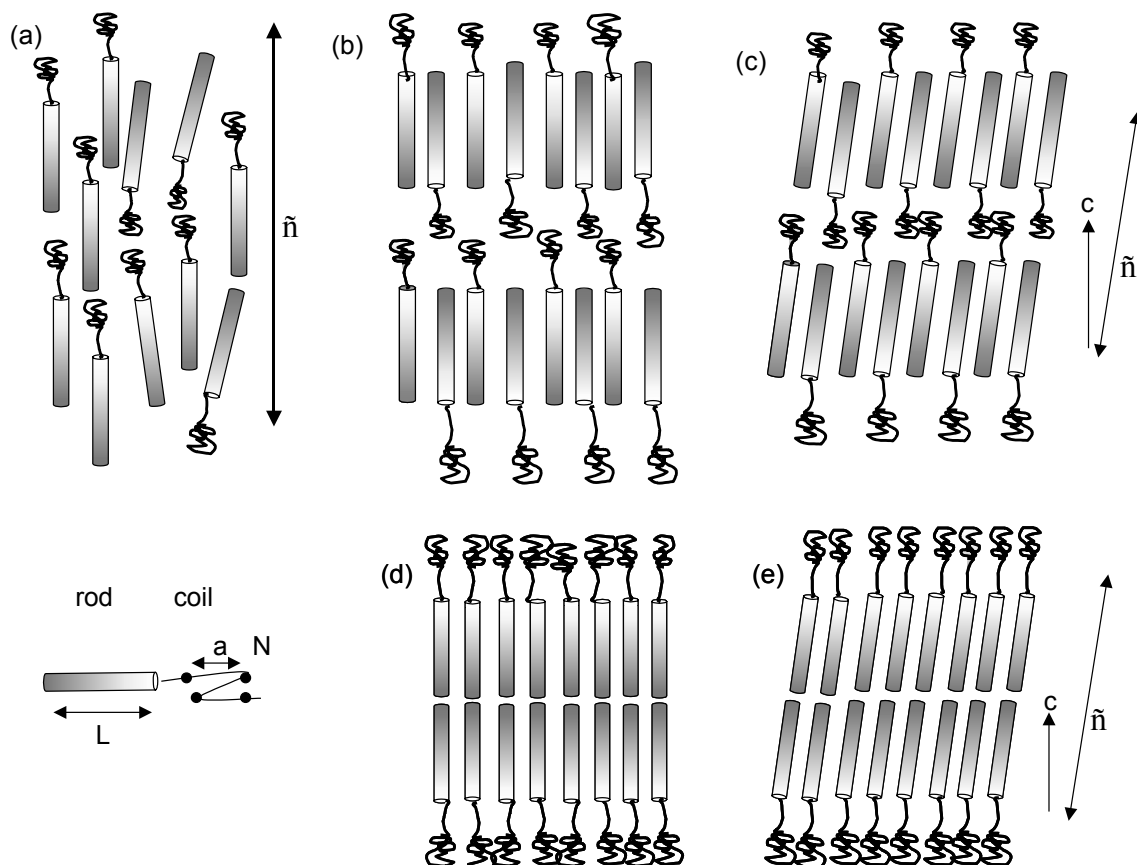


Figure 1.9: Schematic representation of rod-coil diblock morphologies proposed by Semenov and Vasilenko^{26,27} (a) nematic (b) interdigitated SmA (c) interdigitated SmC (d) bilayer SmA and (e) bilayer SmC

In order to test the theoretically predicted lamellar phases by Semenov^{26,27} and Halperin²⁸ with experiments, Chen *et al.*^{30,31} synthesized a series of five rod-coil diblock copolymers by coupling a polyhexyl-isocyanate block to a polystyrene block. Thin film samples were cast from toluene solutions and showed lamellar phases, which were not anticipated by the existing theories. The copolymer with the largest coil fraction $f=0.58$ displayed an interdigitated SmC phase with undulating layers (SmC_{1,und}) having a tilt angle of 60°. Because of the poor-long range order of this phase it was named “wavy lamellar phase”. Copolymers with higher rod fraction showed better-developed long-range order and the tilt angle reduced to 45°. This phase was referred to as the “zig-zag” phase. By increasing the rod fraction an interdigitated - bilayer phase transition (SmC_{1,und} – SmC_{2,und}) occurs. In Figure 1.10 a

schematic illustration of the interdigitated and bilayer “zig-zag” phase is shown. Even at very high rod fractions lamellar morphologies were observed. If $f < 0.04$ the authors observed smectic O (SmO) phases which were named “arrowhead” morphology. Characteristic of the SmO phase is that the tilt angle of the rods flips from layer to layer. This phase is similar to a smectic C phase with alternating tilt angles (SmC_A). For $f = 0.04$ a bilayer morphology and for $f = 0.02$ an interdigitated morphology was suggested. These “arrowhead” morphologies are also shown in Figure 1.10. That the above-mentioned phases were not predicted before by theory is possibly the consequence of non-equilibrium effects associated with the solvent casting process, which indicates that the preparation method strongly influences the phase behaviour and opens up perspectives for the preparation of a range of morphologies which are not anticipated for by theory.

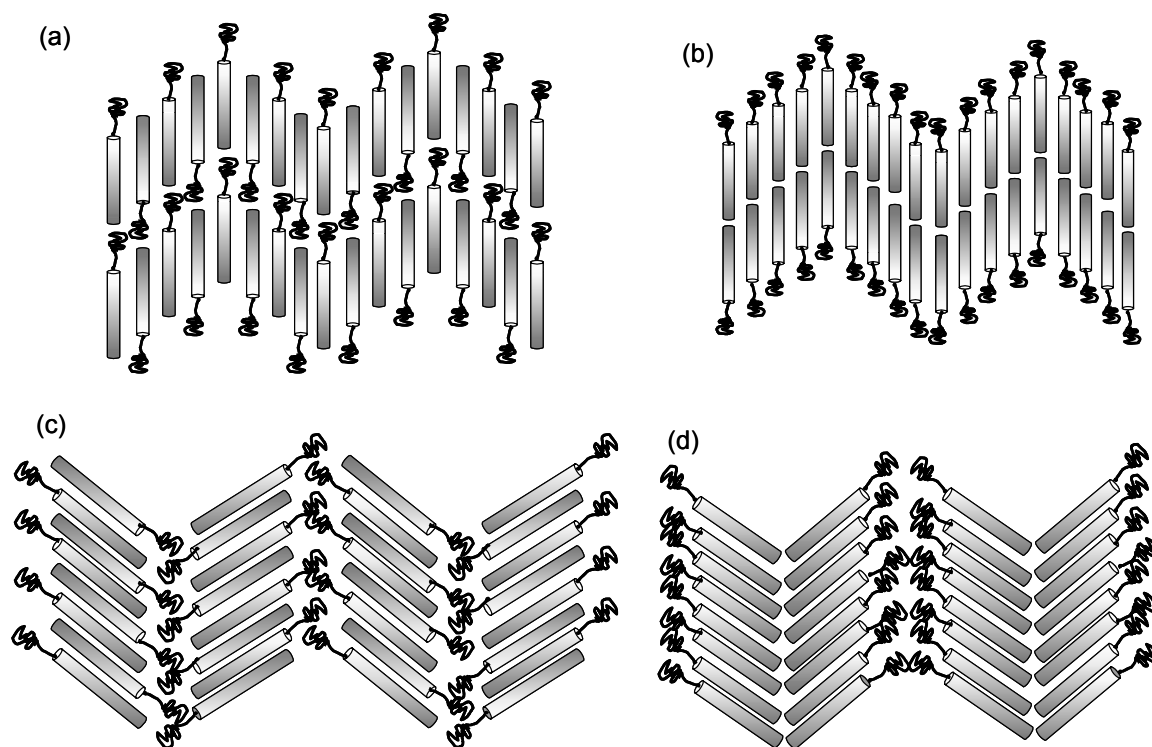


Figure 1.10: Schematic representation of rod-coil diblock morphologies proposed by Chen *et al.*³⁰ (a) an interdigitated “zigzag” phase (b) a bilayer “zigzag” phase (c) interdigitated “arrowhead” phase, and (d) bilayer “arrowhead” phase

Non-Lamellar Phases

Upon increasing the coil fraction f the stretching penalty of the coils in the lamellar phase of a rod-coil diblock copolymer will rapidly increase. In order to relieve coil stretching the lamella may undergo a tilting transition^{27,28} or transform from a bilayer to an interdigitated morphology²⁶ as described in the previous section. For even higher coil fractions the lamella are forced to break up into smaller aggregates, which allows the highly stretched coils to spread out and occupy space lateral to the rigid rod domains. As a result the average coil stretching significantly decreases. Williams and Fredrickson³² extended the Semenov-Vasilenko²⁶ theory and predicted a phase where the rods organize in a disc-like layer (so called “hockey pucks”) surrounded by a corona of coils when the fraction of coils $f > 0.88$. These “hockey pucks” are supposed to pack into cylinders and form a three-dimensional superstructure. In order to investigate non-lamellar structures Radzilowski *et al.*³³⁻³⁵ synthesized a series of rod-coil diblock copolymer with high coil fractions. Radzilowski *et al.*³³⁻³⁵ connected a perfectly monodisperse rod-like segment containing eight phenyl groups onto a coil-like segment of polyisoprene ($M_n \sim 3000-8000$) and showed by increasing the coil fraction that the smectic phase first broke up into a strip-like morphology at $f \sim 0.64$ which subsequently broke up into the “hockey puck” morphology at $f \sim 0.75$. For both phases the rods are arranged in hexagonal fashion. A schematic representation of both the “hockey puck” and rectangular “strip” morphology is shown in Figure 1.11. Remarkably similar transitions occur for multiblock rod-coil block copolymers upon increasing the number of repeat units. Lee *et al.*³⁶ synthesised a series of rod-coil block copolymers of the (rod-coil) _{n} type with ($n=1,2,3,13$) composed of 3 biphenyls which are separated by methylene ether linkages as a rigid block connected to poly(propylene oxide). The rod-coil diblock (rod-coil)₁ showed a lamellar structure. In contrast, the (rod-coil)₂ multiblock copolymer displayed a rectangular strip morphology. Rod-coil multiblock copolymers with $n \geq 3$ displayed a hexagonal cylindrical phase. Similar argumentation holds here in order to explain the phase transitions, i.e. increasing the number of repeating units in the multiblock copolymer induces more topological constraints and as a result the coils will be highly stretched. To overcome this unfavourable coil stretching the sheet-like domains will break up (into strips or cylinders) to make room for the coils.

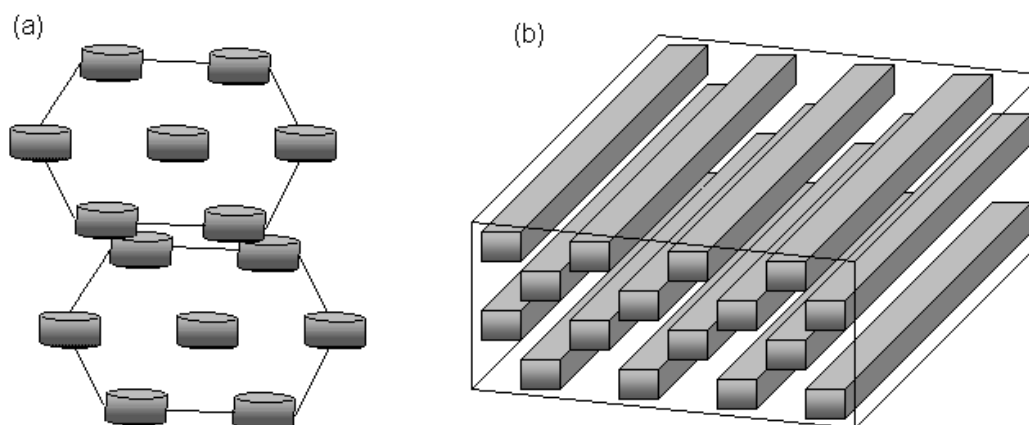


Figure 1.11: Schematic representation of (a) a hexagonal superlattice of a “hockey puck” morphology and (b) a hexagonal “strip” morphology proposed by Radzilowski *et al.*³⁵

Recently some more elaborate self-consistent field theory (SCFT) models have been developed to predict the phase behaviour of (diblock) rod-coil copolymers where numerical calculations have been employed in a 2D framework, and as a consequence the model allows for the presence of non-lamellar phases. Pryamitsyn and Ganesan³⁷ presented a theory where the orientational interactions were modelled through a Maier-Saupe^{12,13} interaction and 2D phase diagrams were computed which showed that the stripe and puck phases observed in the experiments of Radzilowski *et al.*³³ covered a major portion of the phase diagram for $f > 0.5$. In addition the theory allowed for the presence of non-equilibrium and meta-stable (arrowhead, bilayer and zigzag) lamellar phases. For comparison with the 1D phase diagram proposed by Matsen and Barrett²⁹ the 2D phase diagram proposed by Pryamitsyn and Ganesan³⁷ is shown in Figure 1.12.

Although research on rod-coil block copolymers is relatively new, already successful results have been achieved both by experimental and theoretical investigations in order to obtain new supramolecular phases and in describing the phase behaviour of rod-coil block copolymers. However a full understanding of the complete range of structures of rod-coil diblock copolymers has not been achieved. Recent experiments also showed the possibility for rod-coil block copolymers to exhibit intermediate structures like the gyroid³⁸ and perforated lamellar³⁹ phases, which formerly were only known from flexible coil diblock copolymers and have not yet been found by any rod-coil diblock copolymer theory.

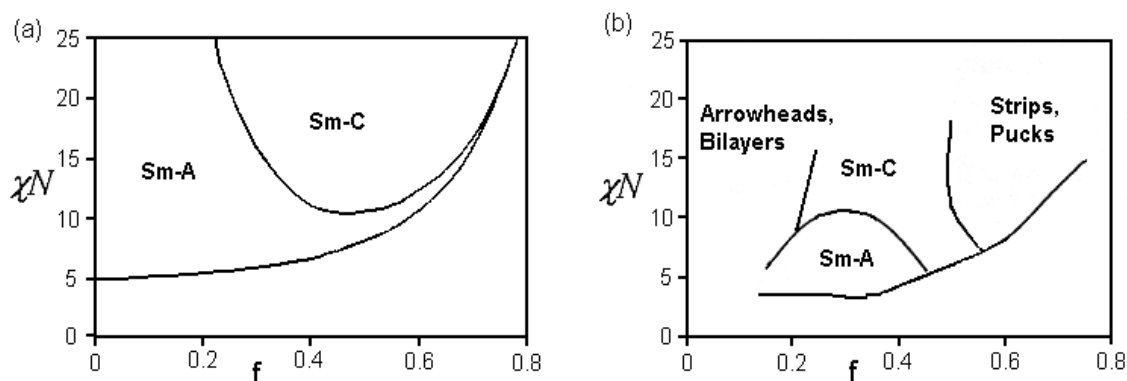


Figure 1.12: Phase diagrams for rod-coil diblock copolymers for $v=0.25$ from (a) 1D calculations by Matsen and Barrett²⁹ and (b) 2D calculations by Pryamitsyn and Ganesan³⁷.

1.5 Scope of this Thesis

1.5.1 Incentive for this Work

In the past a considerable amount of work has been done on the blending of thermotropic LCP's with standard flexible chain polymer matrix materials. The main objective of this concept is to reinforce a cheap matrix material with a small amount of expensive LCP material, which is dispersed in a fibrillar form. This work was initiated by Jackson⁴⁰ who prepared blends of polyhydroxybenzoic acid (PHB) in polyethylene terephthalate (PET). The concept of self-reinforcing polymer blends (SRPB's) however never completely reached its targets due to various problems resulting from the incompatibility of the constituent polymers, these include: high interfacial tension, large differences in viscosity, and large differences in thermal properties to name a few. All these aspects result in that the obtained fibrillar morphology of the LCP filler was not sufficiently stable. Due to the above mentioned disadvantages of self-reinforced blends not much later the concept of molecular composites was initiated by the groups of Takaynagi⁴¹ and Helminiak⁴². Molecular composites differ from SRPB's in the way the liquid crystalline reinforcement is dispersed in the matrix. SRPB's are phase-separated mixtures of LCP's and thermoplastic polymers whereas in molecular composites the aim is to homogeneously disperse a rigid rod polymer in a flexible matrix. However molecular composites also have some important drawback due to the incompatibility of the constituents. Because different polymers tend to phase separate upon heating melt

processing of molecular composites is limited. Also the fabrication is limited by the large amount of strong acids that are needed to optimally disperse the reinforcement. Block copolymers of rigid rods and flexible coil segments have been proposed in order to improve heat stability. Blends tend to phase separate on a macroscopic scale resulting that the reinforcement effect is largely lost whereas block copolymer only phase separate on a microscopic scale.

Despite these difficulties, the concepts of self-reinforcing blend and molecular composites still remains intriguing as it has the potential to combine the properties of both type of polymers to lead to e.g. high modulus, high energy absorption, high ductility, high temperature in addition to a tuneable degree of anisotropy. From our point of view the best way to obtain such properties is in the form of a liquid crystalline block copolymer, where the rigid segments give rise to the formation of a nematic domain. The aim is obtain a material, which forms both a LC phase and a microphase-separated structure. Due to this phase separation we assume that the flexible blocks are anchored onto the aligned LC layers and therefore due to packing constraints will tend to become aligned as well, i.e. a stretched conformation of the flexible blocks become favoured upon minimization of the free energy term. Therefore the coils in the copolymer will be stiffer compared to unstretched coils, and the mechanical properties will be better than expected from the pure flexible coils.

It is expected that the structure of this type of block copolymers, at least conceptually, may be compared to the structure of dragline silk. This type of block copolymer should therefore display high-energy absorption because of the combination of rigid blocks providing stiffness and flexible (amorphous) blocks providing elasticity. In addition we want to gain insight into the evolution of the microstructure of such materials as function of composition and processing conditions in relation with the macroscopic mechanical properties.

The polymer structure of our choice is a block copolymer that is composed of poly(*p*-phenylene terephthalate) (PPTA, commercial names Kevlar[®] or Twaron[®]) and polyamide 6,6 (PA 6,6) (chemical name: hexamethylene adipamide, commercial name: Nylon 6,6). It should be noted that this type of polyamides in general have relatively strong intermolecular hydrogen bonding, which improves the properties compared to polyesters. In addition by using this type of polyamides problems related to transesterification, which destroys the block structure, can be avoided. This type of alternating PPTA-PA 6,6 block copolyamide was first synthesised by the group of Takayanagi⁴¹ who blended it with aliphatic polyamides to explore the concept of molecular composites. The block copolymer prepared by Takayanagi was not liquid crystalline because the PPTA content was not sufficiently high. The synthesis of the

block copolymers was via a conventional polycondensation route. As a consequence multiblock copolymers are obtained which have rather broad distribution of block lengths and overall block copolymer length. This has some important consequences for the phase behaviour of the block copolymer. Because of the multiple connections between the different blocks a multiblock has considerably increased topological constraints compared to a diblock copolymer and because the blocks are polydisperse the phase separation is expected to be less well defined than for the examples mentioned in the previous paragraphs. In order to study the effect of processing on the mechanical properties we will investigate the orientation and morphology under simple shear flows in films and using fiber drawing. Despite the broad MW distribution in the polymers control of the morphology is to some extent possible by changing composition of the blocks. In the end it is the purpose to gain a better understanding of the relation between the molecular composition, the microstructure and the mechanical macroscopic properties.

1.5.2 Preview of the Following Chapters

In Chapter 2 the synthesis and initial characterization of a series of four block copolymers of different compositions, comprised of alternating PPTA and PA 6,6 blocks is described. Chapter 3 deals with the phase behaviour of the copolymers in sulfuric acid. In Chapter 4 a structural study in the solid state is given. The relations between the mechanical properties and orientational order of aligned copolymer films and of copolymer fibers are discussed in Chapters 5 and 6, respectively.

1.6 References

- (1) Reinitzer, F. *Monatsh.* **1888**, *9*, 421.
- (2) Lehmann, O. *Z. Phys. Chem.* **1889**, *4*, 462.
- (3) Lehmann, O. *Verhandl., d. Deutschen Phys. Ges., Sitzung* **1900**, *16*(3), 1.
- (4) Akutagawa, T.; Matsunaga, Y.; Yasuhara, K. *Liquid Crystals* **1994**, *17*, 659.
- (5) Herrmann-Schönherr, O.; Wendorff, J. H.; Ringsdorf, H.; Tschirner, P. *Makromol. Chem., Rapid Commun.* **1986**, *7*, 97.
- (6) Ballauff, M. *Makromol. Chem., Rapid Commun.* **1986**, *7*, 407.
- (7) Onsager, L. *Proc. NY Acad. Sci.* **1949**, *51*, 627.
- (8) Flory, P. J. *Proc. R. Soc. London, Ser. A* **1956**, *234*, 73-89.
- (9) Khokhlov, A. R.; Semenov, A. N. *Physica A* **1981**, *108*, 546-556.
- (10) Khokhlov, A. R.; Semenov, A. N. *Physica A* **1982**, *112*, 605-614.
- (11) Ronca, G.; Yoon, D. Y. *J. Chem. Phys.* **1982**, *76*, 3295-3299.
- (12) Maier, W.; Saupe, A. *Z. Naturforsch.* **1959**, *14A*, 882-889.
- (13) Maier, W.; Saupe, A. *Z. Naturforsch.* **1960**, *15A*, 287-292.
- (14) Jahmig, F. *J. Chem. Phys.* **1979**, *70*, 3279-3290.
- (15) Warner, M.; Gunn, J. M. F.; Baumgartner, A. B. *J. Phys., A* **1985**, *18*, 3007-3026.
- (16) Kratky, O.; Porod, G. *Rec. Trav. Chim. Pays-Bas* **1949**, *68*, 1106-1123.
- (17) Khokhlov, A. R.; Semenov, A. N. *J. Stat. Phys.* **1985**, *38*, 161-182.
- (18) Nakano, T.; Hasegawa, Y.; Okamoto, Y. *Macromolecules* **1993**, *26*, 5494.
- (19) Hamley, I. W. In *The physics of block copolymers*, Oxford University Press: New York, 1998.
- (20) Matsen, M. W.; Schick, M. *Phys. Rev. Lett.* **1994**, *72*, 2660.
- (21) Matsen, M. W.; Schick, M. *Macromolecules* **1996**, *29*, 1091.
- (22) Fink, Y.; Urbas, A. M.; Bawendi, M. G.; Joannopoulos, J. D.; Thomas, E. L. *J. Lightwave Tech.* **1999**, *17*, 1963-1969.
- (23) Jenekhe, S. A.; Chen, X., L. *J. Phys. Chem. B* **2000**, *104*, 6332-6335.
- (24) de Boer, B.; Stalmach, U.; Melzer, C.; Hadziioannou, G. *Synth. Met.* **2001**, *121*, 1541-1542.
- (25) Li, M; Cho, B-K; Zin, W-C. *Chem. Rev.* **2001**, *101*, 3869-3892
- (26) Semenov, A. N.; Vasilenko, S. V. *Sov. Phys. JETP* **1986**, *63*, 70-79.
- (27) Semenov, A. N. *Mol. Cryst. Liq. Cryst.* **1991**, *209*, 191.
- (28) Halperin, A. *Europhys. Lett.* **1989**, *10*, 549-553.
- (29) Matsen, M. W.; Barrett, C. *J. Chem. Phys.* **1998**, *109*, 4108-4118.

- (30) Chen, J. T.; Thomas, E. L.; Ober, C. K.; Hwang, S. S. *Macromolecules* **1995**, *28*, 1688-1697.
- (31) Chen, J. T.; Thomas, E. L.; Ober, C. K.; Mao, G.-P. *Science* **1996**, *273*, 343-346.
- (32) Williams, D. R. M.; Fredrickson, G. H. *Macromolecules* **1992**, *25*, 3561-3568.
- (33) Radzilowski, L. H.; Wu, J. L. *Macromolecules* **1993**, *26*, 879-882.
- (34) Radzilowski, L. H.; Stupp, S. I. *Macromolecules* **1994**, *27*, 7747-7753.
- (35) Radzilowski, L. H.; Carragher, B. O.; Stupp, S. I. *Macromolecules* **1997**, *30*, 2110-2119.
- (36) Lee, M.; Cho, B.-K.; Oh, N.-K.; Zin, W.-C. *Macromolecules* **2001**, *34*, 1987-1995.
- (37) Pryamitsyn, V.; Ganesan, V. *J. Chem. Phys.* **2004**, *120*, 5824-5837.
- (38) Lee, M.; Cho, B.-K.; Kim, H.; Zin, W.-C. *Angew. Chem. Int. Ed.* **1998**, *37*, 638-640.
- (39) Ryu, J.-H.; Oh, N.-K.; Zin, W.-C.; Lee, M. *J. Am. Chem Soc.* **2004**, *126*, 3551-3558.
- (40) Jackson Jr., W. J.; Kuhfuss, H. F. *J. Pol. Sci.* **1976**, *14*, 2043.
- (41) Takayanagi, M.; Ogata, T.; Morikawa, M.; Kai, T. *J. Macromol. Sci., Phys.* **1980**, *B17*, 591-615.
- (42) Hwang, W.-F.; Wiff, D. R.; Benner, C. L.; Helminiak, T. E. *J. Macromol. Sci., Phys.* **1983**, *B22*, 231-257.

Chapter 2

Synthesis and Characterization of PPTA-*block*-PA 6,6 Multiblock Copolymers

Abstract

A series of block copolymers that contain rigid liquid crystal forming blocks of poly(*p*-phenylene terephthalamide) (PPTA) and flexible blocks of polyamide 6,6 (PA 6,6) have been synthesized. The polymers have been prepared in a one-pot procedure by addition of PA 6,6 monomers to an amine-terminated PPTA-oligomer via a low-temperature polycondensation reaction in *N*-methyl-2-pyrrolidone. Via this method block copolymers are formed that were characterized by inherent viscosity measurements, size exclusion chromatography (SEC), NMR, Soxhlet extraction and TGA. The molecular weights of the synthesized rod-coil block copolymer materials are estimated from their intrinsic viscosities by a semiempirical model that combines both the intrinsic viscosity relations of the homopolymers and the mean-square end-to-end distance of the rod-coil copolymer.

Based on:

Synthesis and Characterization of Lyotropic Rod-Coil Poly(amide-block-aramid) Alternating Block Copolymers, de Ruijter, C.; Jager, W.F.; Groenewold J.; Picken S.J. Macromolecules 2006, 39, 3824-3829

2.1 Introduction

The study of block copolymers containing rigid liquid crystal forming segments is of great interest both from a scientific and from a technological point of view. Monodisperse rod-coil diblock copolymers have served as a model system to examine both theoretically¹⁻⁵ and experimentally⁶⁻⁹ the self-assembly resulting from the interplay between liquid crystalline (LC) ordering and microphase separation. Because both processes compete during the minimization of free energy, morphologies that are distinctly different from flexible block copolymers will be obtained, showing LC order at a molecular scale together with long-range orientational order. From a technological point of view monodisperse rod-coil block copolymers offer numerous opportunities for designing nano-structured materials in a wide field of applications. In particular rod-coil block copolymers bearing a conjugated segment as the rod block received great interest and have been proposed for electro-optic and photonic devices.¹⁰⁻¹²

The phase behaviour of rod-coil diblock (and multiblock) polymers with a broad molecular weight distribution is much less understood and up to now there are no theories available describing the phase behaviour of such materials. Over the past two decades numerous publications have appeared dealing with synthesis and characterization of polydisperse multiblock copolymers comprised of alternating rigid, liquid crystal forming, and flexible (amorphous or crystalline) segments. A considerable amount of research on LC multiblock copolymers has been done in the field of thermoplastic elastomers where LC segments replace the hard segments of conventional thermoplastic elastomers. Several publications are available that deal among others with LC poly(ether-ester),¹³ poly(ether-amide),^{14,15} and polyurethane¹⁶ block copolymers where the rigid segments are polyurethane blocks and the flexible segments are usually polyether or polyester blocks.

Block copolymers containing LC segments can also be considered as a molecular composite. The concept of a molecular composite was introduced in the early 1980s by the groups of Takayanagi¹⁷ and Helminiak,¹⁸ and the concept can be defined as a homogenous dispersion of rigid polymer microfibrils of high aspect ratio (L/D) in a flexible coil polymer matrix in order to improve the mechanical and physical properties of the matrix polymer. These materials can be seen as an interesting alternative for conventional fiber reinforced composites. The main drawback observed in preparing molecular composites is the incompatibility between the rigid and the flexible polymer. Because of this incompatibility, the rigid polymer tends to phase separate in macroscopic aggregates, causing the reinforcement effect to a

large extent to be lost. An alternative approach is to prepare a block copolymer composed of rigid and flexible segments. Because of the covalent bond between the different segments, phase separation on macroscopic scale is prevented. On the basis of this principle, Takayanagi¹⁷ prepared block copolymers of a flexible aliphatic polyamide PA 6 or PA 6,6 with a rigid aromatic polyamide poly(*p*-phenylene terephthalamide) (PPTA) or poly(benzamide) (PBA). Takayanagi showed that PA reinforced with the block copolymer displayed improved mechanical properties compared to a corresponding blend of the aramid and PA.

Since this pioneering work other research groups also prepared block copolyamides composed of segments of different rigidity. Martin¹⁹ synthesized a block copolymer of PBA with a random copolymer of PA 6 and PA 6,6. Both Takayanagi and Martin prepared the block copolymers via the Morgan²⁰ method, i.e. a low temperature acid chloride-amine polycondensation reaction in a mixed hexamethylphosphoramide/*N*-methyl-pyrrolidone (HMPA/NMP) solution. Krigbaum²¹⁻²³ reported on several types of wholly aromatic block copolyamides prepared by the phosphorylation reaction²⁴ and studied the phase behaviour of these block copolymers when dissolved in dimethylacetamide (DMAc) containing 3 wt% LiCl. Helgee²⁵ reported on the preparation of fibers from liquid crystalline solutions of a wholly aromatic block copolyamide synthesized via the conventional acid chloride-amine polycondensation method. Aromatic-aliphatic triblock copolyamides prepared via anionic ring opening polymerisation have been reported by Mathias²⁶ and Marek Jr.²⁷ According to the Marek Jr. method a short rigid aromatic polyamide oligomer was prepared with *N*-acyl-6-hexanelactam end-groups. These groups act as an initiator for the anionic polymerisation of PA 6. The main drawback of this method is that only a limited amount of aromatic activator with a low degree of polymerisation can be dissolved in the ϵ -caprolactam monomer. Recently Huang reported on synthesis of block copolymers of PA 6²⁸ and PA 6,6²⁹ with various aromatic semi-rigid polyamides in order to improve the mechanical properties of PA. Via a low temperature polycondensation reaction, acid chloride terminated rigid oligomers were reacted with amine-terminated PA oligomers to produce block copolymers. The majority of the publications mentioned above deal with block copolymers for the purpose of making molecular composites. The key condition to prepare such materials is that the rigid segments are homogeneously distributed in the flexible matrix to fully benefit from the reinforcement. These systems contain a low fraction of the rigid component and films or fibers should be prepared via rapid coagulation from a dilute (isotropic) solution both in order to prevent phase separation. Another limitation of molecular

composites is their lack of thermal stability. Molecular composites based on block copolymers tend to microphase separate if the temperature exceeds the glass transition point of the flexible component.

In contrast to the molecular composite approach the focus in this thesis will be on microphase-separated polyamide-*b*-aramid multiblock copolymers. Basically this approach can be seen as a reversal of the general perspective; i.e.; the aim is not to improve the properties of PA with PPTA as reinforcement (molecular composite approach) but to modify PPTA with PA aiming to enhance the impact resistance of PPTA by introducing more elasticity and to obtain higher fracture energy.

In this study the focus will be on the block copolymer composed of alternating PPTA and PA 6,6 blocks, similar to those originally reported by Takayanagi¹⁷ although the polymerisation route has been slightly altered. Takayanagi prepared copolymers via the Morgan²⁰ route which makes use of hexamethylphosphoramide (HMPA) as a cosolvent. This solvent is known to be carcinogenic³⁰; so therefore the synthesis route of our choice is the Vollbracht³¹ route, and the solvent is a mixture of NMP/CaCl₂. The block length can be altered easily by adjusting the ratio of the monomers. Takayanagi synthesized the block copolymer from an acid-chloride PPTA oligomer. The block copolymers for this research have been prepared from an amine-terminated oligomer because amine end groups tend to be more stable in the solvent mixture. The chemical structure of a repeat unit of the prepared block copolymers is shown in Figure 2.1.

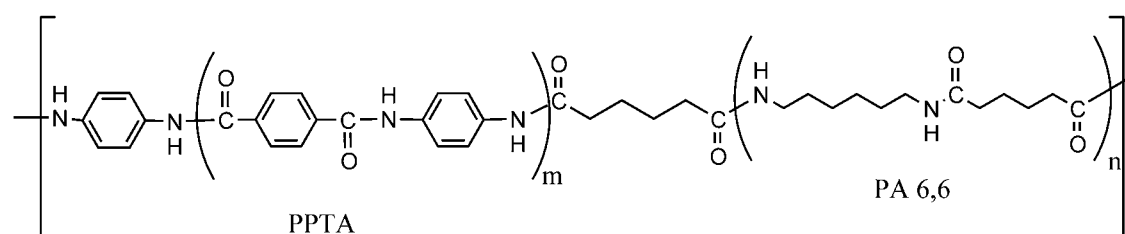


Figure 2.1: Chemical structure of a repeating unit of a PPTA-*b*-PA-6,6 block copolymer

2.2 Experimental

2.2.1 Materials

N-methyl-2-pyrrolidone NMP (Acros) was vacuum-dried over CaH₂ and stored on molecular sieves. Terephthaloyl chloride TDC (Acros), *p*-phenylenediamine PDA (Acros) and hexanediamine HDA (Acros) were purified by vacuum sublimation before

use. Calcium chloride (Boom) was dried overnight under vacuum at 200 °C. Triethylamine TEA (Merck) was distilled over CaH₂ and stored over molecular sieves. Adipoyl chloride AC (Fluka) was purified by vacuum distillation.

2.2.2 Measurements

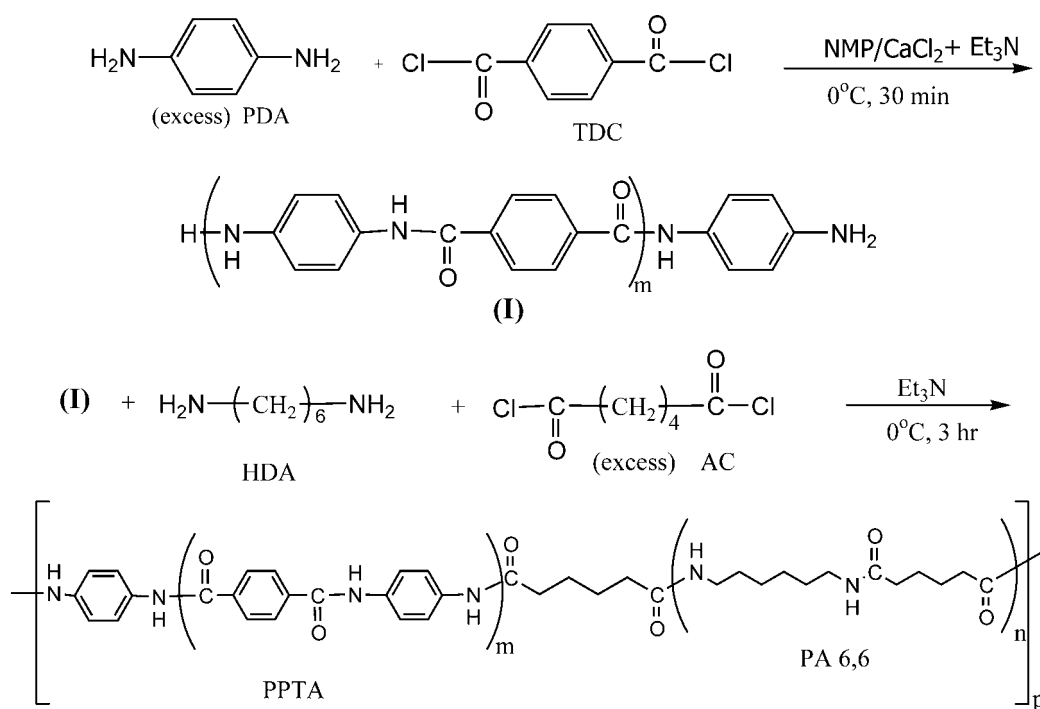
The block copolymers were extracted in a Soxhlet apparatus using formic acid, which is a solvent for PA 6,6, but a nonsolvent for PPTA. In each case, 3 g of polymer was exposed to 80 mL of formic acid and extracted for 24 h. Next the unextracted part was filtered. The extracted part was precipitated in ethanol and then filtered. Both the extracted and unextracted part were washed with water and dried under vacuum at 50 °C. ¹H-NMR spectra of the polymer specimen in D₂SO₄ were obtained with a 400 MHz UR-400S Varian spectrometer.

The inherent viscosities (η_{inh}) of the polymers were determined with an Ubbelohde viscometer. For all polymers a 0.5 g dL⁻¹ solution in concentrated sulfuric acid at 30 °C was used. The intrinsic viscosities [η] of the polymers were determined by extrapolating the reduced viscosities (η_{sp}/c) obtained at four concentrations (0.2, 0.3, 0.4, and 0.5 g dL⁻¹) to zero concentration. Size exclusion chromatography (SEC) analysis of the samples was performed at Teijin Twaron Arnhem. The polymers were dissolved in concentrated sulfuric acid (0.1 mg/mL) which was used as the mobile phase and separated by SEC using a Zorbax GPC column (250 x 6.2 mm). For detection a UV detector at 340 nm was used. The molecular weight values were calculated using Cirrus version 1.1 GPC software (Polymer Laboratories). As a reference a high-MW Twaron (PPTA) yarn type 1010 and a PPTA trimer were used. Thermal gravimetric analysis (TGA) in nitrogen was performed with a Perkin-Elmer 7a using a heating rate of 10 °C/min. Differential scanning calorimetric (DSC) measurements were performed with a Perkin-Elmer TAC 7/DX DSC using a heating rate of 10 °C/min.

2.2.3 General Procedure for the One-Pot Block Copolymer Polycondensation Reaction

A typical block copolymerisation experiment was performed as follows: in a four-neck reaction vessel equipped with a mechanical stirrer and a dropping funnel under an argon atmosphere, 6.00 g (0.0556 mol) of PDA was placed in a mixed solvent of 22 mL of TEA and 200 mL of NMP containing 22 g of CaCl₂, which was partially in the

solid state. After the mixture was cooled in an ice bath to 0 °C, 9.02 g (0.0444 mol) of finely powdered TDC was added to the solution under vigorous stirring. The solution was kept in an ice bath for 30 min to obtain a clear dark yellow fairly viscous solution containing an amino-terminated PPTA oligomer. To this mixture was added successively 5.16 g (0.0444 mol) of HDA, 18 ml of TEA and 100 ml of NMP. To this solution 10.17 g (0.0556 mol) of AC was added dropwise. The reaction mixture was kept in an ice bath for 1 h and at room temperature for another two h to obtain a viscous gel. This gel was precipitated into a large amount of water, blended in a blender jar, repeatedly washed with water, and dried under vacuum at 50 °C. According to this method a random block copolymer is prepared that consist of 50 mol% PPTA and 50 mol% PA 6,6. The theoretical degree of polymerisation of the individual blocks is 9 and the polymer is denoted as P4-4 where the numbers refer to the number of repeat units of respectively the aramid and aliphatic amide blocks (m and n in Figure 2.1). By simply varying the monomer ratio according to Carothers' equation, every desired composition can be made. A series of four different types of block copolymers have been synthesized, i.e., P10-4, P4-4, P10-10, and P4-10. The composition and inherent viscosities $[\eta]_{inh}$ of the copolymers and the aramid and polyamide prepolymers are given in Table 2.1. The synthesis route of the copolymer is schematically shown in Scheme 2.1. The inherent viscosities are measured at a concentration of 0.5 g dL⁻¹ in 96 wt% H₂SO₄ at 30°C.



Scheme 2.1: Synthetic scheme for the synthesis of a PPTA-*b*-PA-6,6 multiblock copolymer

Table 2.1: Inherent viscosities and compositions of the block copolymers and oligomers

Polymer	η_{inh} (dL g ⁻¹) ^a	Amount of flexible (PA 6,6) block (mol%)	Number of repeat units ^b of		
			PPTA m (-) ^c	PA 6,6 n (-) ^c	PPTA-b-PA 6,6 p (-) ^{c,d}
P10-4	1.87	29	10	4	3.1
P10-10	1.71	50	10	10	2.4
P4-4	2.06	50	4	4	8.3
P4-10	0.75	71	4	10	2.1
P4-0	0.42	0	4	0	2.0
P10-0	0.76	0	10	0	-
P0-4	0.22	100	0	4	-
P0-10	0.39	100	0	10	-

^a Measured at a concentration of 0.5 g dL⁻¹ in 96 wt% H₂SO₄ at 30°C

^b The number of repeat units based on stoichiometry using Carothers equation

^c m and n and p refer to Figure 2.1

^d p is calculated from M_w values obtained by SEC (Table 2.3)

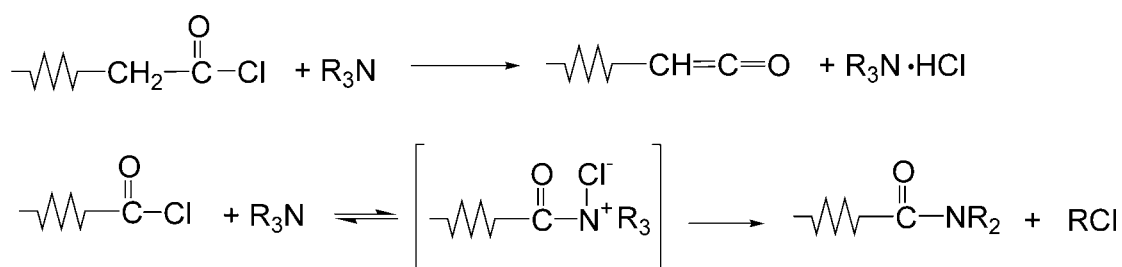
2.3 Results and Discussion

2.3.1 Polymer Synthesis

The synthesis of this type of aromatic-aliphatic block copolyamides by the low-temperature solution method is rather complex. The feature that complicates the synthesis is that during the polymerisation hydrogen chloride is released which can react with the diamine reactant. In this way the diamine is deactivated and the stoichiometric balance is disturbed, resulting in a decreased molecular weight. To circumvent this problem a base should be added which is stronger than the diamine monomer. Triethylamine (TEA) was chosen to act as hydrogen chloride scavenger. For the synthesis of pure PPTA the addition of TEA is not necessary to obtain high molecular weight polymer since PDA is a weak base. However, HDA is a stronger base than PDA and the use of an acid scavenger is essential to obtain high molecular weight PA 6,6. The next problem that occurs is that TEA is reactive with acid chloride end groups. Especially aliphatic acid chlorides are sensitive for side reactions and can react with TEA to form ketenes,³² and both aliphatic and aromatic acid chlorides can react with TEA to form a monoamide group and an alkyl halide.³³ These side reactions are shown in Scheme 2.2. The reaction rate of these chain-terminating side reactions compared to the amide-forming condensation reaction can be suppressed significantly by decreasing the temperature. Temperatures in the

range of -40 to 0 °C are desirable, and therefore the polymerisation reactor was kept in an ice-bath during the synthesis. Because of the reactivity of the TEA toward acid chloride, the block copolymer was synthesized from an amine-terminated PPTA oligomer; i.e., an excess of PDA in the oligomer synthesis was used.

Because of the complications mentioned above the final molecular weight of the PPTA-*b*-PA block copolymer will be lower than obtained for pure PPTA. Because aliphatic acid chloride is more sensitive to side reactions than aromatic acid chlorides, the molecular weight of the final copolymer in general will decrease with increasing PA content (see Table 2.3).



Scheme 2.2: Side-reactions of acid chlorides with tertiary amines

2.3.2 Extraction and $^1\text{H-NMR}$ Analyses of PPTA-*b*-PA 6,6 Block Copolymers

All copolymer samples were extracted with formic acid, which is a solvent for PA 6,6 but a nonsolvent for PPTA, by a Soxhlet extraction procedure. The results of the extraction procedure are shown in Table 2.2. The absence of any components in the precipitate of copolymer samples **P10-4**, **P4-4**, and **P10-10** along with the increase of the inherent viscosity of the copolymers compared to the oligomers (as shown in Table 2.1) are good indications that the PA is indeed copolymerized with the PPTA. However, a substantial part of the **P4-10** sample could be extracted by formic acid. This does not necessarily mean that the entire extracted fraction was not copolymerized (i.e., is pure PA). The

$^1\text{H-NMR}$ spectrum of the extracted fraction of **P4-10**, see Figure 2.2, shows the presence of PPTA in the extracted fraction. This indicates that the PPTA in the extracted fraction must be copolymerized with the PA because pure PPTA even with low degree of polymerisation is insoluble in formic acid. Therefore, these results indicate that copolymer chains with low PPTA content (up to approximately 15 wt%) are soluble in formic acid. From Figure 2.2 it is also clear that the molecular weight of the extracted part of **P4-10** is significantly lower than of **P4-10** because the absorption peaks in the $^1\text{H-NMR}$ spectrum are sharper.

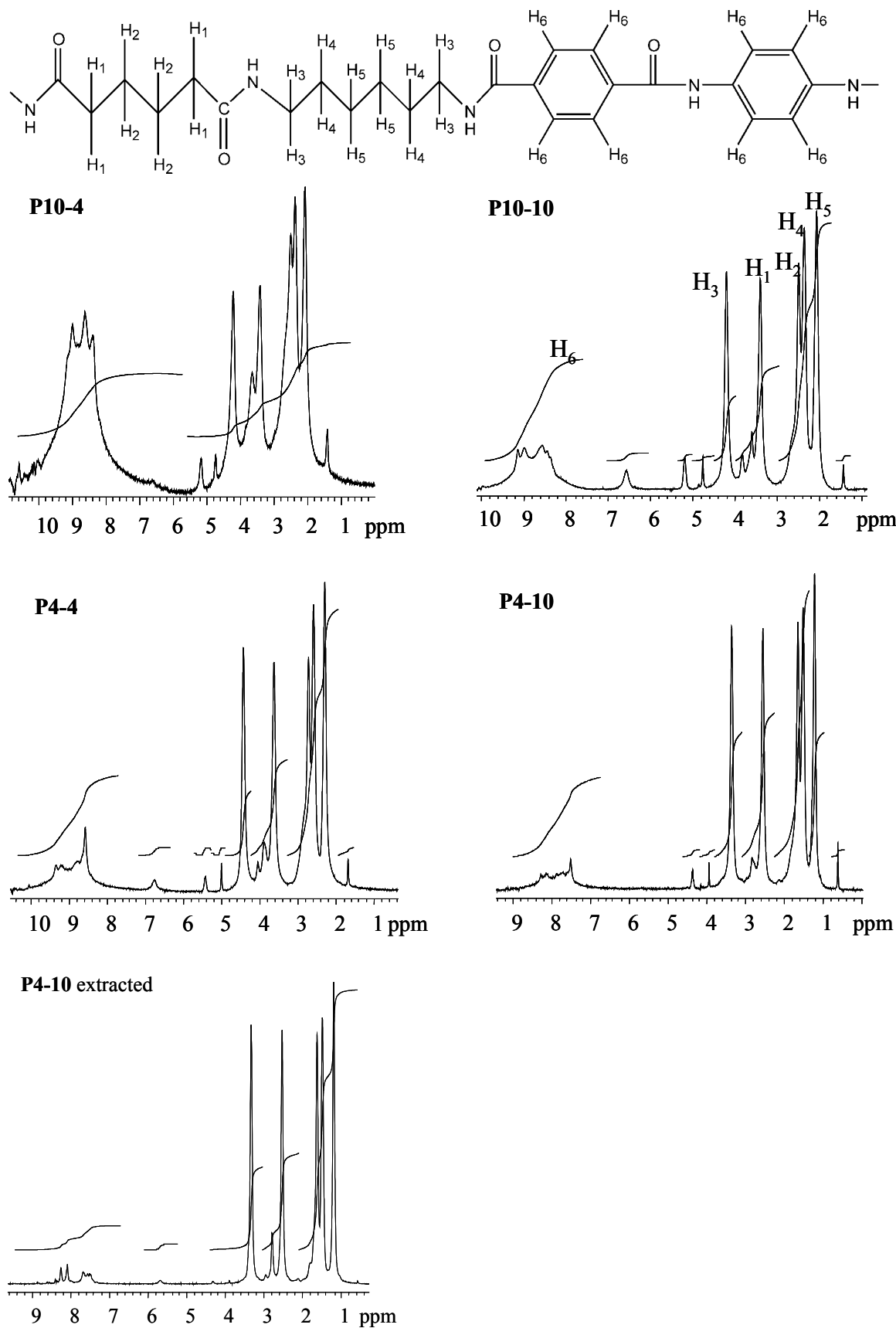


Figure 2.2: ¹H-NMR spectra of the copolymers

¹H-NMR measurements in D₂SO₄ were done for all copolymer samples and the spectra are shown in Figure 2.2. The peak assignment is shown for sample **P10-10**. The area underneath the peaks from the protons in the PPTA (δ range 7.0-9.0 ppm) was compared to area from the absorption of the protons in the PA 6,6 (δ range 1.0-5.0 ppm). From the ratio of the two areas the copolymer composition is determined. The weight fraction of PA 6,6 ($\varphi_{PA\ 6,6}$) in the copolymer is calculated by

$$\varphi_{PA\ 6,6} = \frac{\frac{A_{PA\ 6,6}}{20} M_{PA\ 6,6}}{\frac{A_{PA\ 6,6}}{20} M_{PA\ 6,6} + \frac{A_{PPTA}}{8} M_{PPTA}} \quad [2.1]$$

where $A_{PA\ 6,6}$ is the area underneath the peaks in the NMR-spectrum assigned to PA 6,6, A_{PPTA} is the area underneath the peaks in the NMR-spectrum assigned to PPTA. $M_{PA\ 6,6} = 226\ \text{g}\cdot\text{mol}^{-1}$ and $M_{PPTA} = 238\ \text{g}\cdot\text{mol}^{-1}$ are the molecular weights of a repeat unit and 20 and 8 are the number of protons per repeat unit of respectively PA 6,6 and PPTA. The amide protons of both PPTA and PA 6,6 are capable of exchanging with the deuterium of D₂SO₄ and will therefore be part of the intense sulfuric acid signal observed around 12 ppm. The weight fraction of flexible polyamide calculated from the NMR spectra is compared with the fraction calculated from the feed ratio, and the results are shown in Table 2.2. According to Table 2.2, the $\varphi_{PA\ 6,6}$ for all copolymer samples calculated from NMR analysis is significantly higher than the predicted weight fraction according to the theoretical composition. This overestimation of the weight fraction of the aliphatic part can be attributed to the process that the aromatic protons are capable of deuterium exchange in concentrated D₂SO₄.^{34, 35} Tam-Chang³⁵ observed that this deuterium exchange process increases with increasing temperature but already to some extent takes place at room temperature. Because of this deuterium exchange process, a systematic error is made that results in an overestimation of $\varphi_{PA\ 6,6}$ in the range of 5-10% for all our copolymers.

Table 2.2: Copolymer compositions calculated from ¹H-NMR analyses and extraction results

Polymer	Weight fraction of PA 6,6 repeat units in copolymer by stoichiometry	Weight fraction of PA 6,6 repeat units in copolymer by NMR-analysis	Amount extracted by formic acid (wt%)
P10-4	0.29	0.35	0
P10-10	0.49	0.55	0
P4-4	0.49	0.60	0
P4-10	0.69	0.76	16.7
P4-10 (extracted part)^a	N.A.	0.87	N.A.

^a extraction with formic acid in a Soxhlet apparatus

2.3.3 Molecular Mass Determination

Viscosimetry

Viscosimetry in concentrated (96 wt%) sulfuric acid was performed in order to determine the intrinsic viscosities $[\eta]$ of the block copolymers. The intrinsic viscosities were calculated by extrapolating the reduced viscosities to zero concentration. For all copolymers the reduced viscosity was linearly dependent on c for $0.2 \leq c \leq 0.5 \text{ g dL}^{-1}$, which means there was no observable “polyelectrolyte effect” for this concentration range. This behaviour is in accordance with the results reported by Schaeffgen *et al.*,³⁶ who observed that for pure PPTA the positive charges generated by protonation along the polymer backbone are shielded due to the high concentration of counterions in 96 wt% H₂SO₄ and therefore allowing the polymer molecules to take a natural conformation over a this concentration range. The intrinsic viscosity relates to the viscosity average molecular weight M_v according to the well-known Mark-Houwink equation

$$[\eta] = K \cdot M_v^a \quad [2.2]$$

where K and a are constants for a given system. Determination of molecular weights of the type of block copolymers considered here is somewhat troublesome, because no values for the parameters K and a are available. In fact, dilute solution behaviour of block copolymers in general remains an area of controversy, and particularly for

block copolymers comprised of rigid and flexible segments only few theories are available.

The intrinsic viscosity of a block copolymer material $[\eta]_{\text{block}}$ in a nonselective solvent can be estimated by a simple linear average of the corresponding intrinsic viscosities of the homopolymers if the polymer chain is considered as an idealized random-flight model with no mutual interactions.³⁷ For a binary block copolymer this results in

$$[\eta]_{\text{block}} = \phi_1 [\eta]_1 + \phi_2 [\eta]_2 \quad [2.3]$$

where ϕ_1 and ϕ_2 represent the weight fraction and $[\eta]_1$ and $[\eta]_2$ the intrinsic viscosities of the individual components. Of course, if polymers are comprised of rigid segments the use of random flight statistics is far from plausible and a simple linear relationship of the intrinsic viscosities will not suffice. A useful model that describes the intrinsic viscosity behaviour of rod-coil diblock copolymers has been developed recently by Cavalleri *et al.*³⁸ Although, since the prepared polymers in this research are multiblock copolymers this model is not fully applicable. Therefore this approach is modified in order to describe the intrinsic viscosity behaviour of a rod-coil multiblock copolymer. Here an alternating rod-coil copolymer is assumed of which the chains are composed of a sequence of rigid rod-like blocks A of length L and flexible coil blocks B that are described as a freely jointed chain of n segments with length l . The unperturbed mean-square-end-to-end distance $\langle R^2 \rangle$ of the individual blocks is

$$\langle R^2 \rangle_A = L^2 \text{ for the rigid blocks and} \quad [2.4]$$

$$\langle R^2 \rangle_B = nl^2 \text{ for the flexible blocks.} \quad [2.5]$$

To calculate the unperturbed mean-square-end-to-end distance of the block copolymer we need to take the average of the squares, because we do a summation of statistically independent (Gaussian) events. The $\langle R^2 \rangle$ of a rod-coil block copolymer consisting of N repeating units can be given by

$$\langle R^2 \rangle = N(L^2 + nl^2) \quad [2.6]$$

The intrinsic viscosity $[\eta]$ in general is proportional to the ratio of the hydrodynamic volume V_h of the polymer to its molar mass M

$$[\eta] = 2.5 N_{AV} \frac{V_h}{M} = 2.5 N_{AV} \frac{\langle R^3 \rangle}{M} \quad [2.7]$$

where N_{AV} is the Avogadro number.

The molar mass of the block copolymer $M_{v,copolymer}$ can be written as

$$M_{v,copolymer} = N M_{AB} \quad [2.8]$$

where M_{AB} the mass of the repeating unit in the block copolymer. By substituting Eqs. 2.6 and 2.8 into Eq. 2.7 the intrinsic viscosity of the rod-coil block copolymer $[\eta]_{copolymer}$ can be written as:

$$[\eta]_{copolymer} = 2.5 N_{AV} \frac{\left(N(L^2 + nl^2) \right)^{3/2}}{N M_{AB}} = \frac{2.5 N_{AV}}{M_{AB}} (L^2 + nl^2)^{3/2} N^{1/2} \quad [2.9]$$

Analogous equations can be written for the individual blocks:

$$M_A [\eta]_A = 2.5 N_{AV} (L^2)^{3/2} \quad [2.10]$$

$$M_B [\eta]_B = 2.5 N_{AV} (nl^2)^{3/2} \quad [2.11]$$

where M_A and M_B represent the molar masses and $[\eta]_A$ and $[\eta]_B$ the corresponding intrinsic viscosities of respectively the A and B blocks. If Eqs. 2.10 and 2.11 are substituted into Eq. 2.9:

$$M_{AB} [\eta]_{copolymer} = N^{1/2} \left((M_A [\eta]_A)^{2/3} + (M_B [\eta]_B)^{2/3} \right)^{3/2} \quad [2.12]$$

is obtained, and because $N = M_{v,copolymer} / M_{AB}$ the final result will be:

$$M_{AB}^{3/2} [\eta]_{copolymer} = M_{v,copolymer}^{1/2} \left((M_A [\eta]_A)^{2/3} + (M_B [\eta]_B)^{2/3} \right)^{3/2} \quad [2.13]$$

According to this result the intrinsic viscosity of the rod-coil block copolymer scales with the molecular weight to the power 0.5. This is analogous to a polymer that obeys random chain statistics dissolved in a Θ solvent. In reality however this is not true, nonideal behaviour of the individual blocks in a good solvent, and the rigidity of the aramid blocks will cause that parameter a will be higher than 0.5. It is more plausible that parameter a for the block copolymer is between the values of the individual homopolymers. Values for parameter a of PA 6,6 and PPTA in sulfuric acid are respectively 0.69³⁹ and 1.09⁴⁰. Therefore Eq.2.13 is rewritten and an α -parameter is defined which is between 0.69 and 1.09, which replaces the scaling factor of 0.5:

$$M_{AB}^{1+\alpha} [\eta]_{copolymer} = M_{v,copolymer}^{\alpha} \left((M_A [\eta]_A)^{2/3} + (M_B [\eta]_B)^{2/3} \right)^{3/2} \quad [2.14]$$

Using this semiempirical approach, the molecular weight range for the block copolymer can be estimated. The molecular weight ranges of our copolymer samples calculated with Eq. 2.14 are shown in Table 2.3; the values of the intrinsic viscosities of the individual blocks needed for the calculations are given in Table 2.1. Results are compared with results obtained from SEC analysis treated in the next section.

SEC Analysis

Results obtained by SEC analyses, i.e., values for M_n , M_w and the polydispersity index (PDI), are also displayed in Table 2.3. The applicability of SEC for measurements of molecular weights of aramid type polymers is limited because only few solvents for aramids are known, and most of them are harmful for columns and filters of the SEC apparatus. Another limitation of the use of SEC is that absolute values of molecular weights cannot be obtained because no aramid fractions with well-defined molecular weight are available for calibration. The apparatus used was calibrated with polystyrene standards in THF. In addition, the polymers concerned here are not aramids but block copolymers containing aramid segments; therefore, the results obtained by SEC analyses should be regarded as a rough estimation for the molecular weights. However, results obtained from SEC do give an indication of the molecular weight distribution. The SEC elution curves of the block copolymer samples and the PPTA homopolymer reference are shown in Figure 2.3. Next, the results of the molecular weights calculated from intrinsic viscosities (M_v) will be compared with the results obtained by SEC (M_n and M_w). In general M_v is between M_n and M_w and tends to be close to M_w for rigid polymers and polymers with a broad

molecular weight distribution, i.e. high index of polydispersity. Since both factors are valid here it is plausible to state that M_v should be close to M_w . From our results it is clear that that $M_v > M_n$ for all copolymer samples and we found M_w to be in the same range as the M_v values obtained via viscosimetry using Eq. 2.14. This indicates that by combination of the results of both methods a reasonable approximation for the molecular weights of this type of aramid-amide block copolymers is obtained.

Table 2.3: Molecular weight of the copolymers as obtained by SEC and viscosimetry

Polymer	$[\eta]$ (dL g ⁻¹)	$M_{v,copolymer}^a$	M_n	M_w	PDI
P10-4	2.16	9200-16100	3600	11000	3.1
P10-10	1.99	11000-17700	3600	11600	3.2
P4-4	2.44	9800-23600	5500	17200	3.2
P4-10	0.94	5500-7300	2900	7200	2.5
P4-0	0.46	2800	800	2100	2.6

^a $M_{v,copolymer}$ values calculated from Eq. 2.14 with α range of 0.69-1.09, **P4-0** from the Mark-Houwink equation for PPTA

Nevertheless, it is clear that the determination of molecular mass of rod-coil block copolymers is not straightforward. The present approach gives consistent results between the various methods, but it should be noted that Eq. 2.14 is only a rough estimate. So far we have not succeeded in finding a more rigorous derivation for the $[\eta]$ of a rod-coil block copolymer. This is due to the fact that both block are nonideal and have different Mark-Houwink exponents a .

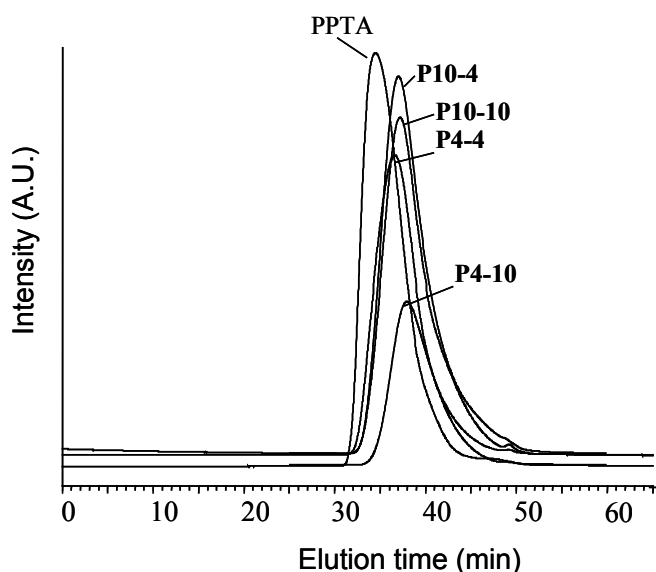


Figure 2.3: SEC elution curves for PPTA 1010 reference yarn ($M_w \cong 32000$) and for the copolymers

2.3.4 TGA

TGA measurements in nitrogen have been performed to determine the thermal stability of the block copolymer samples. Pure PPTA and PA 6,6 samples were used as a reference. From the curvature of a TGA plot it is possible to distinguish between random and block copolymers because with increasing block length a block copolymer tends to behave more like a blend of the homopolymers. A block copolymer should therefore show two distinct degradation zones, while for a random copolymer a more gradual degradation is expected. Our results of the TGA measurements are shown in Figure 2.4.

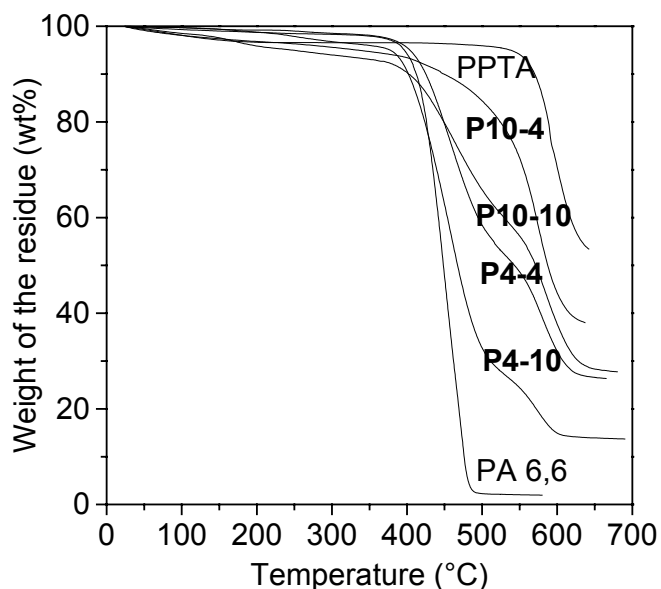


Figure 2.4: TGA of PPTA (MW \cong 32000), PA 6,6 (MW \cong 16000) and the copolymers

From this figure it is clear that the stability of the polymers increases with increasing amount of PPTA. However, copolymer sample **P10-10** shows a somewhat higher thermal stability than sample **P4-4**. Block copolymer samples **P4-4**, **P10-10** and **P4-10** show two distinct reductions in mass at 400 °C due to degradation of the PA 6,6 blocks and at 550 °C due to degradation on the PPTA blocks. Copolymer **P10-4** with highest amount of PPTA does not show a distinct degradation of the PA blocks but shows a more gradual reduction in mass. The degradation of PA 6,6 in this sample is therefore somewhat protected by the PPTA which can be an indication that the PA 6,6 is more or less randomly distributed in the PPTA. By plotting the

derivative of the weight loss as a function of temperature, as shown in Figure 2.5, the distinction between random-like and block-like behaviour can be visualized more clearly.

From this figure it can be seen that polymer **P10-4** only shows one distinct peak while the other polymer samples show two distinct peaks indicating separate degradation of PA and PPTA blocks.

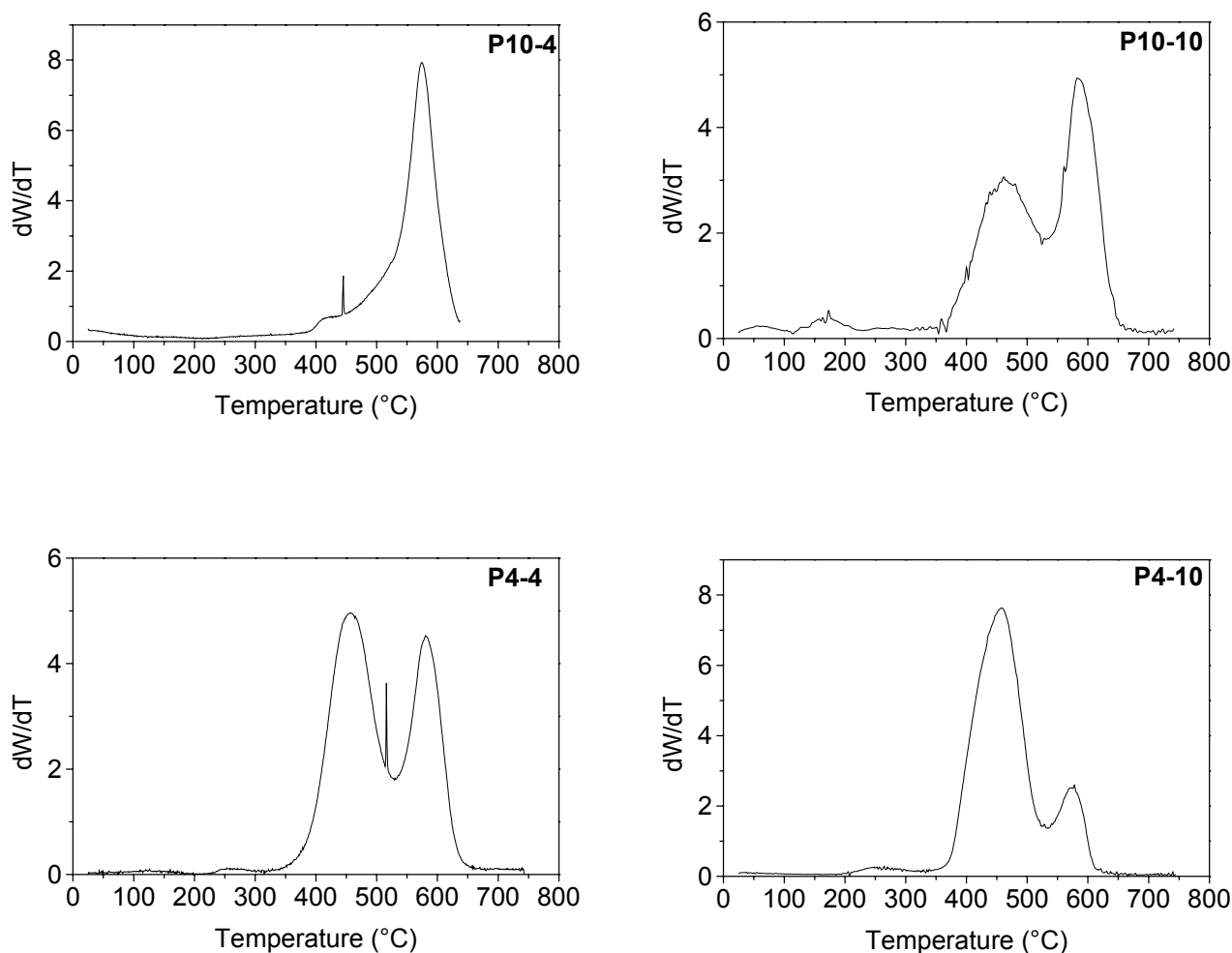


Figure 2.5: Derivative of the weight loss of the copolymers from Figure 2.4

2.4 Conclusions

Four rod-coil block copolymers that are composed of alternating flexible PA 6,6 and rigid PPTA blocks differing in block length have been synthesized by a low-temperature polycondensation method. Molecular weights of the copolymers are lower than for pure PPTA obtained by the same synthetic procedure. Nevertheless,

the molecular weights of copolymers with an aramid content of at least 50 mol% are sufficiently high for preparing films and fibers. By means of a combination of the characterization methods, notably Soxhlet extraction, NMR, and TGA as well as the observation that the intrinsic viscosity of the block copolymers increases substantially compared to the corresponding PPTA oligomers, it has been proven that block copolymers are obtained. Because the block copolymers have been synthesized via a condensation method, a broad distribution in molecular weight is obtained which is confirmed by SEC analysis. A semiempirical model is described that relates the intrinsic viscosity of a rod-coil multiblock copolymer to its molecular weight, which in combination with SEC analysis appears to give a good approximation of the molecular mass of this type of alternating aramid-amide block copolymers.

Concentrated solutions of this type of block copolymers are able to form a lyotropic liquid crystalline phase in sulfuric acid. The phase behaviour in sulfuric acid will be dealt with in the next chapter.

2.5 References

- (1) Semenov, A. N.; Vasilenko, S. V. *Sov. Phys. JETP* **1986**, *63*, 70-79.
- (2) Halperin, A. *Europhys. Lett.* **1989**, *10*, 549-553.
- (3) Williams, D. R. M.; Fredrickson, G. H. *Macromolecules* **1992**, *25*, 3561-3568.
- (4) Matsen, M. W.; Barrett, C. J. *J. Chem. Phys.* **1998**, *109*, 4108-4118.
- (5) Li, W.; Gersappe, D. *Macromolecules* **2001**, *34*, 6783-6789.
- (6) Perly, B.; Douy, A.; Gallot, B. *Makromol. Chem.* **1976**, *177*, 2569-2589.
- (7) Radzilowski, L. H.; Stupp, S. I. *Macromolecules* **1994**, *27*, 7747-7753.
- (8) Chen, J. T.; Thomas, E. L.; Ober, C. K.; Mao, G.-P. *Science* **1996**, *273*, 343-346.
- (9) Lee, M.; Cho, B.-K.; Kim, H.; Yoon, J.-Y.; Zin, W.-C. *J. Am. Chem. Soc.* **1998**, *120*, 9168-9179.
- (10) Fink, Y.; Urbas, A. M.; Bawendi, M. G.; Joannopoulos, J. D.; Thomas, E. L. *J. Lightwave Technol.* **1999**, *17*, 1963-1969.
- (11) Jenekhe, S. A.; Chen, X., L. *J. Phys. Chem. B* **2000**, *104*, 6332-6335.
- (12) de Boer, B.; Stalmach, U.; Melzer, C.; Hadziioannou, G. *Synth. Met.* **2001**, *121*, 1541-1542.
- (13) Pietkiewicz, D.; Roslaniec, Z. *Polimery* **2000**, *45*, 69-80.
- (14) Higashi, F.; Nakajima, K.; Watabiki, M.; Zhang, W. X. *J. Polym. Sci., Part A: Polym. Chem.* **1993**, *31*, 2929-2933.
- (15) Garcia, J. M.; De La Campa, J. G.; De Abajo, J. *J. Polym. Sci. Part A: Polym. Chem.* **1996**, *34*, 659-667.
- (16) Padmavathy, T.; Srinivasan, K. S. V. *J. Macromol. Sci., Part C: Polym. Rev.* **2003**, *43*, 45-83.
- (17) Takayanagi, M.; Ogata, T.; Morikawa, M.; Kai, T. *J. Macromol. Sci., Phys.* **1980**, *B17*, 591-615.
- (18) Hwang, W.-F.; Wiff, D. R.; Benner, C. L.; Helminiak, T. E. *J. Macromol. Sci., Phys.* **1983**, *B22*, 231-257.
- (19) Martin, R.; Götz, W.; Vollmert, B. *Angew. Makromol. Chem.* **1985**, *132*, 91-109.
- (20) Bair, T.; Morgan, P. *U.S. Pat. 3,817,941 (1974)*.
- (21) Krigbaum, W. R.; Preston, J.; Ciferri, A.; Zhang, S. F. *J. Polym. Sci., Part A: Polym. Chem.* **1987**, *25*, 653-667.
- (22) Krigbaum, W. R.; Shufan, Z.; Preston, J.; Ciferri, A.; Conio, G. *J. Polym. Sci., Part B: Polym. Phys.* **1987**, *25*, 1043-1055.

- (23) Jadhav, J. Y.; Krigbaum, W. R.; Ciferri, A.; Preston, J. J. *Polym. Sci., Part C: Polym. Lett.* **1988**, *27*, 59-63.
- (24) Yamazaki, N.; Matsumoto, M.; Higashi, F. *J. Polym. Sci., Part A: Polym. Chem.* **1975**, *13*, 1373-1380.
- (25) Helgee, B.; Flodin, P. *Polymer* **1992**, *33*, 3616-3620.
- (26) Mathias, L. J.; Moore, D. R.; Smith, C. A. *J. Polym. Sci., Part A: Pol. Chem.* **1987**, *25*, 2699-2709.
- (27) Marek Jr., M.; Stehlicek, J.; Doskocilova, D. *Eur. Pol. J.* **1995**, *31*, 363-368.
- (28) Wang, H.-H.; Lin, M.-F. *J. Appl. Pol. Sci.* **1998**, *68*, 1031-1043.
- (29) Wang, H.-H. *J. Appl. Pol. Sci.* **2001**, *80*, 2167-2175.
- (30) Kimbroug, R.; Gaines, T. **1966**, *211*, 146-147.
- (31) Vollbracht, L.; Veerman, T. *U.S. Pat. 4,308,374 (1981)*.
- (32) Hanford, W. E.; Sauer, J. C. In *Organic Reactions*, Wiley-Interscience: New York, 1946; Vol. 3, Chapter 3.
- (33) Hess, O. *Ber.* **1885**, *18*, 685.
- (34) Gabellini, A.; Novi, M.; Ciferri, A.; Dell'Erba, C. *Acta Polym.* **1999**, *50*, 127-134.
- (35) Tam-Chang, S.-W.; Seo, W.; Iverson, I. K. *J. Org. Chem.* **2004**, *69*, 2719-2726.
- (36) Schaeffgen, J. R.; Foldi, V. S.; Logullo, F. M.; Good, V. H.; Gulrich, L. W.; Killian, F. L. *Polym. Prepr.* **1976**, *17*, 69-74.
- (37) Stockmayer, W. H.; Moore Jr, L. D.; Fixman, M.; Epstein, B. N. *J. Polym. Sci.* **1955**, *16*, 517-530.
- (38) Cavalleri, P.; Chavan, N. N.; Ciferri, A.; Dell'Erba, C.; Novi, M.; Marurucci, G.; Renamayar, C. S. *Macromol. Chem. Phys.* **1997**, *198*, 797-808.
- (39) Burke, J. J.; Orofino, T. A. *J. Polym. Sci., Part A-2: Polym. Phys.* **1969**, *7*, 1-25.
- (40) Arpin, M.; Strazielle, C. *Polymer* **1977**, *18*, 591-598.

Chapter 3

Phase Behaviour in Sulfuric Acid

Abstract

In this chapter the results are presented of the phase behaviour in sulfuric acid of a series of rod-coil multiblock copolymers of which the synthesis was described in the previous chapter. Concentrated solutions of the copolymers in sulfuric acid show a liquid crystalline phase if the content of PPTA exceeds 50 mol%. A block copolymer with 30 mol% PPTA does show a distinct structure by OPM, however the birefringence of this structure is very low. The critical concentration for the transition from the isotropic to the liquid crystalline state increases with increasing amount of flexible PA 6,6 segments. Comparison of the phase behaviour of the copolymer with that of PPTA provides strong evidence that the coils in the copolymer are significantly stretched in the nematic solutions.

Based on:

Lyotropic Rod-Coil Poly(amide-block-aramid) Alternating Block Copolymers: Phase Behaviour and Structure, de Ruijter, C.; Jager, W.F.; Li J.; Picken S.J. Macromolecules **2006**, 39, 4411-4417

3.1 Introduction

In the previous chapter the synthesis of a series of rod-coil poly(amide-*b*-aramid) alternating multiblock copolymers using a low temperature polycondensation method was reported. From a combination of viscosimetry, TGA, ¹H-NMR and via an extraction procedure it was shown that block copolymers are obtained. In this chapter the phase behaviour of the block copolymers in 100 wt% sulfuric acid will be reported. It is commonly accepted that block copolymers comprised of alternating rigid and flexible segments are potentially able to form liquid crystalline (LC) phases, however, only a limited number of reports on liquid crystalline block copolyamides have appeared in the literature. Most reports on rod-coil block copolyamides deal with synthesis of the materials for the purpose of preparing molecular composites. So far, two articles dealing with the lyotropic behaviour of wholly aromatic block copolyamides have been published. Krigbaum *et al.*¹ reported on the phase behaviour of multiblock copolymers, composed of rigid poly(*p*-benzamide) (PBA) blocks and flexible blocks composed of either polyterephthalamide or *p*-aminobenzhydrazide (PABH-T) or poly(*m*-phenylene isophthalamide) (MDP-I), that were dissolved in *N,N*-dimethylacetamide (DMAc) containing 3 wt% LiCl. Later, Cavalleri *et al.*^{2,3} extended the work of Krigbaum and reported on the phase behaviour of diblock copolymers of PBA with either MDP-I² or poly(*m*-benzamide)³ as the flexible block in the same solvent system. Cavalleri synthesized diblock copolymers in order to more accurately compare the phase behaviour with the theoretical models of Matheson-Flory⁴ and Vasilenko.⁵ The authors observed that a block copolymer bearing a longer flexible block than allowed by the Matheson-Flory model was still able to form a LC phase. The authors attributed this to partial ordering of the flexible component by the self-consistent orientational field of the rigid component. In the Matheson-Flory model⁴ chain stretching is not taken into account, and as a consequence the flexible chains would only act as a diluent for the mesophase. The authors concluded that it would be better to compare the phase behaviour with the Vasilenko model because this model does account for conformational changes of the flexible component by the orientational field of the mesophase. In addition the authors observed an increased stability of the mesophase when a semiflexible chain was coupled to a rigid homopolymer, which means that the concentration range where the mesophase was present was

considerably increased. This was concluded from the observations that although the critical concentration for mesophase formation was slightly increased, the biphasic gap was strongly reduced and also the solubility of the copolymer was strongly enhanced compared to the rigid homopolymer. To relate the phase behaviour of the block copolymers to the model, the authors constructed phase diagrams as a function of concentration and composition at a fixed (ambient) temperature since both the Matheson-Flory and Vasilenko theories originate from athermal lattice models. In this chapter the phase behaviour is reported as a function of composition, concentration and temperature, which means that evaluation of the obtained results with athermal theories is not applicable. However, Yurasova and Semenov⁶ as well as Wang and Warner⁷ recently developed more sophisticated models based on a mean-field approach of the Maier-Saupe^{8,9} type that describes temperature dependent phase behaviour of block copolymers with rigid and flexible segments. In this chapter the results will be compared to a modified Maier-Saupe mean-field theory adapted by Picken,¹⁰ which also take temperature and concentration effects into account, in order to estimate the effective persistence length of the block copolymers in sulfuric acid.

3.2 Experimental

3.2.1 Materials

A series of four block copolymers composed of alternating blocks of PPTA and PA 6,6 were synthesized as described Chapter 2.2. The chemical structure of a repeat unit of the block copolymer is shown in Figure 2.1 and Table 3.1 summarizes some characteristics of the block copolymers.

Table 3.1: Inherent viscosities and composition of the studied copolymers

Polymer	η_{inh} (dl g ⁻¹)	M_w ^a	Amount of flexible (PA 6,6) block (mol%)	Number of repeat units ^b of PPTA m (-) ^c PA n (-) ^c	
P10-4	1.87	11000	29	10	4
P10-10	1.71	11600	50	10	10
P4-4	2.06	17200	50	4	4
P4-10	0.75	7200	71	4	10

^a Obtained by using SEC

^b Theoretical degree of polymerisation depends on stoichiometry

^c m and n refer to figure 2.1

3.2.2 Measurements

Nematic-isotropic transition (clearing) temperatures were determined as a function of polymer concentration in sulfuric acid by OPM (optical polarization microscopy). A Nikon Eclipse E600 Pol. polarizing microscope equipped with a Mettler-Toledo FP82HT hot-stage was used.

3.3 Results and Discussion

3.3.1 Phase Behaviour in Sulfuric Acid

The phase behaviour of the PPTA-PA 6,6 block copolymers in 100 wt% sulfuric acid as function of temperature was examined by OPM. Because of the high viscosity of the polymeric samples phase transitions are not instantaneous. In addition, because we are dealing with polymer solutions, there is a temperature range where the isotropic and nematic phases coexist (biphasic regime). OPM images of the nematic phase and the biphasic regime for copolymer **P10-4** are shown in Figure 3.1. The obtained phase diagrams are shown in Figure 3.2. The upper curve describes the transition from the biphasic (I + LC) to the isotropic (I) phase and the bottom curve describes the transition of the LC phase to the biphasic region. To construct a phase diagram five different polymer concentrations were measured at a heating rate of 4 °C/min. Each polymer concentration was measured at least five times. By taking the average of these measurements reasonably accurate and reproducible values of the transition temperatures were obtained. According to Figure 3.2, all copolymers show LC behaviour when dissolved in sulfuric acid although in sample **P4-10** only very weak birefringence was observed. The observed texture of this sample might indicate a phase-separated structure rather than a LC phase.

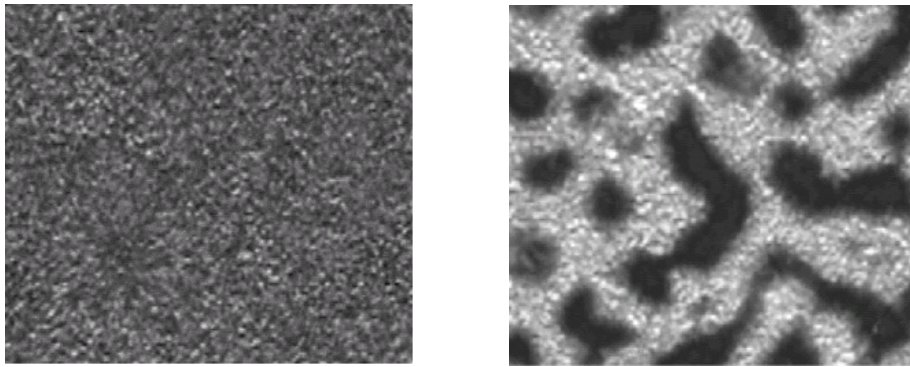


Figure 3.1: OPM images at 200 x magnification of the nematic phase (left) at 60°C and the biphasic regime (right) at 115 °C of a 15 wt% solution of copolymer sample **P10-4** in sulfuric acid

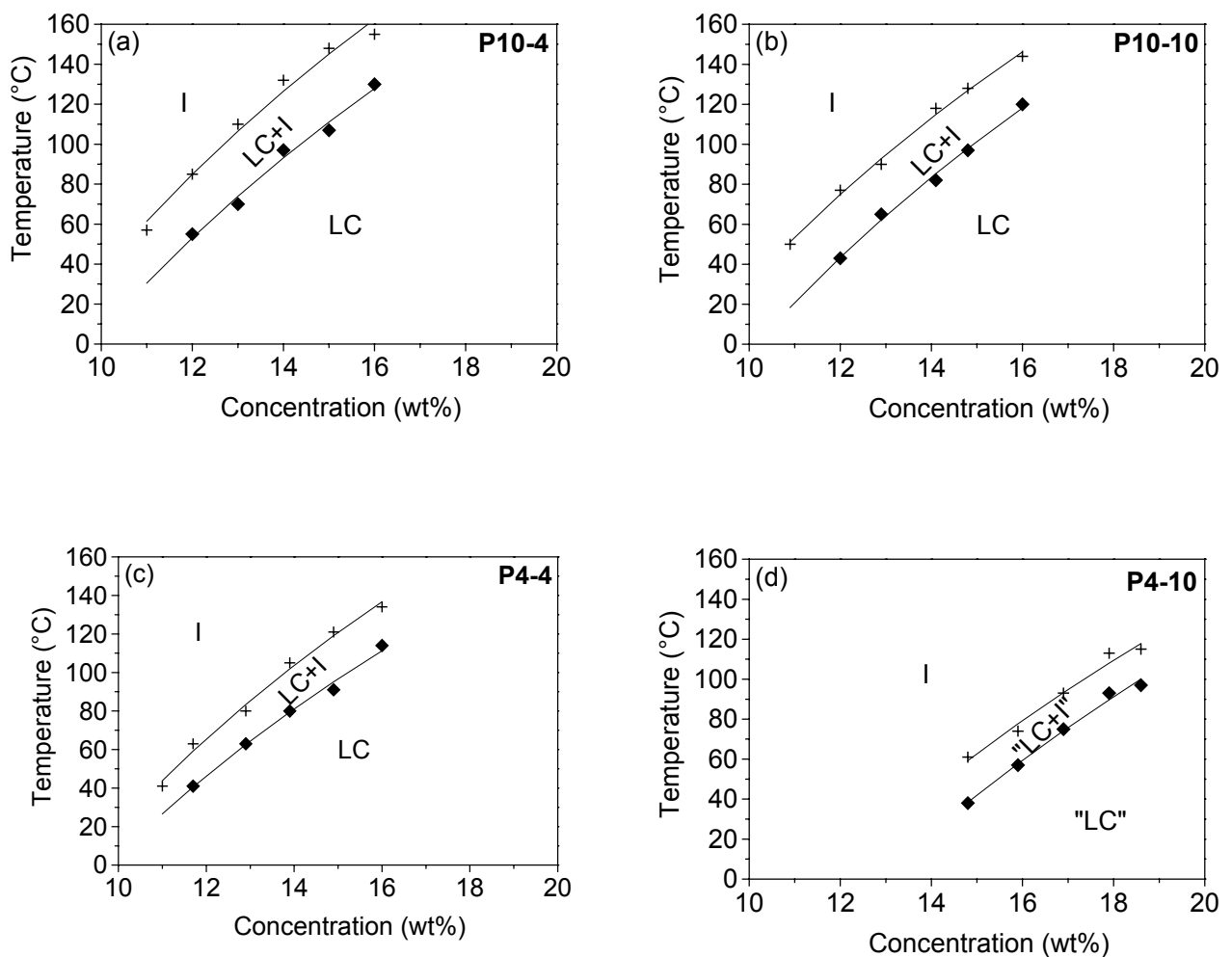


Figure 3.2: Phase behaviour of copolymer samples **P10-4** (a), **P10-10** (b), **P4-4** (c) and **P4-10** (d) in 100 wt% H₂SO₄. Sample **P4-10** shows hardly any birefringence by OPM.

To compare the phase behaviour of the polymer samples, Figure 3.3 shows the clearing temperature T_{ni} at which 50% phase transition is observed versus polymer concentration. In this figure the phase behaviour of the copolymer samples, a high molecular weight PPTA sample ($\eta_{inh}=4.2 \text{ dL g}^{-1}$, $M_w=32000$) and a low molecular weight PPTA-oligomer with a number of repeat units of $m = 4$ ($\eta_{inh}=0.42 \text{ dL g}^{-1}$), is shown. From Figure 3.3 it is clear that the critical concentration for the formation of a LC phase increases with increasing fraction of the flexible fragments in the block copolymer. Another striking observation that results from Figure 3.3 is that coupling of flexible chains to rod-like oligomers increases the stability of the LC phase, i.e., the LC phase of copolymer **P4-4** shows a greater thermal stability compared to the PPTA oligomer (**P4-0**), while the average lengths of the rigid units in the copolymer and the oligomer are the same. Another indication of the increased stability of the LC phase of the block copolymer can be seen when we compare the curves of sample **P4-4** and **P10-10** with the curve of pure PPTA. Pure PPTA shows a LC to I transition at ambient temperature at about 8 wt%. If the flexible segments in the copolymer only would act as a diluent the phase transition for samples **P4-4** and **P10-10** would be expected around 16 wt% since these copolymers contains about 50 mol% PPTA. However, the phase transition already occurs at about 11 wt%, indicating that the polyamide coils are significantly stretched and therefore actually contribute to the stability of the LC phase.

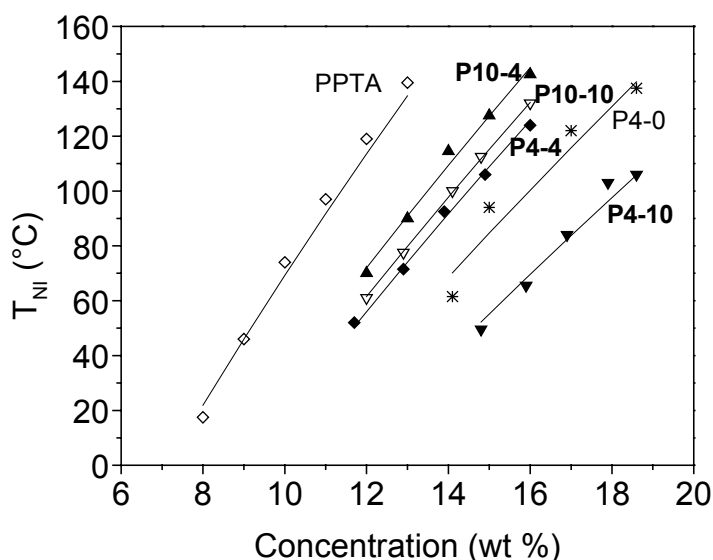


Figure 3.3: The clearing temperature T_{ni} at 50% phase separation as a function of polymer concentration in 100 wt% H_2SO_4 of copolymer samples **P10-4**, **P10-10**, **P4-4** and **P4-10**, PPTA ($M_w \sim 32000$) and a PPTA-oligomer with number of repeat units of m of 4. Data points were fitted with Eq. 3.7 with an α parameter of $2/3$: $T_{ni} = Ac^{2/3}$. A values of PPTA of 73.7, **P10-4** of 65.8, **P10-10** of 63.8, **P4-4** of 62.8, **P4-0** of 58.7 and **P4-10** of 53.9 were found

3.3.2 Comparison of the Phase Behaviour with an Extended Maier-Saupe (EMS) Theory

Next we will compare our results to a modified Maier-Saupe mean field theory developed by Picken.¹⁰ The original Maier-Saupe theory^{8,9} is developed for low molecular weight thermotropic liquid crystals and is based on a mean-field potential U that can be written as:

$$U = -\varepsilon \langle P_2 \rangle P_2(\cos \varphi) \quad [3.1]$$

and describes the influence of a nematic field on the orientation of one particle in that field. The strength of the potential is given by the parameter ε . $P_2(\cos \varphi) = \frac{1}{2}(3\cos^2 \varphi - 1)$ is the second order Legendre polynomial of $\cos(\varphi)$ and $\langle P_2 \rangle$ is the average value, weighted by the orientational distribution function, of the Legendre polynomial $P_2(\cos \varphi)$ and is usually called the order parameter. $\langle P_2 \rangle$ is 0 in the case of an isotropic phase and would be 1 in the case of perfect molecular alignment.

Solving the self-consistency equation

$$\langle P_2 \rangle = \frac{\int_{-1}^1 d(\cos \varphi) P_2(\cos \varphi) \exp\left(\frac{\varepsilon}{kT} \langle P_2 \rangle P_2(\cos \varphi)\right)}{\int_{-1}^1 d(\cos \varphi) \exp\left(\frac{\varepsilon}{kT} \langle P_2 \rangle P_2(\cos \varphi)\right)} \quad [3.2]$$

as well as requiring minimization of the free energy with respect to $\langle P_2 \rangle$ gives a phase transition at $kT/\varepsilon \approx 0.22$ from the nematic (N) to the isotropic (I) phase. The critical value of the order parameter $\langle P_2 \rangle$ at the phase transition is about 0.43. Picken¹⁰ adapted the original Maier-Saupe theory for application to lyotropic polymer liquid crystals. This model takes both the influence of the concentration of the polymer in a solvent and molecular flexibility of the polymer into account since LC polymers are not completely rigid. The molecular flexibility of a LC polymer is often described by the persistence length, which is a measure of the tendency of segments in a polymer chain to “remember” the orientation of adjoining segments in the chain.¹¹ The persistence length is a measure for the rigidity of a polymer in a specific solvent at

ambient temperature and can be obtained from light-scattering experiments. In the modified Maier-Saupe theory the “contour projection length” $L(T)$ was introduced, which like the persistence length is a measure of the rigidity of a polymer but is a function of both temperature and molecular weight as given by:

$$L(T) = L_p \frac{1 - \exp\left(-\frac{L_c T}{L_p T_p}\right)}{T/T_p} \quad [3.3]$$

where L_p is the persistence length at temperature T_p and L_c is the average contour length of a polymer chain. The limit of this equation for infinitely long polymer chains gives $L(T) \cong L_p T_p / T$ and for a very short molecule (compared to the persistence length) $L(T) \cong L_c$, i.e., the length of a rod. Next it is assumed that the strength of the potential can be given by:

$$\varepsilon = \varepsilon^* c^2 L^2(T) \quad [3.4]$$

where ε^* is a scaling constant and c the concentration. The dependence on the factor c^2 is based on the observation that dispersive van der Waals interactions scale as $1/r^6$, where r is the distance between molecules. This dependence is proportional to $1/V^2$ or c^2 , where V is the volume. The dependence on the factor L^2 originates from the Maier-Saupe potential which is an average over all two-particle interactions leading to an L^2 dependence. Substitution of Eq. 3.3 into Eq. 3.4 leads to:

$$\varepsilon = \varepsilon^* c^2 L_p^2 \left(\frac{1 - \exp\left[-\frac{L_c T}{L_p T_p}\right]}{T/T_p} \right)^2 \quad [3.5]$$

At the nematic-isotropic transition temperature T_{ni} it was already shown that $kT_{ni}/\varepsilon \approx 0.22$ holds; as a consequence, at T_{ni} , Eq. 3.5 can be written as:

$$\varepsilon^* c_{ni}^2 L^2(T_{ni}) = kT_{ni}/0.22 \quad [3.6]$$

Rearrangement of this equation provides a prediction of the clearing temperature on the concentration that can be approximated quite well by:

$$T_{ni} = Ac_{ni}^{\alpha} \quad [3.7]$$

where A and α are constants. For the infinite chain limit, i.e., $L_c \gg L_p$ it can be derived that $\alpha = 2/3$. This power-law behaviour of the T_{ni} as a function of the concentration is also clearly visible in the phase diagrams (Figures 3.2 and 3.3). Clearing temperature versus concentration behaviour of all polymer samples displayed in Figure 3.3 was fitted with Eq. 3.7 with a fixed parameter α of $2/3$. From Figure 3.3 it is clear that there is a remarkably good agreement of the clearing temperature versus the concentration with Eq. 3.7 with $\alpha = 2/3$.

Estimation of the Effective Persistence Length of the PPTA-*b*-PA 6,6 Block Copolymers with a the Extended Maier-Saupe Theory

At a fixed value of T_{ni} the terms on the right hand side of Eq. 3.6 are all constant and it can be simplified further to

$$c_{ni}L(T_{ni}) = const \quad [3.8]$$

This also means that the product $c_{ni}L$ at T_{ni} of PPTA is equal to $c_{ni}L$ at T_{ni} of the copolymer, or written slightly differently

$$\frac{c_{ni,PPTA}}{c_{ni,copolymer}} = \frac{L_{copolymer}(T_{ni})}{L_{PPTA}(T_{ni})} \quad [3.9]$$

If we can also neglect the influence of molecular weight on the flexibility, i.e., if the molecular weight of the copolymer is sufficiently high that its flexibility can be characterized by the persistence length, then Eq. 3.9 can be further simplified into

$$\frac{c_{ni,PPTA}}{c_{ni,copolymer}} = \frac{L_{p,copolymer}}{L_{p,PPTA}} \quad [3.10]$$

From light scattering experiments it is found that the persistence length of PPTA at ambient temperature is 29 ± 5 nm.¹² From Eq. 3.10 therefore the persistence length

of the block copolymer $L_{p,copolymer}$ can be estimated if we know the c_{ni} of PPTA and the copolymer at temperature T_{ni} , which can easily be determined from the phase diagrams. The results of the calculation of the persistence length for our copolymers are given in Table 3.2.

An alternative way to calculate the persistence length of the copolymer is by taking the weighted average of the persistence lengths of the individual polymers. As a result a series model is obtained

$$L_{p,copolymer} = \phi_{PPTA} L_{p,PPTA} + \phi_{PA6,6} L_{p,PA6,6} \quad [3.11]$$

where $L_{p,PA6,6}$ is the persistence length of PA 6,6, which is about 1.0 nm.^{13, 14} A series model is chosen because this should be considered as the upper bound of the copolymer persistence length in the absence of specific interactions of the LC phase on the flexible segment conformation. Values for the persistence lengths of our copolymer samples calculated from the series model are also shown in Table 3.2. From this table it is clear that the persistence lengths of the copolymers obtained from the extended Maier-Saupe theory with phase transition data obtained from the phase diagram are significantly higher than predicted by the series model which quantifies the statement that the polyamide coils in the copolymer are significantly stretched by the mesophase.

Table 3.2: Estimated persistence lengths of high M_W PPTA and the copolymers

Polymer	Critical concentration for (I-LC) phase transition at T=25°C (wt%)	L_p according to phase behaviour (via Eq. 3.10) (nm)	L_p according to series model (via Eq.3.11) (nm)
PPTA ($M_W \approx 32000$)	8.1	N.A.	29
P10-4	10.3	24.3	20.6
P10-10	10.3	23.7	15.0
P4-4	10.5	22.4	15.0
P4-10	13.8	18.1	9.4

3.4 Conclusions

In this chapter the phase behaviour of four rod-coil block copolymers differing in block length which are composed of alternating flexible PA 6,6 and rigid PPTA blocks

is described. Concentrated solutions of these copolymers in sulfuric acid are liquid crystalline if the aramid content in the copolymer is at least 50 mol%. The phase behaviour of these solutions demonstrates that the liquid crystallinity involves induced orientation of the flexible polyamide coils because liquid crystallinity of the block copolymer is found to occur at a lower PPTA concentration compared to a PPTA oligomer with the same block length. This means that the incorporation of aramid blocks in the copolymer induces stretching of the flexible coils, and this stretching will make the copolymer stiffer than expected initially. Complementary to the study on the LC behaviour of the copolymer samples reported here, films have been prepared of which the orientational order is determined by means of X-ray scattering. This will be reported in Chapter 5.

3.5 References

- (1) Krigbaum, W. R.; Shufan, Z.; Preston, J.; Ciferri, A.; Conio, G. *J. Polym. Sci., Part B: Polym. Phys.* **1987**, *25*, 1043-1055.
- (2) Cavalleri, P.; Ciferri, A.; Dell'Erba, C.; Novi, M.; Purevsuren, B. *Macromolecules* **1997**, *30*, 3513-3518.
- (3) Cavalleri, P.; Ciferri, A.; Dell'Erba, C.; Gabellini, A.; Novi, M. *Macromol. Chem. Phys.* **1998**, *199*, 2087-2094.
- (4) Matheson Jr., R. R.; Flory, P. J. *Macromolecules* **1981**, *14*, 954-960.
- (5) Vasilenko, S. V.; Khokhlov, A. R.; Shibaev, V. P. *Macromolecules* **1984**, *17*, 2270-2275.
- (6) Yurasova, T. A.; Semenov, A. N. *Molec. Cryst. Liq. Cryst* **1991**, *199*, 301.
- (7) Wang, X. J.; Warner, M. *Liq. Cryst.* **1992**, *12*, 385-401.
- (8) Maier, W.; Saupe, A. *Z. Naturforsch.* **1959**, *14A*, 882-889.
- (9) Maier, W.; Saupe, A. *Z. Naturforsch.* **1960**, *15A*, 287-292.
- (10) Picken, S. J. *Macromolecules* **1989**, *22*, 1766-1771.
- (11) Xu, Z. D.; Hadjichristidis, N.; Fetters, L. J.; Mays, J. W. *Adv. Polym Sci.* **1995**, *120*, 1-50.
- (12) Ying, Q. C.; Chu, B. *Makromol. Chem., Rapid Commun.* **1984**, *5*, 785-791.
- (13) Taylor, G. B. *J. Am. Chem Soc.* **1947**, *69*, 638-644.
- (14) Howard, G. J. *J. Polym. Sci.* **1959**, *37*, 310-313.

Chapter 4

Structural Study in the Solid State

Abstract

In this chapter a structural investigation in the solid state by DSC and SAXS of a series of rod-coil multiblock copolymers comprised of alternating PPTA and PA 6,6 blocks is presented. DSC experiments showed that the crystallization of the PA 6,6 is to a large extent suppressed by the presence of PPTA, but the degree of crystallization increases upon annealing. SAXS experiments revealed that, although some block copolymers show a broad peak in the SAXS diffraction patterns, there is no clear evidence for long-range lamellar order in any block copolymer because of the absence of higher order peaks.

Based on:

Lyotropic Rod-Coil Poly(amide-block-aramid) Alternating Block Copolymers: Phase Behaviour and Structure, de Ruijter, C.; Jager, W.F.; Li J.; Picken S.J. Macromolecules, 2006, 39, 4411-4417

4.1 Introduction

This chapter concerns the structural investigation of the block copolymers in the solid state. Structural investigation of LC rod-coil block copolyamides in the solid state is not common although it is commonly accepted that, due to incompatibility of the components, a block copolymer material will tend to phase separate and may possibly show long-range order if the polydispersity of the blocks is narrow. A rod-coil block copolymer will display even higher incompatibility because of the strong structural difference between the blocks that results in an increased tendency toward phase separation.¹ To our knowledge the only structural study of monodisperse rod-coil block multiblock copolymers has been done by Lee *et al.*² The authors synthesized a series of rod-coil copolymers of which the rigid rod segments were made up of three biphenyls connected through methylene ether linkages, and the flexible segments were made of poly(propylene oxide) with a degree of polymerization of 13. By using SAXS, the authors observed that the diblock copolymer displayed a lamellar structure and the multiblock copolymers with a number of repeating units of 3 and more displayed a hexagonal columnar phase. The authors also observed a rapid decrease of the long period of the observed structure with increasing number of repeating units.

In the present study the polydispersity index of the block copolyamides is rather high, and therefore the formation of well-defined long-range ordered structures is not anticipated. Small-angle X-ray scattering (SAXS) measurements and differential scanning calorimetry (DSC) have been performed in order to get better insight into the extent of phase separation in the copolymers and the melting and crystallization behaviour of the PA 6,6 blocks, respectively.

4.2 Experimental

4.2.1 Materials

A series of four block copolymers composed of alternating blocks of PPTA and PA 6,6 were synthesized as described Chapter 2.2. The chemical structure of a repeat unit of the block copolymer is shown in Figure 2.1 and Table 3.1 summarizes some characteristics of the block copolymers.

4.2.2 Measurements

Differential scanning calorimetric (DSC) measurements were performed with a Perkin-Elmer TAC 7/DX DSC. All samples were heated from 25 °C to 325 °C, next cooled to 25 °C, and heated again to 325 °C. The heating and cooling rates were 10 °C/min.

Small-angle X-ray scattering (SAXS) experiments were performed on finely powdered copolymer samples at the SAXS facility at the FOM Institute for Atomic and Molecular Physics (Amolf) in Amsterdam, The Netherlands. In this set-up a rotating anode X-ray generator generates a highly parallel beam of monochromatic CuK α radiation. A Linkam CSS450 shear cell was used as a sample stage. A brass sample holder with Kapton windows is used to replace the original glass windows. The SAXS patterns were recorded with a Bruker High-Star area detector. The two dimensional SAXS patterns were integrated azimuthally and corrected for the background to obtain one-dimensional plots of the intensity as a function of the scattering vector $q=4\pi\sin\theta/\lambda$, where λ is the X-ray wavelength (0.154 nm) and 2θ the scattering angle.

4.3 Results and Discussion

4.3.1 Effect of Copolymer Composition on Thermal Behaviour using DSC

DSC analysis of the block copolymer samples is shown in Figures 4.1 and 4.2. Figure 4.1 shows the DSC traces from the second heating scan of all copolymer samples. From this figure it is clear that crystallization of PA 6,6 is to a large extent hindered by the presence of PPTA. Only samples **P4-10** and **P10-10** show a melting peak for PA 6,6 but the melting points ($T_m = 217$ °C for **P4-10** and $T_m = 208$ °C for **P10-10**) are strongly reduced compared to the melting point of pure PA 6,6 ($T_m \approx 265$ °C). For copolymer samples with short polyamide chains (**P4-4** and **P10-4**) crystallization of the PA 6,6 is fully suppressed. Traditionally, melting point depression can be described by means of the Hoffmann-Weeks³ equation. The melting point of a semicrystalline polymer according to this equation is given by

$$T_m = T_m^\circ \left(1 - \frac{2\gamma_e}{\Delta H_f l_c} \right) \quad [4.1]$$

where T_m is the observed (typically 265 °C) and T_m° equilibrium melting point ($T_m^\circ = 300$ °C for PA 6,6⁴), γ_e the surface free energy, ΔH_f the heat of fusion, and l_c the lamellar crystal thickness. If PA 6,6 crystallites melt in a matrix that only contains PA 6,6, the surface free energy between matrix and crystallites is (much) smaller than if PA 6,6 crystallites melt in a matrix that also contains PPTA.

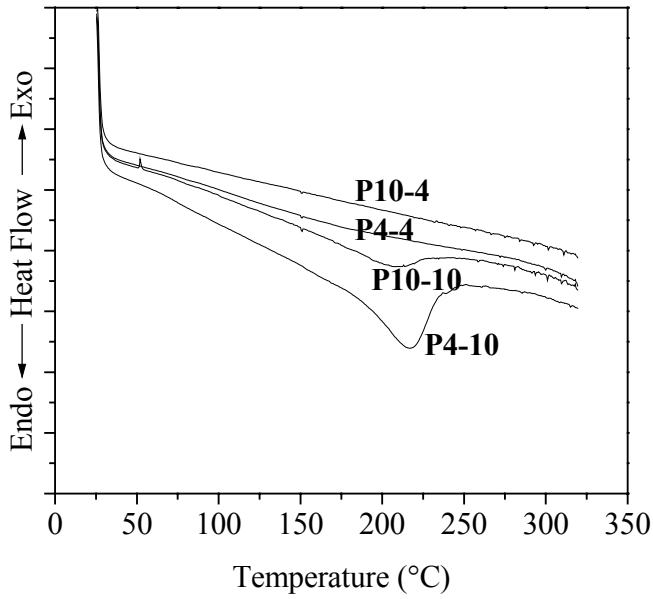


Figure 4.1: DSC plots of the copolymers

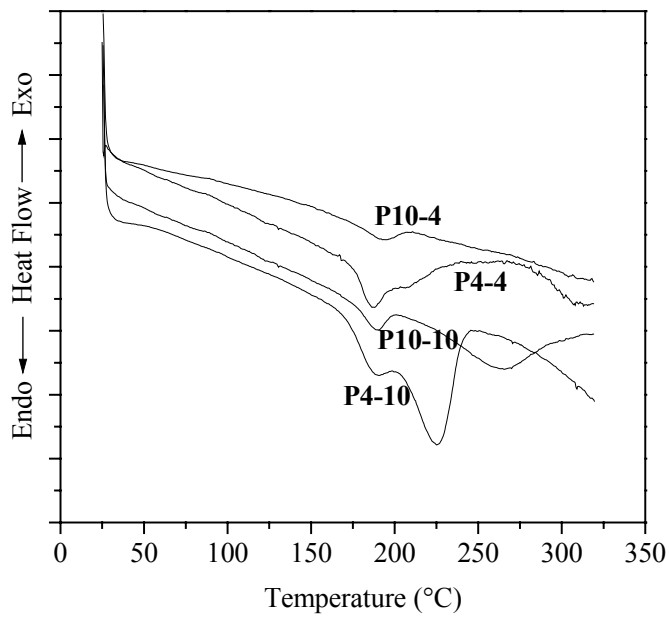


Figure 4.2: DSC plots of the annealed copolymers

Therefore, with increasing PPTA content in the copolymer the PA 6,6 melting point should reduce if the lamellar crystal thickness remains constant. From Figure 4.1 it is clear that the melting point of **P4-10** is higher than for **P10-10** whereas the polyamide block length remains constant. To investigate the melting of PA 6,6 by introducing PPTA in more detail, DSC analysis was performed on all copolymer samples after annealing overnight at a temperature of 160 °C. Figure 4.2 shows the curves of the first heating scan. It is clear that the annealing process induces crystallization since all copolymer samples show at least one melting peak. The overall degree of crystallinity increases with increasing the fraction of polyamide and with increasing the length of the polyamide blocks, as expected. The sequence of the degree of crystallinity is **P4-10 > P10-10 > P4-4 > P10-4**.

Remarkably all polymer samples show a melting peak around 190°C but for copolymer samples **P4-10**, **P10-10** and **P4-4** also a second melting peak is observed at 225 °C, 267 °C and 310 °C respectively. This shift to a higher melting point might be explained by a better-developed phase separation due to the annealing process, which induces higher orientation of the PA 6,6 coils. The improved orientation of the coils decreases the conformational entropy, and as a consequence the melting point increases since $T_m = \Delta H/\Delta S$.

It is expected that the glass transition temperature of the PA in the rod-coil copolymers considered here will progressively increase with increasing amount of PPTA because the mobility of the amorphous polyamide chains will be significantly constrained by the surrounding PPTA chains. However, with the DSC apparatus we have used no clear glass transition was observed in the DSC curves even for the sample with the highest the amount of PA (**P4-10**). DMA measurements on copolymer films have been performed in order to detect glass transitions of the PA 6,6 blocks. The results of the DMA measurements will be presented in Chapter 5.

4.3.2 Microstructure of PPTA-b-PA 6,6 Copolymers using SAXS

SAXS measurements were performed on copolymer samples **P10-4**, **P4-4**, and **P4-10**. For each samples two diffraction patterns were recorded, one at a temperature far below the melting point and one above the melting point of the PA blocks. The intensity of the small-angle scattering depends on the composition ratio and the difference of the electron densities of the rigid and flexible component ($\rho_R - \rho_F$)

$$I(q) \sim \phi_R \phi_F (\rho_R - \rho_F)^2 \quad [4.2]$$

where ϕ_R and ϕ_F are the volume fraction of rigid and flexible segments, respectively. The scattering intensity $I(q)$ was transformed from the partially oriented three-dimensional object to the one-dimensional intensity $I(q)_1$ by Lorentz correction according to:

$$I(q)_1 = c \cdot q^2 \cdot I(q) \quad [4.3]$$

where c is a constant. This correction was used since the original data did not show distinct maxima to calculate the block length. This correction compensates for the random orientations of periodic systems⁵ and results in the peaks being sharpened and moved to slightly higher q values, compared to the uncorrected SAXS curves. SAXS profiles of our block copolymer samples are shown in Figure 4.3. The block length was calculated from the maxima after Lorentz correction by means of Eq. 4.4. For each block copolymer sample first a measurement was made above the melting point of the polyamide blocks. Next, the sample was cooled and a second measurement was made at a temperature far below the melting point of the polyamide blocks.

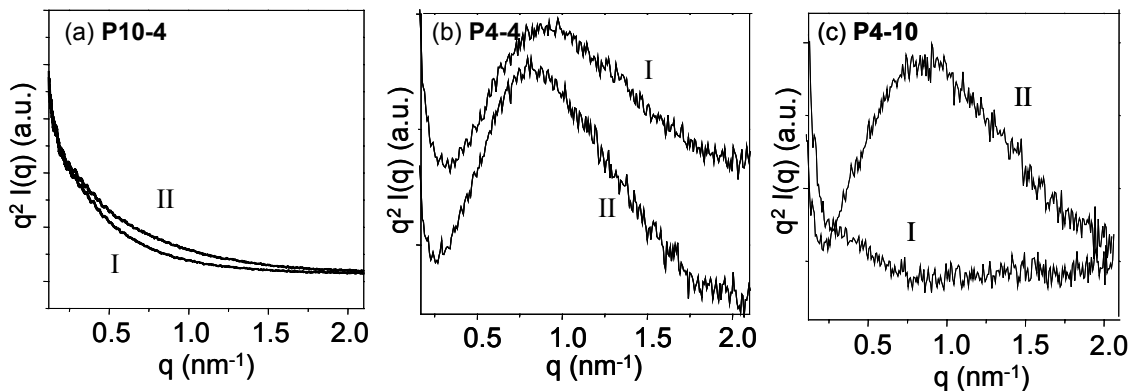


Figure 4.3: SAXS images of copolymer samples **P10-4** (a) measured at $T=25$ °C (I) and $T=220$ °C (II), **P4-4** (b) measured at $T=25$ °C (I) and $T=260$ °C (II) and **P4-10** (c) measured at $T=50$ °C (I) and $T=230$ °C (II)

Figure 4.3 reveals that all copolymers show different patterns. Sample **P10-4** shows no peak in SAXS. This can possibly be explained by assuming that the small PA blocks are more or less randomly distributed in the rigid polymer and therefore do not phase separate into an ordered structure. Sample **P4-4** is the only sample that shows

a peak in SAXS both above and below the melting point of PA. The observed peaks, however, are rather broad, and the spectrum shows no higher order peaks. This observation is typical for block copolymers obtained via a polycondensation method having a rather high polydispersity index. Sample **P4-10** only shows a peak in SAXS at high temperature. Since crystallization of the PA blocks in this polymer will increase its density, the density contrast between regions with rigid and flexible blocks will be reduced. The crystallization destroys the ordering and reduces density contrast, which leads to no scattering peaks at room temperature. After the melting of PA 6,6, the ordering is reconstructed, and a clear scattering peak appears in the small-angle x-ray scattering pattern. Since **P4-4** does not crystallize at room temperature as well as at high temperature, there is no destructive effect of the phase-separated layer structure from crystallization. The SAXS curve of sample **P4-4** measured above the melting point of PA 6,6, is sharper indicating a more developed phase separation compared to the curve measured at ambient temperature. Because the phase separation is better developed the polyamide coils are more stretched and the observed peak is shifted to a lower q value.

Estimation of the Block Period of the Block Copolymers using SAXS

The position of the scattering maxima, q_{\max} can be used to estimate L_{obs} , the average observed block period of the structure given by

$$L_{\text{obs}} = \frac{2\pi}{q_{\max}} \quad [4.4]$$

If we assume that the domains repeat one-dimensionally, we can calculate the block length as the sum of the domain lengths of a rigid block and a flexible block ($L_{\text{cal}} = L_{\text{R}} + L_{\text{F}}$). If, for the sake of simplicity, the effect of molecular weight distribution of both components is not taken into account the rigid-segment domain length L_{R} for a perfect rigid rod is the product of the monomer length a and the degree of polymerization DP_{R}

$$L_{\text{R}} = a \cdot DP_{\text{R}} \quad [4.5]$$

In the case of a perfect lamellar rearrangement in a rod-coil multiblock copolymer, the flexible coil segments will not be able to adopt a Gaussian conformation and as a

consequence would be significantly stretched. A schematic structure of such a lamellar phase of a rod-coil block multiblock copolymer is shown in Figure 4.4a.

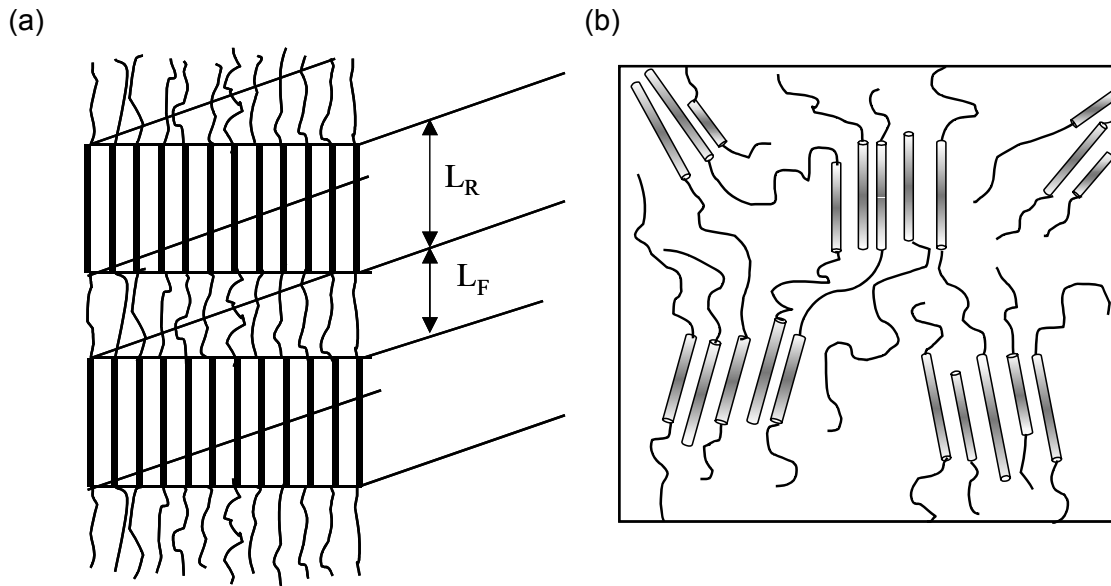


Figure 4.4: A schematic illustration of (a) a lamellar structure, (b) a broken lamellar structure of a multiblock rod-coil block copolymer. To make space for the coils to adopt a less stretched conformation the sheet-like rod domains break up.

The length of the flexible domain can be calculated if the mass of the rigid and flexible domains is known. The mass of a rigid domain M_R can be written as

$$M_R = L_R A \rho_R \quad [4.6]$$

where A is the interfacial area between a rigid and flexible domain and ρ_R the density of the rods. The mass of a rigid domain can also be given by

$$M_R = N m_R DP_R \quad [4.7]$$

where N is the number of rods and m_R the mass of a repeat unit of the rods. Similar equations can be written for a flexible coil domain

$$M_F = L_F A \rho_F = N m_F DP_F \quad [4.8]$$

where M_F is the mass of a flexible domain, ρ_F the density, m_F the mass of a repeat unit of the coils, and DP_F the degree of polymerization of the coils. The number of coils in a domain is the same as the number of rods N . The length of the flexible

domain L_F can be calculated by substitution of Eqs. 4.5, 4.6, and 4.7 into Eq. 4.8 and is given by

$$L_F = \frac{\rho_R}{\rho_F} \frac{m_F}{m_R} aDP_F \quad [4.9]$$

The densities of amorphous PA 6,6 and PPTA are respectively 1.14 g/cm³ and 1.44 g/cm³.

Results for the observed block period L_{obs} for our copolymers samples are given in Table 4.1, and are much smaller than the calculated values L_{cal} of a lamellar phase. An explanation for this large difference might be because a perfect lamellar arrangement in which the coils are significantly stretched is highly unfavorable in terms of entropy. This strong entropic penalty can be reduced if the sheet-like rod-domains break up into smaller domains. In this case the flexible coils are less confined because they can occupy space lateral to the rigid-segment domains, and as a result the observed block period is significantly decreased^{2,6,7}. A schematic structure of such a broken lamellar phase is shown in Figure 4.4b.

Assigning a structure simply by comparing the observed and the measured long order is for our copolymers not straightforward because the observed peaks in SAXS are rather broad and because of the high polydispersity index.

Table 4.1: SAXS results

Polymer	Temperature (°C)	L_{obs} (nm)	L_F (nm)	L_R (nm)	L_{cal} (nm)
P10-4	20	-	7.0	13.6	20.6
	220	-	7.0	13.6	20.6
P4-4	25	7.1	7.0	5.8	12.8
	230	7.7	7.0	5.8	12.8
P4-10	50	-	16.2	5.8	22.0
	230	7.7	16.2	5.8	22.0

4.4 Conclusions

SAXS and DSC measurements were undertaken to study solid-state properties of the prepared block copolymers. DSC measurements revealed that crystallization of the

PA blocks was to a large content suppressed by the presence of the aramid blocks. In addition, the melting point of the amide blocks is decreased strongly due to the presence of the aramid blocks. The SAXS curves obtained from polymer samples **P4-4** and **P4-10** showed a broad peak, indicating that the microphase separation was not very well developed compared to the ideal lamellar structure. This observation is also supported by the absence of higher order peaks. This also may be obscured due to the polydispersity of the block-lengths. Also the observed periodicity is significantly smaller than that expected for a perfect lamellar phase. Therefore, it is plausible to suppose a less well-developed broken lamellar or cylindrical phase where the block period is strongly reduced to diminish the unfavorable entropic penalty for chain stretching of the flexible coils.

4.5 References

- (1) Flory, P. J. *Macromolecules* **1978**, *11*, 1138-1141.
- (2) Lee, M.; Cho, B.-K.; Oh, N.-K.; Zin, W.-C. *Macromolecules* **2001**, *34*, 1987-1995.
- (3) Hoffman, J. D.; Weeks, J. J. *J. Res. Natl. Bur. Stand.* **1962**, *A66*, 13-28.
- (4) Magill, J. H.; Girolamo, M.; Keller, A. *Polymer* **1981**, *22*, 43-55.
- (5) Roe, R.-J. In *In Methods of X-ray and Neutron Scattering in Polymer Science*, Oxford University Press: New York, 2000.
- (6) Williams, D. R. M.; Fredrickson, G. H. *Macromolecules* **1992**, *25*, 3561-3568.
- (7) Sakurai, S.; Okamoto, Y.; Sakaue, H.; Nakamura, T.; Banda, L.; Nomura, S. *J. Polym. Sci., Part B: Polym. Phys.* **2000**, *38*, 1716-1728.

Chapter 5

Orientational Order and Mechanical Properties PPTA-*b*-PA 6,6 Block Copolymer Films

Abstract

In this chapter the mechanical properties and orientational order of a series of uniaxially oriented block copolymer films of alternating blocks of PPTA and PA 6,6 have been investigated. The prepared block copolymers differ in aramid content and average block length. The films were prepared by shearing polymer solutions (in sulfuric acid) followed by rapid coagulation of the solutions in water. From wide-angle X-ray scattering (WAXS) and optical polarisation microscopy (OPM) it was found that films with a mole fraction of PPTA of at least 0.5 showed a distinct anisotropy. Both increasing the aramid content as well as the average aramid block length at constant aramid fraction influences the observed orientation in the copolymer films. It was found that the mechanical properties of the anisotropic block copolymer films are similar to the properties of isotropic films, as determined with dynamical mechanical analyses (DMA) and from tensile tests. This was attributed to the relative low $\overline{\langle P_2 \rangle}$ parameter of the anisotropic films obtained by using WAXS. Copolymerisation of the PPTA blocks with the flexible polyamide blocks resulted in an increase of storage and Young's modulus, a decrease of the elongation at break while the tensile strength was unaffected compared to normal PA 6,6. Above the melting point of the PA 6,6 blocks all prepared copolymers exhibit a plateau where the storage modulus remains rather constant.

Based on:

Orientational Order and Mechanical Properties of Poly(amide-block-aramid) Alternating Block Copolymer Films and Fibers, de Ruijter, C.; Mendes, E.; Boerstael, H.; Picken, S.J. Polymer (Under Review)

5.1 Introduction

Block copolyamides that consist of alternating rigid and flexible blocks have received increasing attention recently. Takayanagi *et al.*¹ introduced the molecular composite concept to reinforce a conventional aliphatic polyamide with small amounts of a multiblock copolymer containing alternating aromatic and aliphatic polyamide blocks. The authors showed that the mechanical properties of flexible polyamide were improved more, if the polyamide was reinforced with the block copolymer instead of with the corresponding rigid homopolymer. Later Krigbaum *et al.*² synthesized fully aromatic block copolyamides from aramid blocks with different rigidity, and showed that these block copolymers were able to show a nematic phase in solution³. In our group, we have synthesized a series of liquid crystalline block copolymers comprised of alternating aramid and aliphatic polyamide blocks of which the synthesis was described in Chapter 2. OPM observations of concentrated solutions of these copolymers in sulfuric acid were described in Chapter 3 and indicated that they form a LC phase if the fraction of PPTA is at least 0.5. Besides the aramid content it was observed that the phase behaviour also depended on the average block length of the rigid aramid block as well as on temperature. From the phase diagrams (Figures 3.2 and 3.3) it was concluded that the mesophase induces significant stretching of the polyamide coils. Next it was observed that a block copolymer with a fraction of PPTA of 0.3 did show a distinct birefringent texture using OPM, the observed birefringence of the texture however was very small. To evaluate if such observed textures are indeed LC phases we will further analyse the solutions in this chapter. In this chapter therefore, the focus will be on the analyses of aligned polymer films, which were prepared by shearing the polymer solutions followed by rapid coagulation of the solutions in water. Films have been prepared from both isotropic and concentrated, possibly LC, solutions. The orientational order of these copolymer films was determined by means of wide-angle X-ray Scattering (WAXS) measurements and the effect of the orientation on the overall mechanical properties of the copolymer films is considered. The mechanical properties of the polymers were obtained by means of DMA measurements and tensile tests. Also the effect of aramid content and block length in the copolymer films in relation to the observed orientational order and the resulting mechanical properties will be discussed.

5.2 Experimental

5.2.1 Materials

The block copolymers were synthesized as described in Chapter 2.2. The chemical structure of a repeat unit of the block copolymer is shown in Figure 2.1 and Table 3.1 summarizes some characteristics of the block copolymers.

5.2.2 Film Preparation

The films were prepared by manually shearing a polymer solution in sulfuric acid of 50 °C between two microscope slides and immediately coagulating the aligned solution in water. In this way the obtained orientation is 'frozen-in' in the films. Films of PPTA and the copolymers were prepared from both isotropic (10 wt%) and birefringent (possibly) LC solutions (15 wt%). For copolymer sample **P4-10** a 17 wt% solution was used since these solutions at 50 °C are certainly isotropic up to 15 wt% according to the phase diagram shown in Figure 3.2d. For PA 6,6 only one reference solution was prepared because PA 6,6 exhibits no LC phase. The coagulated films were thoroughly washed with water, neutralized using a CaCO₃ solution, and once again washed with water. Subsequently the films were dried overnight in vacuum at 50 °C, and hot pressed for a few seconds at 250 °C. The films were kept dry in a vacuum oven at 110 °C for an extended period of time before DMA and WAXS measurements, and tensile tests were performed. The thickness of all films was about 100 μm. The applied shear rate (velocity/film thickness) was in the order of 100 s⁻¹. The applied shear strain is approximately 15 units of strain assuming that the distance in which the strain can build up in our sample geometry was about 1 cm. An OPM image of an aligned block copolymer film is shown in Figure 5.1, the arrow denotes the shearing direction.

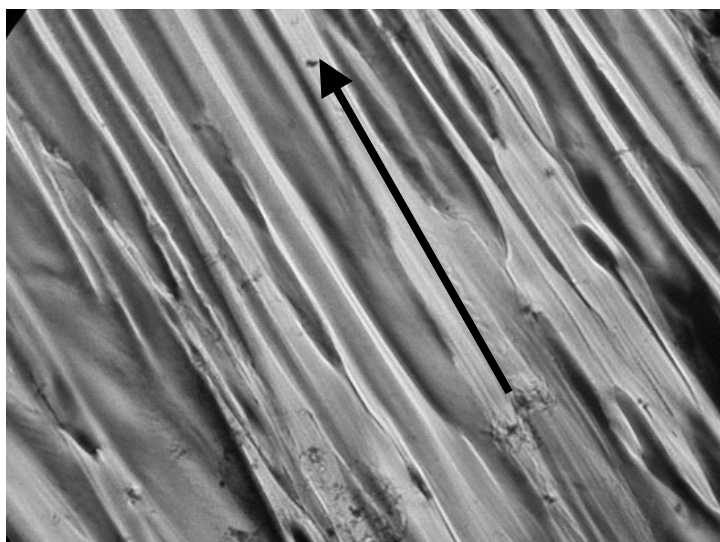


Figure 5.1: OPM image of an aligned block copolymer sample **P4-4**, prepared from a 15 wt% solution in sulfuric acid, the arrow reflects the direction of the shear flow.

5.2.3 Measurements

X-ray scattering experiments were performed on a Bruker-Nonius D8-Discover set-up with a 2D detector in order to estimate the orientational order of the polymer films. Monochromatic CuK_α radiation with a wavelength of 0.154 nm was used. The direction of the incident X-ray beam was normal to the film surface and the molecular orientation was parallel to the film surface. The detector-sample distance was set at 6 cm. The diffraction data was recorded using a 2 hour exposure time and corrected by subtraction of the background scattering.

DMA measurements were performed using a Perkin Elmer DMA 7a apparatus. The measurements were performed at a frequency of 1 Hz. The temperature of the measurements was raised at a constant rate of 5 °C/min, from 25 °C to 350 °C, which is well above the melting point of the polyamide blocks.

The samples were tested on a Zwick 1445 tensile tester with a 100 N force cell, equipped with a climate chamber. The films were tightened by hand between 2 grips with a rough surface to minimize slippage between the specimen and the grip. The test speed was 0.5 mm/min and the temperature was kept at 20 °C. For each type of film five samples were tested to determine the average values of the tensile properties.

5.3 Results and Discussion

5.3.1 WAXS Measurements

Observed Reflections

In Figure 5.2, the 2-D X-ray scattering patterns of the diffraction of PPTA, PA 6,6 and the block copolymer films prepared from the most concentrated solutions are displayed. Figure 5.3, shows the corresponding intensity curves as a function of the scattering angle 2θ .

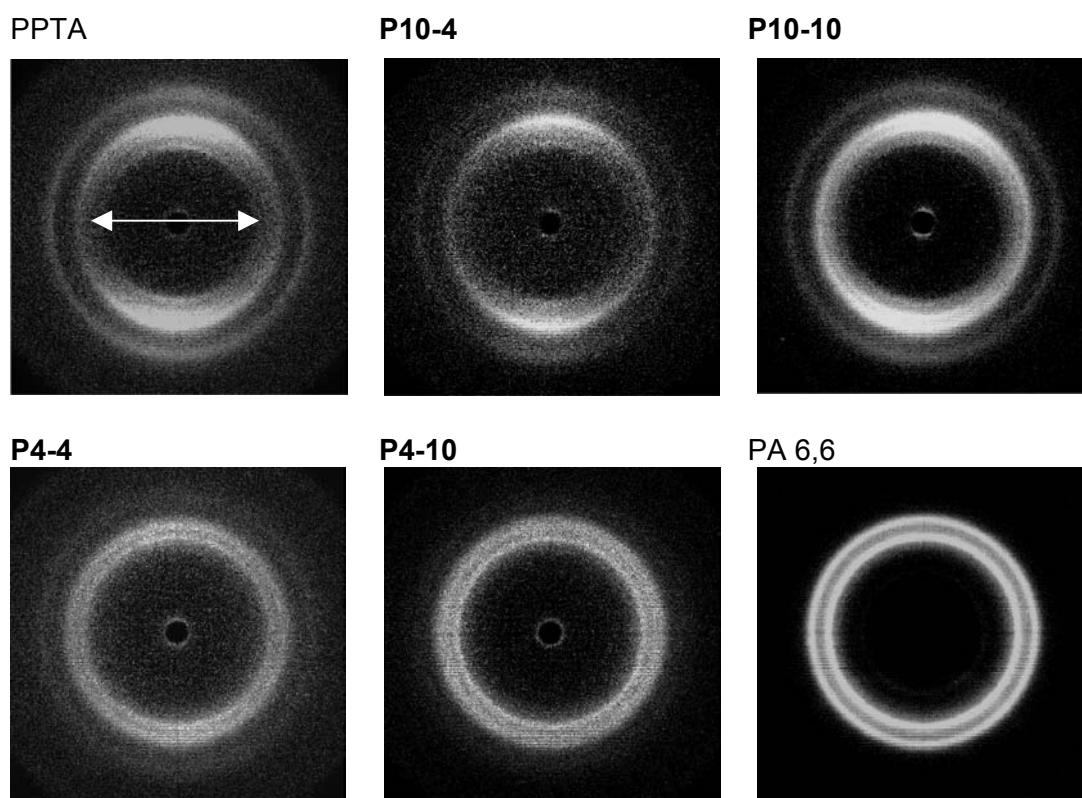


Figure 5.2: 2D X-ray scattering patterns of the diffraction of the aligned polymer films of PPTA, **P10-4**, **P10-10**, **P4-4**, **P4-10** and PA 6,6 (the arrow reflects the direction of the shear flow which is horizontal for all films)

From Figures 5.2 and 5.3, it is clear that all polymers show rather sharp reflections indicating a regular packing of the molecules. The peaks obtained from isotropic solutions are relatively less intense and slightly broader indicating less ordered structures. The degree of alignment of the polymer films can be obtained from an azimuthal scan over the obtained reflections and this will be treated in more detail in the next section. It is, however, clear from Figure 5.2 that the anisotropy of the peaks

decreases with decreasing aramid content, and is absent for copolymer sample **P4-10** and for pure PA 6,6. Also the films obtained from isotropic solutions did not show any orientation. The diffraction patterns of these polymers exhibit rings which are uniform in intensity indicating no significant anisotropy.

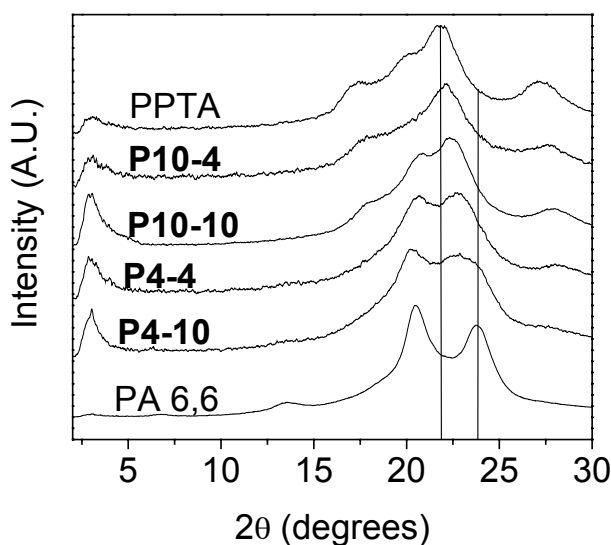


Figure 5.3: Radial scattering intensity distribution of the aligned polymer films of PPTA, **P10-4**, **P10-10**, **P4-4**, **P4-10** and PA 6,6

At small scattering angles, close to the beam stop, reflections of moderate intensity are observed which can be attributed to the presence of phase-separated structures. These reflections are observed for all copolymer samples but are much more pronounced for **P4-10**, **P10-10**, and **P4-4** than for **P10-4** and the homopolymers. These results are in accordance with our observations obtained from SAXS measurements⁴. We observed a reflection in the SAXS data for samples **P4-4** and **P4-10** (copolymer **P10-10** was not measured) and an absence of a reflection for sample **P10-4**. We explained the absence of a reflection of copolymer **P10-4** by assuming that the minor PA part is more or less randomly distributed in the rigid polymer and, therefore, does not have the freedom to phase separate into an ordered structure. Because all the observed peaks in SAXS were very broad, it is assumed that the phase separation is not very well developed compared to the perfect lamellar phase. The present WAXS data suggest that the microphase separation is more developed for copolymers with longer blocks, as the relative intensity of the reflection near the beam stop of **P10-10** is higher than for **P4-4**.

The diffraction pattern of the PPTA film displayed in Figure 5.2, corresponds to a polymorphic crystal structure, i.e., the pattern shows the characteristics of both the Northolt⁵ and the Haraguchi⁶ crystal structure. Characteristic of both structures are the strong reflections observed at a diffraction angle 2θ of 22.04° and 27.78° for the (200) and (211) planes respectively. The main difference between the diffraction patterns of the two structures is the presence of a strong (110) reflection at a 2θ of 20.73° for the Northolt structure⁵ and the presence of a (010) reflection of moderate intensity at a 2θ of 17.46° for the Haraguchi structure⁶. In Figure 5.4 the c-axis projections of the crystal structures of the Northolt and the Haraguchi crystal are shown. The Northolt crystal structure has a monoclinic unit cell with pseudo-orthorhombic symmetry and two chains per cell. ($a=0.787$, $b=0.518$, $c=1.29$ (repeat distance)) Along the direction of the b-axis the chains are laterally bonded by hydrogen bonds (broken lines in Fig. 5.4). The Haraguchi crystal has almost the same unit cell dimensions ($a=0.80$, $b=0.51$, $c=1.29$) but the hydrogen-bonded plane through the center of the unit cell is shifted along the b-axis over a distance $b/2$.

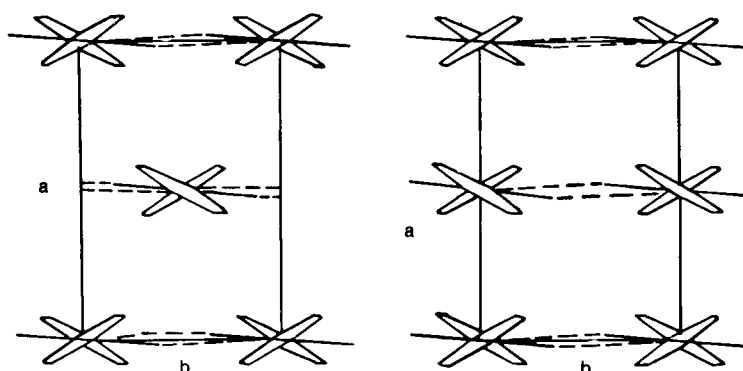


Figure 5.4: Crystal structures for PPTA: Northolt structure (left), Haraguchi structure (right)

The Haraguchi crystal structure is a transient crystal structure which is observed for PPTA fibers which are prepared from an isotropic or an anisotropic solution of low polymer concentration.⁷ Fibers prepared from solutions of intermediate concentrations exhibit both Northolt and Haraguchi crystal forms. Upon annealing, the Haraguchi structure transforms into the Northolt structure. This process reveals itself by a gradual increase of the (110) reflection with increasing annealing temperature. Since reflections of both structures are observed in the scattering pattern of the PPTA film the resulting structure is a polymorphic structure. The observed pattern of PA 6,6 shows sharp Debye rings for 2θ values of 13.55° (weak),

20.45° (very strong) and 23.75° (strong) corresponding to the (002), (100), and (010) planes of the triclinic α structure proposed by Bunn and Garner⁸. If we compare the diffractograms of the block copolymers with the pure components it is striking that the intensity profile of block copolymers **P10-4** and **P10-10** resemble to great extent to the profile of PPTA. The sharpest reflection of all these polymers is the (200) reflection. Because of the partial overlap of the (200) PPTA and the PA 6,6 (010) reflections a gradual shift of this maximum is observed in $2\theta = 22-23^\circ$ range as is clear from the vertical lines drawn in Figure 5.3. Because the hydrogen bonding sheets in the PPTA are forming the (200) lattice planes and the H-bonded sheets in PA 6,6 forming the (010) planes, this shift might be attributed to cross-hydrogen bonding between PPTA and PA 6,6. Another observation is that the intensity of the (211) PPTA reflection indeed decreases with increasing PA 6,6 content and remains constant with respect to the scattering angle. The most intense PA 6,6 reflection, the (100) reflection, becomes visible if the PA 6,6 fraction in the copolymer is at least 0.5. For copolymer **P4-10** this is the most intense observed reflection.

Determination of the Orientational Order using WAXS

The experimental order parameter S_{exp} of a material can be estimated from an azimuthal integration over a single reflection in the scattering pattern. The experimental order parameter can be defined as a product of three contributions⁹

$$S_{\text{exp}} = K \langle P_2 \rangle \overline{P_2} \quad [5.1]$$

where $\langle P_2 \rangle$ is the local molecular order parameter, $\overline{P_2}$ is the macroscopic director order parameter and K is a parameter that describes azimuthal broadening of meridional reflections due to translational disorder. Since we are dealing with only equatorial reflections the K factor is absent and Eq. 5.1 can be simplified to:

$$S_{\text{exp}} = \langle P_2 \rangle \overline{P_2} = \overline{\langle P_2 \rangle} \quad [5.2]$$

For pure PPTA fibers the orientational order is normally determined from the azimuthal profile of the (200) equatorial reflection.^{10,11} The $\overline{\langle P_2 \rangle}$ order parameters of the polymer films considered here are also estimated from an azimuthal integration along the equatorial (200) reflection, which is the pattern with the highest peak intensity for the polymers PPTA, **P10-4**, **P10-10** and **P4-4** and is observed in the $2\theta =$

22-23° range. The intensity profiles an azimuthal peak can be fitted to a Maier-Saupe distribution function¹² with a free baseline I_0 and position of the maximum φ_0 :

$$I = I_0 + A e^{\alpha \cos^2(\varphi - \varphi_0)} \quad [5.3]$$

where φ is the azimuthal angle and α is a parameter which determines the width of the distribution. From the α parameter the average orientational order parameter $\overline{\langle P_2 \rangle}$ is determined using

$$\overline{\langle P_2 \rangle} = \frac{\int_{-1}^1 P_2(\cos \varphi) e^{\alpha \cos^2 \varphi} d \cos \varphi}{\int_{-1}^1 e^{\alpha \cos^2 \varphi} d \cos \varphi} \quad [5.4]$$

where $P_2(\cos \varphi)$ is de second order Legendre polynomial of $\cos(\varphi)$:

$$P_2(\cos \varphi) = \frac{1}{2} (3 \cos^2 \varphi - 1) \quad [5.5]$$

Eq. 5.4 is solved by a numerical integration. The obtained order parameters for all films are listed in Table 5.1. Films prepared from concentrated (15 wt%) solutions of PPTA, **P10-4**, **P10-10** and **P4-4** in sulfuric acid all displayed an anisotropic scattering pattern. In Figure 5.5, the azimuthal scans of these polymers are shown which all are corrected for the baseline. For all the other films, no significant anisotropy was observed from the azimuthal scans. This suggests that the corresponding precursor polymer solutions were not in a liquid crystal phase. Also, a concentrated (17 wt% in sulfuric acid) solution of sample **P4-10** which exhibited a slightly birefringent texture by OPM does not seem to be in a LC phase because of the absence of an anisotropic azimuthal peak in the corresponding film. Therefore, the observed texture in this polymer might be related to microphase separation. From Figure 5.5, it is clear that the sequence of the $\overline{\langle P_2 \rangle}$ values is PPTA > **P10-4** > **P10-10** > **P4-4** > **P4-10**. The orientational order is found to increase if the aramid content in the polymer increases,

as anticipated. Also increasing the aramid block length increases the order parameter. This is clear from comparing samples **P10-10** and **P4-4**; the aramid content in the copolymers is the same but the $\overline{\langle P_2 \rangle}$ parameter of **P10-10** is distinctly higher. Although the copolymers with an aramid content of at least 50 mol% exhibit orientational ordering the value of the $\overline{\langle P_2 \rangle}$ parameter is rather small. This relative low orientational order could be explained due to a significant degree of recoiling during the coagulation process. Since the films are rather thick and the coagulation rates are quite low this may cause inhomogeneous orientation in the film, i.e., only the polymer at the surface of the film is well aligned, in the remaining bulk the orientation is distinctively lower.

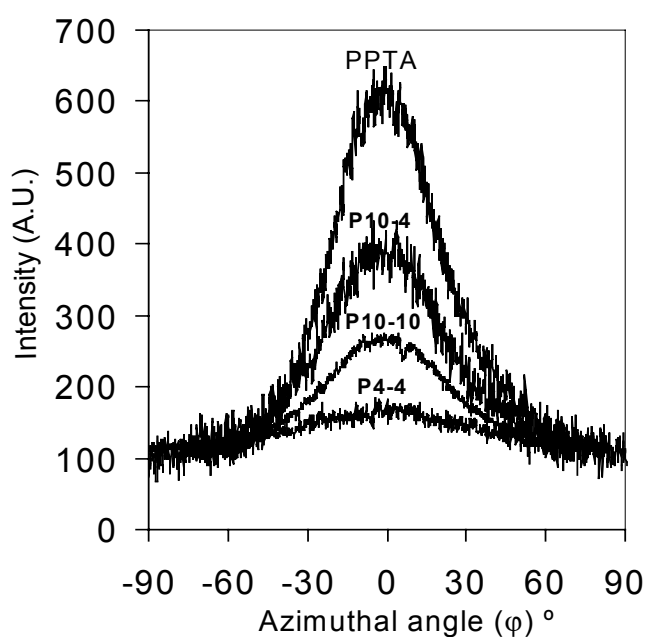


Figure 5.5: Azimuthal profiles of PPTA and copolymer samples **P10-4**, **P10-10** and **P4-4**

Table 5.1: $\overline{\langle P_2 \rangle}$ values of the polymer films determined by using WAXS

Polymer	Concentration in sulphuric acid (wt%)	$\overline{\langle P_2 \rangle}$ (-)
PPTA	5	0
	15	0.51
P10-4	10	0
	15	0.47
P10-10	10	0
	15	0.36
P4-4	10	0
	15	0.16
P4-10	10	0
	17	0
PA 6,6	20	0

5.3.2 Mechanical Properties

Mechanical properties of the copolymer films were obtained by performing tensile tests and by Dynamical Mechanical Analysis (DMA). Figure 5.6 displays the storage modulus and Figure 5.7 the loss modulus of the polymer films as a function of temperature. Figure 5.8 displays the stress-strain curves of the polymer films as determined by tensile tests. The shown curves are all measured on the samples obtained from the most concentrated solutions. For these films we have shown using WAXS that PPTA, **P10-4**, **P10-10** and **P4-4** exhibit anisotropic behaviour, while the **P4-10** and PA 6,6 films were isotropic. DMA curves obtained from the less concentrated (isotropic) solutions have also been measured but the differences in mechanical properties between the anisotropic and isotropic films turned out to be small. An explanation for this is that the orientational order of the anisotropic films is not yet high enough for the mechanical properties to benefit from the alignment. Table 5.2 gives a schematic overview of the mechanical properties obtained by both methods (DMA and tensile tests). The storage modulus is reported both at ambient temperature as well as at 300 °C. Above 300 °C, the modulus for the copolymer films remains more or less constant. Also, the Young's moduli, tensile strength and

elongation at break are given in this table. As mentioned before the polymer concentration in sulfuric acid did not play a significant role for the mechanical properties according to DMA. Therefore the tensile tests were performed only for the films prepared from the highest concentrations (see Table 5.2).

Determination of Temperature Dependent Mechanical Properties using DMA

Results of the DMA measurements are shown in Figures 5.6 and 5.7. The storage modulus of the polymers increases with increasing aramid content and decreases with increasing temperature, as anticipated. The largest drop in the modulus of the copolymers **P10-10**, **P4-4** and **P4-10** is between 120 and 150 °C, which is considerably higher than the glass transition temperature of PA 6,6. At high temperatures (above ~280 °C) the modulus of all prepared copolymers show a plateau value. This indicates the presence of a rubbery plateau above the melting point of the soft segments. This is a common feature for segmented block copolymers and therefore is a clear indication that a phase-separated block copolymer structure is formed. As a result, the structure of the copolymers can be envisaged as a physical network where the rigid blocks act as cross-linked zones for the flexible blocks. Such a structure can be represented as the broken lamellar structure shown in Figure 4.4b.

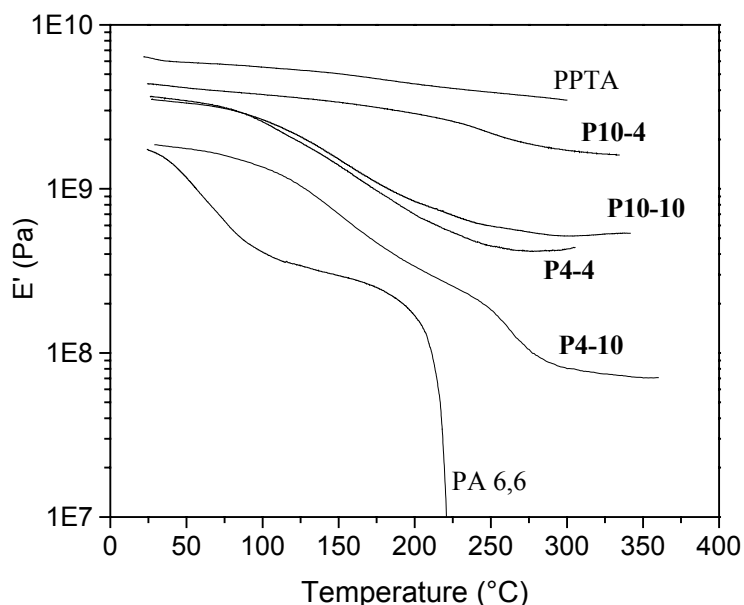


Figure 5.6: Storage modulus of PPTA, **P10-4**, **P10-10**, **P4-4**, **P4-10** and PA 6,6

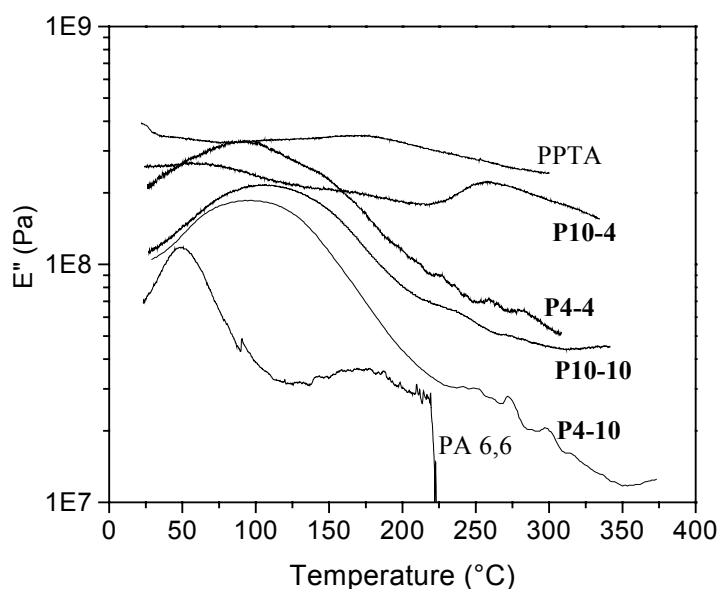


Figure 5.7: Loss modulus of PPTA, **P10-4**, **P10-10**, **P4-4**, **P4-10** and PA 6,6

Even copolymer sample **P4-10**, containing only about 30 mol% aramid, exhibits a plateau value above the melting point of the PA blocks of approximately 0.07 GPa. Since no sign of melting of the PPTA blocks is observed up to the degradation temperature of PA 6,6, which is around 400 °C, it is clear that none of the synthesized copolymers are expected to be melt-processable. On the other hand, since the mechanical properties of the block copolymers remain intact up to at least 400°C high temperature applications of this material may be considered.

Figure 5.7 displays the loss modulus versus temperature of the polymer films. The PA 6,6 sample exhibit a distinct peak at about 52 °C indicating the location of the glass transition temperature. The glass transition temperature for dry PA 6,6 reported in literature is 66 °C¹³. Also copolymer samples **P4-10**, **P4-4** and **P10-10** exhibit a peak corresponding to the T_g of PA 6,6 although the peak is much broader and is shifted to a higher temperature, around 120 °C. This shift towards a higher temperature can be explained by the reduced segmental mobility of the polyamide, which is constrained due to the presence of the rigid aramid blocks. Another observation that can be made from Figure 5.7 is that copolymer **P10-4** exhibits a peak in the loss modulus around the melting temperature of the PA 6,6 blocks.

Determination of Tensile Properties

Tensile properties of the prepared polymer films are listed in Table 5.2, the accompanying stress-strain curves of characteristic specimens are shown in Figure 5.8

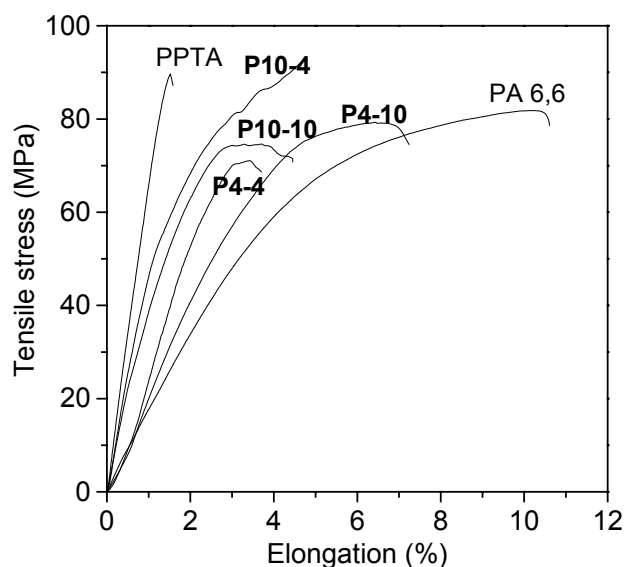


Figure 5.8: Stress-strain curves of PPTA, **P10-4**, **P10-10**, **P4-4**, **P4-10** and PA 6,6

Table 5.2: Mechanical properties of the polymer films obtained by DMA and tensile tests

Polymer	Concentration in sulphuric acid (wt%)	E' (GPa) ^a (30°C)	E'(GPa) ^a (300°C)	E (GPa) ^b (20°C)	σ (Mpa) ^c (20°C)	ϵ (%) ^d (20°C)
PPTA	15	6.2	3.5	7.1	90	1.5
	5	4.1	1.9			
P10-4	15	4.3	1.7	5.6	83	3.6
	10	3.9	1.3			
P10-10	15	2.8	0.8	4.5	75	4.4
	10	3.5	0.5			
P4-4	15	3.6	0.4	3.7	71	3.7
	10	3.1	0.3			
P4-10	17	1.8	0.08	2.7	79	7.1
	10	1.8	0.07			
PA6,6	20	1.7	0	2.0	81	10.6

^a Storage modulus

^b Young's modulus

^c Tensile strength

^d Elongation at break

From Table 5.2 it is clear that with increasing aramid content in the copolymer, the initial Young's modulus gradually increases and the elongation at break gradually decreases. The tensile strength of the polymer seems largely unaffected by the incorporation of aramids. Both the measured modulus of the PPTA and PA 6,6 films are almost a factor 2 lower than that of available commercial films.¹⁴⁻¹⁶ It should be noted that the commercial PPTA films are 2D-isotropic. Uniaxially oriented PPTA films are not commercially available since properties in transversal direction of unidirectional oriented films are rather poor. Flood *et al.*¹⁷, however, prepared both uniaxially oriented and 2D-isotropic PPTA films and measured mechanical properties that are comparable to our results, that is, 8.3 GPa for uniaxially oriented films. The modulus of the biaxially oriented films, however, was 2.3 GPa. This indicates that the ultimate mechanical properties very much depend on the preparation method. Table 5.3 compares the results from tensile experiments performed on PPTA and PA 6,6 in this study with the results obtained from other groups.

Table 5.3: Comparison of tensile properties of the PPTA and PA 6,6 films with results from other groups

Polymer	Orientation	E (GPa) ^a	σ (Mpa) ^b	ϵ (%) ^c
PPTA (this work)	Uniaxial	7.1	90	1.5
PPTA (commercial) ¹⁵	2D-isotropic	12	450	25
PPTA (Flood <i>et al.</i>) ¹⁷	Uniaxial	8.3	290	Not reported
PPTA (Flood <i>et al.</i>) ¹⁷	2D-isotropic	2.3	96	Not reported
PA 6,6 (this work)	Isotropic	2.0	81	10.6
PA 6,6 (commercial) ¹⁴	Isotropic	3.2	83	60

^a Young's modulus

^b Tensile strength

^c Elongation at break

Besides the preparation method, also other factors like test conditions (temperature, humidity and test speed) may influence the ultimate mechanical properties. In the particular for the case of aramid polymers, the mechanical properties of fibers can be improved drastically upon heat treatment. With our simple preparation method the samples are obviously not perfectly homogeneous and may suffer from voids and other structural imperfections. Nevertheless even using this simple preparation method the properties are quite promising. However to obtain better mechanical

properties a higher orientational order in the polymer is needed. It is generally accepted that the modulus of a polymer can increase rapidly with increasing orientational order although there is a threshold value up to which the effect of the $\langle \overline{P_2} \rangle$ parameter on the modulus is small. A useful equation that describes the relation between the modulus of a fiber as a function of orientational order parameter is given by¹⁸

$$\frac{1}{E} = \frac{1}{e_c} + \frac{1 - \langle \overline{P_2} \rangle}{3g} \quad [5.7]$$

where E is the fiber modulus, e_c is the chain modulus (about 240 GPa for PPTA) and g is the shear modulus (about 2 GPa for PPTA). Analysis of this relation shows that the modulus of PPTA fibers increases only slightly with an increasing value of the $\langle \overline{P_2} \rangle$ parameter up to about 0.8, but rapidly increases for $\langle \overline{P_2} \rangle$ values above 0.9. To aim for such values of $\langle \overline{P_2} \rangle$ for our material, fibers have been prepared via a dry-jet wet spinning procedure. Results of the fiber spinning will be presented in the next chapter.

5.4 Conclusions

Uniaxially oriented films have been prepared from a series of four rod-coil block copolyamides comprised of alternating blocks of PPTA and PA 6,6. WAXS measurements made clear that copolymer films with a fraction of rigid aramids of at least 0.5 exhibit anisotropic behaviour if the concentration of the precursor solutions was at least 15 wt% in sulfuric acid. The mechanical properties of the sheared anisotropic films are not superior to the properties of isotropic films. The reason for this is that orientational order of these films is not yet high enough for the mechanical properties to benefit from the LC behaviour.

According to the tensile tests, the Young's modulus of the copolymers increases gradually and the elongation at break decreases with increasing aramid content whereas the tensile strength remains more or less unaltered. From DMA it was clear that the thermostability of the copolymers significantly increases with increasing aramid content. This is expressed by a remarkable increase of the T_g compared to normal PA 6,6 and a storage modulus of more than 1 GPa up to at least 350°C for

copolymers with an aramid fraction of 0.5 or more. The presence of a plateau value of the modulus above the melting point of the soft block is typical for segmented block copolymers and suggest a microphase-separated structure where the rigid blocks act as physical cross-links between the flexible domains (Fig 4.4b).

If a highly oriented material can be obtained from this material it is expected to display high energy absorption and good impact properties because of the combination of the high modulus and strength from the liquid crystallinity and high ductility from the stretch ability of the flexible blocks. For this purpose fibers have been prepared and orientational ordering and mechanical properties have been measured as a function of the spinning conditions. The results are presented in Chapter 6.

5.5 References

- (1) Takayanagi, M.; Ogata, T.; Morikawa, M.; Kai, T. *J. Macromol. Sci., Phys.* **1980**, *B17*, 591-615.
- (2) Krigbaum, W. R.; Preston, J.; Ciferri, A.; Zhang, S. F. *J. Polym. Sci., Part A: Polym. Chem.* **1987**, *25*, 653-667.
- (3) Krigbaum, W. R.; Shufan, Z.; Preston, J.; Ciferri, A.; Conio, G. *J. Polym. Sci., Part B: Polym. Phys.* **1987**, *25*, 1043-1055.
- (4) Chapter 4; this thesis
- (5) Northolt, M. G. *Eur. Polym. J.* **1974**, *10*, 799-804.
- (6) Haraguchi, K.; Kajiyama, M.; Takayanagi, M. *J. Appl. Pol. Sci.* **1979**, *23*, 915-926.
- (7) Northolt, M. G. *Br. Polym. J.* **1981**, *13*, 64-65.
- (8) Bunn, C. W.; Garner, E. V. *Proc. R. Soc. London, Ser. A* **1947**, *189*, 39.
- (9) Zannoni, C. In: *The Molecular Physics of Liquid Crystals* (Eds.: GR Luckhorst, GW Gray), 1979, Chapter 3.
- (10) Northolt, M. G. *Polymer* **1980**, *21*, 1199-1204.
- (11) Hindeleh, A. M.; Halim, N. A.; Ziq, K. A. *J. Macromol. Sci. Phys.* **1984**, *B23*, 289-309.
- (12) Maier, W.; Saupe, A. *Z. Naturforsch.* **1961**, *16A*, 816-824.
- (13) Roerdink, E.; Warnier, J. M. M. *Polymer* **1985**, *26*, 1582-1588.
- (14) Williams, J. C. L.; Watson, S. J.; Boydell, P. In: *Nylon Plastics Handbook* (Ed.: MI Kohan), Hanser Publishers, Munich Vienna New York, 1995, p. 300.
- (15) JP62104713 (1987); JP62174129 (1987); JP62174118 (1987).
- (16) Fujita, T.; Fujiwara, T.; Sato, E.; Nagasawa, K.; Amano, T. *Pol. Eng. Sci.* **1989**, *29*, 1237-1240.
- (17) Flood, J. E.; White, J. L.; Fellers, J. F. *J. Appl. Pol. Sci.* **1982**, *27*, 2965-2985.
- (18) Northolt, M. G.; Van der Hout, R. *Polymer* **1985**, *26*, 310-316.

Chapter 6

Orientational Order and Mechanical Properties PPTA-*b*-PA 6,6 Block Copolymer fibers

Abstract

Mechanical properties and orientational order of a series of fibers comprised of alternating rigid aramid blocks of poly(*p*-phenylene terephthalamide) (PPTA) and flexible blocks of polyamide 6,6 (PA 6,6) have been investigated. The fibers have been spun from liquid crystalline solutions by means of a dry-jet wet spinning process. The only variable parameter was the imposed draw-ratio in the air gap of the spinning process. Increasing the draw-ratio resulted in an increased molecular orientation, Young's modulus and tensile strength of the fibers while its effect on the maximum elongation at break was small. Heat treatment at 300 °C of the fibers resulted in an increase of the Young's modulus, a minor increase of the strength and a decrease of the elongation at break. Scanning electron microscopy (SEM) photographs of the fractured surfaces of the block copolymer fibers do not show a fibrillar fracture surface, which is typically observed for pure PPTA fibers.

Based on:

Orientational Order and Mechanical Properties of Poly(amide-block-aramid) Alternating Block Copolymer Films and Fibers. de Ruijter, C.; Mendes, E.; Boerstael, H.; Picken, S.J. Polymer (Under Review)

6.1 Introduction

In this chapter we report on the relation between the tensile properties and orientational order of fibers spun from liquid crystalline solutions of a PPTA-*b*-PA 6,6 block copolymer in sulfuric acid as a function of the imposed draw-ratio in the air gap. The measured moduli will be compared to a mechanical model that relates the modulus of a fiber to the overall orientational order present.

The preparations of block copolyamide fibers, comprised of alternating rigid and flexible blocks, have been reported recently by Helgee¹ and Goto². Helgee¹ has prepared multiblock copolymers of rigid poly(4,4'-benzanilidylene-terephthalamide) (DABT) and poly(4,4'-diphenylsulphone terephthalamide) and fibers were spun from liquid crystalline solutions whereas Goto² prepared fibers of a block copolymer of PPTA and poly(4,4'-diphenyl ether terephthalamide) from isotropic solutions. In these studies the mechanical properties were reported and the fractured surfaces were investigated, however the influence of the draw-ratio on the mechanical properties was not reported.

6.2 Experimental

6.2.1 Materials

A block copolymer composed of alternating blocks of PPTA and PA 6,6 was synthesised by a two-step low temperature polycondensation method described in a Chapter 2.2. The chemical structure of a repeat unit of the copolymer is shown in Figure 2.1. The theoretical degree of polymerisation of both blocks was 10 (**P10-10**), which corresponds to a molar fraction of 0.5 for both blocks. The inherent viscosity $[\eta]_{\text{inh}}$ of the copolymer measured at a concentration of 0.5 g dL⁻¹ in sulfuric acid of 30°C was 2.07 dL g⁻¹, corresponding to a M_w of about 20000.

6.2.2 Fiber Spinning

The spinning of the fibers was performed at small scale dry-jet wet spinning set-up at the Teijin Twaron Research Institute at Arnhem (the Netherlands). The polymer concentration in sulfuric acid was 15 wt%. At this concentration the liquid crystalline solutions remain stable up to a temperature of about 100°C³. The spinning temperature was about 60 °C. Figure 6.1 schematically represents the experimental

set up for the dry-jet wet spinning process. The copolymer solution was extruded through a single hole spinneret (100 μm diameter) and stretched in the air-gap (6 mm) above the coagulation bath. The water in the coagulation bath was at room temperature. In the coagulation bath the sulfuric acid was removed and the fiber was formed. Finally the fiber was wound up at the take-up reel. During the spinning process the reel speed was kept at a constant speed. By adjusting the extrusion speed the draw-ratio in the air-gap was controlled. To ensure the complete removal of the sulfuric acid the reels were washed with respectively water, a sodium hydroxide solution and finally again with water. A series of five fibers were prepared of which 1 had a draw-ratio smaller than 1. The maximum draw-ratio that could be applied during the spinning process without the frequent occurrence of fiber rupture was about 3.5.

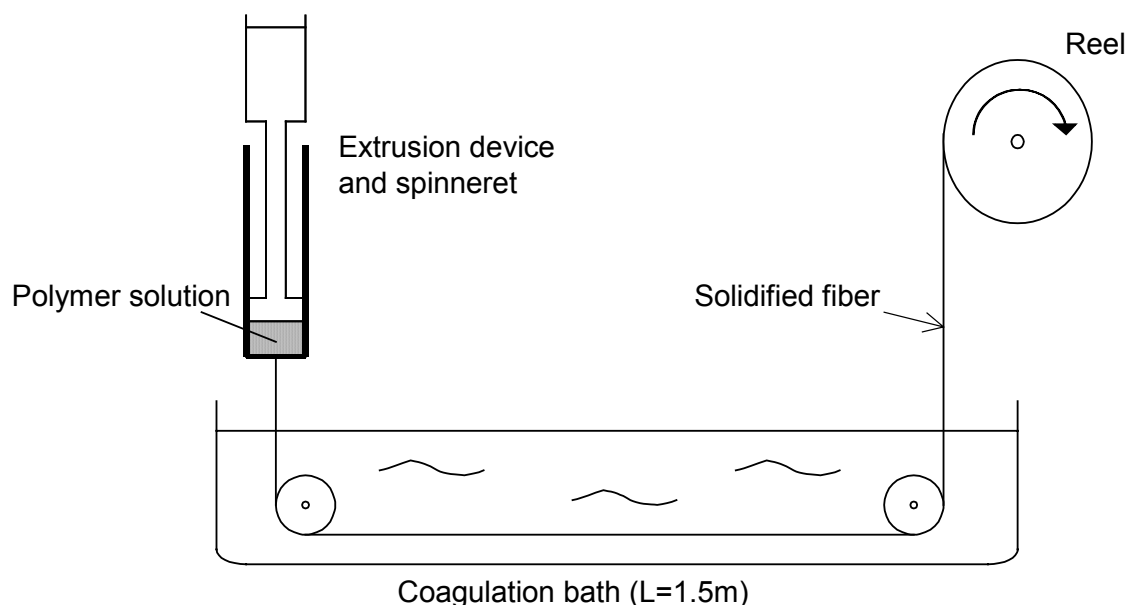


Figure 6.1: Schematic drawing of the experimental set up for the dry-jet wet spinning process

6.2.3 Measurements

Wide-angle X-ray scattering experiments were performed on a Bruker-Nonius D8-Discover set-up with a 2D detector in order to estimate the orientational order of the fibers. Monochromatic $\text{CuK}\alpha$ radiation with a wavelength of 0.154 nm was used. The direction of the incident X-ray beam was normal to the fiber long axes. The detector-sample distance was set at 6 cm. The diffraction data were recorded using a 3 hour exposure time and corrected for the background scattering.

The tensile tests were performed at the tensile test facility at Teijin Twaron in Arnhem (the Netherlands). All fibers were kept in an atmosphere of 65% relative humidity for at least 24h before testing. The test speed was 10 mm/min. and the test temperature was 21.4 °C. Tensile tests were performed on a single filament. For each draw-ratio 10 filaments were tested to determine average values.

6.3 Results and Discussion

6.3.1 WAXS Measurements

Observed Reflections

A 2D X-ray scattering pattern of the diffraction of fiber #4 is shown in Figure 6.2. The fiber major axis is aligned at an angle of 45° with the vertical axis of the figure. The corresponding intensity curve as a function of the scattering angle 2θ is shown in Figure 6.3.

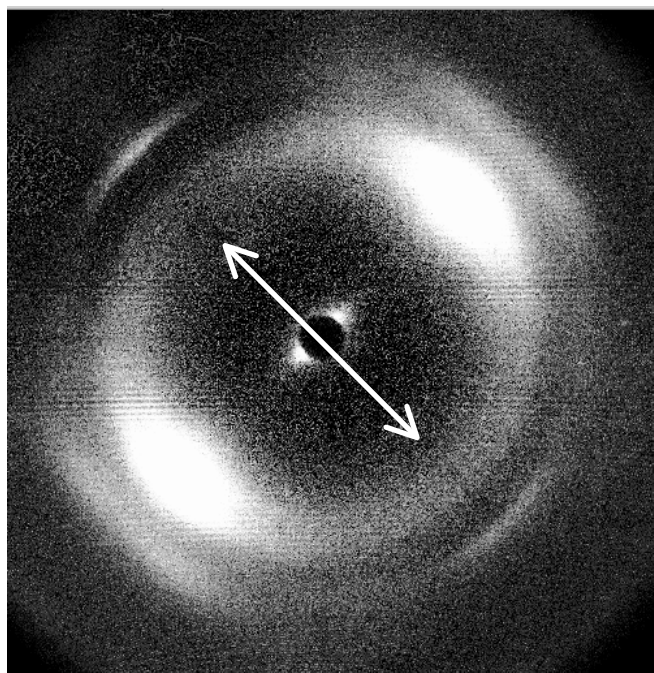


Figure 6.2: 2D X-ray scattering pattern of the diffraction of block copolymer fiber P10-10 #4 (the arrow represents the fiber direction)

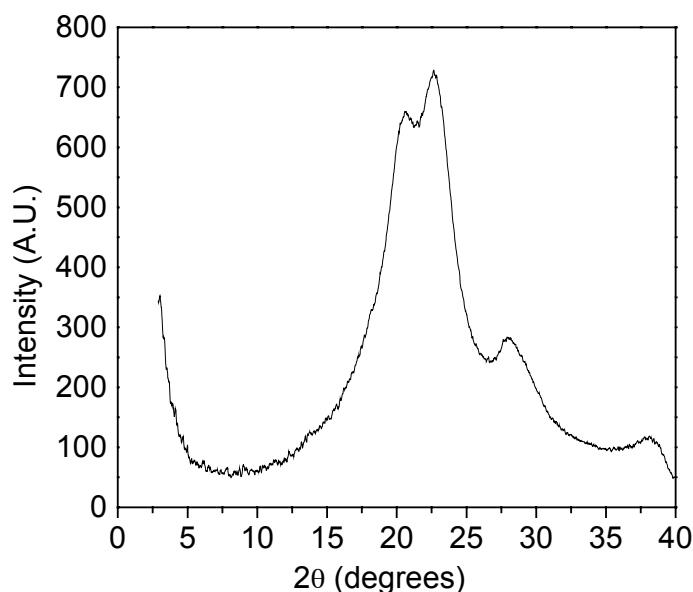


Figure 6.3: Radial scattering intensity distribution of fiber **P10-10 #4**

All prepared fibers show scattering peaks at nearly equal scattering angles. The 2D scattering patterns differ only in the observed degree of alignment. The sharpness of the azimuthal peaks increases rapidly with increasing draw-ratio. The observed reflections for fiber #4 and the aligned **P10-10** film⁴ both prepared from a 15 wt% solution in sulfuric acid, are listed in Table 6.1. The films were prepared by manually shearing the polymer solution at a low shearing rate. Also the reflections of pure PPTA and the reflection indices of PPTA are listed in this table. The scattering curves of the fibers differ to a certain extent from the films, i.e. the fibers show both equatorial and meridional reflections, whereas the films show only equatorial reflections. The scattering pattern of the fiber corresponds largely to the Northolt crystal structure of PPTA, whereas the film exhibit a polymorph crystal form⁴, i.e., a combined Northolt and Haraguchi structure. Another difference is that the reflections of the fibers are observed at slightly higher scattering angles, which corresponds to smaller intermolecular distances as a result of a better packing of the molecules. Also the relative intensity of the reflection of the fibers at small scattering angles, i.e., close to the beam stop, is higher than observed for the films, which suggests that the microphase separation in the fibers is more developed than in the films.

Table 6.1: d-spacings as obtained by WAXS of PPTA and block copolymer **P10-10** fiber #4 and film

d-spacing fiber #4 (Å)	Intensity ^a	d-spacing film (Å)	Intensity ^a	d-spacing PPTA (Å) ^{5,6}	Reflection indices for PPTA ^{5,6}
3.02	w	3.21	m	3.02	211
3.09	m	-	-	3.23	004
3.92	vs	3.98	vs	3.94	200
4.22	s	4.25	s	4.33 ^b	110 ^b
-	-	5.02	w	5.0 ^c	010 ^c
6.23	vw	-	-	6.45	002

^a Visually estimated intensities: vw – very weak, w – weak, m – medium, s – strong, vs – very strong

^b This reflection is observed only for the Northolt PPTA crystal⁵

^c This reflection is observed only for the Haraguchi PPTA crystal⁶

A striking observation that can be drawn here is that the scattering pattern of the copolymer fiber shows great resemblance to the pattern of PPTA; also the d-spacings shown in Table 6.1 are very similar. This means that there is hardly any influence of the PA 6,6 on the scattering from the PPTA blocks, which indicates well-developed phase separation of highly crystalline PPTA, and the amorphous PA.

Determination of the Orientational order using WAXS

The orientational order parameters of the fibers are estimated using to the procedure described in section 5.3.1, i.e., by fitting the azimuthal orientation of the (200) reflection to a Maier-Saupe distribution, and the results are shown in Table 6.2.

Table 6.2: Orientational order and tensile properties of block copolymer **P10-10** fibers as a function of the draw-ratio

Fiber #	Draw ratio (-)	$\langle P_2 \rangle$ (-)	Initial modulus (GPa)	Modulus after yield (GPa)	Theoretical Modulus (Eq. 6.1) (GPa)	Tensile strength (Mpa)	Elongation at break (%)	Toughness (J/g)
1	0.5	0.20	8.7	1.1	7.3	177	7.1	6.4
2	1.1	0.75	23.4	9.1	21.4	423	3.3	6.1
3	1.5	0.79	27.6	10.5	25.2	523	3.4	7.7
4	2.8	0.85	32.2	13.3	34.5	584	2.9	7.4
5	3.3	0.89	46.0	17.6	45.8	748	3.0	9.7

From Table 6.2 it is clear that the $\overline{\langle P_2 \rangle}$ parameter increases with increasing draw-ratio, as anticipated. Another observation that can be made is that fiber #1 with a draw-ratio smaller than 1 already has a $\overline{\langle P_2 \rangle}$ value of 0.2. This indicates that the polymer is already somewhat aligned by the shear-flow in the capillary and by the elongational flow above the entrance zone of the spinneret.

6.3.2 Mechanical Properties

Determination of Tensile Properties

Tensile properties of the fibers as a function of the imposed draw-ratio are listed in Table 6.2. The stress-strain curves for fiber #4 are shown in Figure 6.4 and the corresponding modulus-elongation curves are shown in Figure 6.5. From the character of the stress-elongation and modulus-elongation curves, 3 regimes can be specified. At small elongations a high initial modulus is observed that remains more or less constant up to 0.5% elongation. With increasing the deformation, the hydrogen bonds in the amorphous regions start to break, leading to the formation of a yield point while the initial modulus drops to almost 1/3 of its initial value. At deformations higher than 1.5% the modulus starts to increase with increasing deformation as the amorphous chains readily orient.

From Table 6.2 it is clear that with increasing draw-ratio the initial Young's modulus and the tensile strength rapidly increases. The elongation at break shows the tendency to decrease with increasing draw-ratio. Striking observations, which can be drawn from Table 6.2, are the impressive values for the Young's moduli of the fibers with a high draw-ratio. In Chapter 3 we have already shown that the observed liquid crystallinity involves induced orientation of polyamide segments and therefore it is plausible that also the polyamide segments readily align when the drawing is applied and therefore contribute to the high value of the modulus. Based on the applied draw-ratio, the polymer concentration in sulfuric acid and the temperatures of the spinning dope and coagulation bath, the obtained moduli for the copolymers are in the order of what would be expected for pure PPTA⁷.

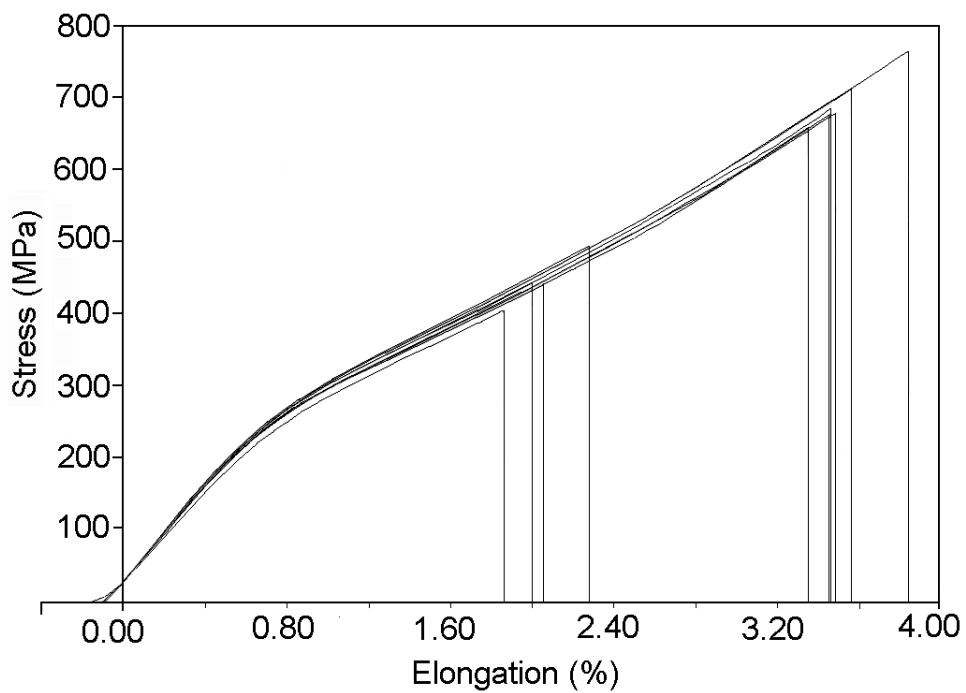


Figure 6.4: Stress-elongation curve for fiber #4

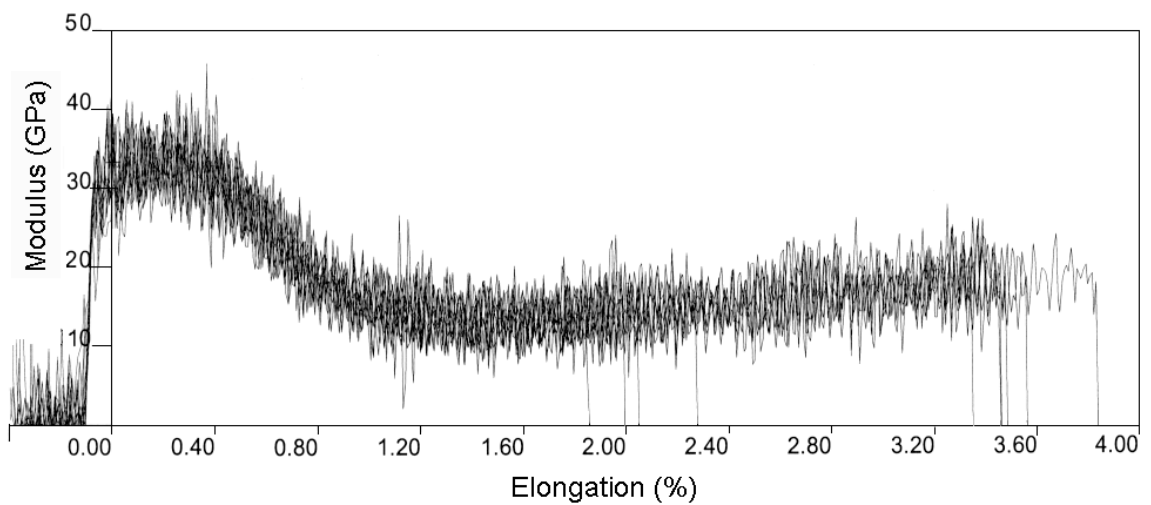


Figure 6.5: Modulus-elongation curve for fiber #4

In order to relate the obtained Young's moduli with the overall orientational order of the copolymers, which were determined by WAXS, the following mechanical model is used⁸

$$\frac{1}{E} = \frac{1}{e_c} + \frac{1 - \langle P_2 \rangle}{3g} \quad [6.1]$$

where E is the modulus of the fiber, e_c is the chain modulus and g the shear modulus. For PPTA the values for chain and shear modulus are respectively 240⁹ and 2 GPa¹⁰. According to Table 6.2 the initial moduli of the block copolymer fibers correspond rather well with the modulus calculated from the mechanical model of Northolt⁸ if the shear and chain modulus of normal PPTA are chosen.

Although the tensile strength of the fibers considerably increases with increasing the draw-ratio, its value measured at even the highest draw-ratio, is still somewhat lower than the tensile strength of PA 6,6. The tensile strength of commercial PA 6,6 and PPTA fibers are respectively around 0.9 GPa and 3 GPa.¹¹ It is commonly accepted that the tensile strength of high-performance fibers may be improved upon heat treatment. Heat treatment has been applied successfully to aromatic polyamide fibers and could even result in a 2 times improvement of both the modulus and tensile strength.^{12,13} Fiber #4 was subjected to heat treatment at 300°C and the results are shown in Table 6.3.

Table 6.3: Effect of heat treatment on fiber properties

Fiber #	Draw ratio (-)	Initial modulus (GPa)	Modulus after yield (GPa)	Tensile strength (Mpa)	Elongation at break (%)	Toughness (J/g)
4	2.6	32.5	13.2	738	4.2	12.5
4 hot-drawn	2.9	55.0	29.2	811	2.0	6.7

Table 6.3 clearly shows that the Young's modulus drastically increases upon heat treatment and that the elongation at break decreases compared to untreated fibers. The tensile strength only slightly increases upon heat treatment. Similar results have been obtained by the groups of Helgee¹ and Goto² who also have investigated the mechanical properties of alternating rigid-flexible block copolyamide fibers. Tensile tests of these copolymers indicated a significant decrease of the tensile strength compared to the rigid homopolymer. Also hardly any influence of heat treatment on the fiber strength of the copolymer was observed, whereas for the rigid homopolymer the modulus drastically increases upon heat treatment. This is an indication that the phase-separated morphology in the fibers contributes to the relatively low strength of the copolymer fibers.

In order to further investigate this relative low strength compared to pure PPTA, the fracture morphology of the fibers was investigated by scanning electron microscopy (SEM). Figure 6.6 show the fracture surfaces of respectively a PPTA and a block

copolymer fiber, which were prepared by the same spinning procedure. From these photographs it is clear that a PPTA fiber has a much stronger tendency to form an fibrillar fracture surface. Because the block copolymers phase separates into small domains it loses the tendency to form these fibrils during breakage and probably a premature tensile rupture will occur. Also the relative low MW of the block copolymers may be a reason for this premature rupture.

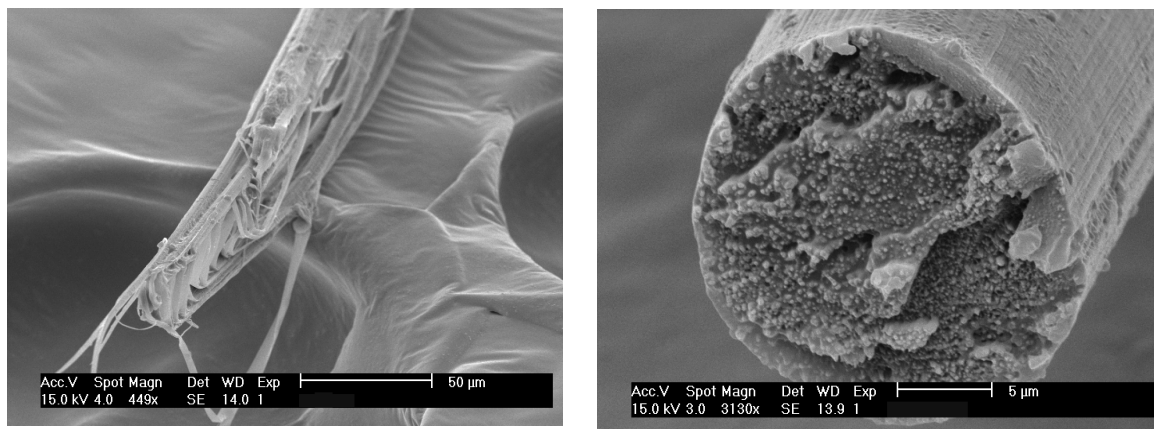


Figure 6.6: Fracture surface of a PPTA fiber (left) and copolymer fiber #4 (right)

Although the mechanical properties of the prepared fibers are already quite promising, additional improvement might be expected by adjusting some of the spinning parameters. A range of parameters are known that can influence the ultimate mechanical properties of fibers prepared via a dry-jet wet spinning process, like e.g. the spinning dope temperature, the coagulation-bath temperature, the polymer concentration, the draw-ratio, the gap size of the spinneret and the size of the air-gap. In our view, a significant improvement of the mechanical properties might be expected by increasing the polymer concentration of the spinning dope, since a higher concentration allows for a higher draw-ratio and the polymer concentration of the spinning dope used was relatively low (15 wt%) compared to the solubility limit which is about 25 wt%. For pure PPTA it is known that the fiber strength approximately doubles if the polymer concentration is doubled¹⁴, which means that probably also for the copolymer an increase in fiber strength can be expected. Another factor that might improve the fiber strength is increasing the block length. By increasing the block length the extent of microphase separation will be enhanced and will probably improve tendency towards fibrillation of the PPTA domains and therefore also could increase the strength.

6.4 Conclusions

Fibers have been prepared according to a dry-jet wet spinning process of a lyotropic multiblock copolymer of alternating blocks of PPTA and PA 6,6. The average degree of polymerisation of both blocks was 10. A series of five fibers were spun from liquid crystalline solutions in sulfuric acid and the only variable parameter during the spinning process was the applied draw-ratio. All fibers displayed a significant degree of alignment and the observed orientation, the Young's modulus and the strength of the fibers increases rapidly with increasing draw-ratio. The observed modulus of the fibers can be modelled nicely with a mechanical model developed by Northolt⁸, which relates the initial modulus to the overall orientation in the fiber. One of the fibers was subjected to heat treatment at 300°C which resulted in a drastic increase of the Young's modulus and a decrease in the elongation at break. These heat-treated fibers exhibited a strength of about 800 MPa, an initial Young's modulus of 55 GPa whereas an elongation at break of 2.0% was obtained.

References

- (1) Helgee, B.; Flodin, P. *Polymer* **1992**, *33*, 3616-3620.
- (2) Goto, T.; Maeda, M.; Hibi, A. *J. Appl. Pol. Sci.* **1989**, *37*, 867-875.
- (3) Chapter 3; this thesis
- (4) Chapter 5; this thesis
- (5) Northolt, M. G. *Eur. Polym. J.* **1974**, *10*, 799-804.
- (6) Haraguchi, K.; Kajiyama, M.; Takayanagi, M. *J. Appl. Pol. Sci.* **1979**, *23*, 915-926.
- (7) Picken, S. J.; Van der Zwaag, S.; Northolt, M. G. *Polymer* **1992**, *33*, 2998-3006.
- (8) Northolt, M. G.; Van der Hout, R. *Polymer* **1985**, *26*, 310-316.
- (9) Yang, H. H. In: Kevlar Aramid Fiber, Wiley, Chisester, 1993, p. 95.
- (10) Deteresa, S. J.; Allen, S. R.; Farris, R. J.; Porter, R. S. *J. Mat. Sci.* **1984**, *19*, 57-72.
- (11) Magat, E. E.; Morrison, R. E. *J. Polym. Sci., Part C: Polym. Symp.* **1975**, *51*, 203-227.
- (12) Kwolek, S. L.; Morgan, P. W.; Schaefgen, J. R.; Gulrich, L. W. *Macromolecules* **1977**, *10*, 1390-1396.
- (13) Bair, T. I.; Morgan, P. W.; Killian, F. L. *Macromolecules* **1977**, *10*, 1396-1400.
- (14) Northolt, M. G.; den Decker, P.; Picken, S. J.; Baltussen, J. J. M.; Schlatmann, R. *Adv. Polym Sci.* **2005**, *178*, 1-108.

Chapter 7

Conclusions and scientific outlook

7.1 Conclusions

The incentive of this project was to investigate block copolymers of alternating rigid and flexible blocks for the spontaneous formation of self-reinforcing materials. Since block copolymers in general will phase separate it was expected that the rigid segments form a nematic domain causing an enhanced orientation of the flexible coil segments. This self-reinforcing effect reveals itself by an enhanced orientation of the flexible chains, resulting in better mechanical properties compared to the pure unstretched flexible polymer. In order to investigate this objective, block copolymers composed of poly(*p*-phenylene terephthalamide) and polyamide 6,6 blocks have been synthesised. By simply comparing the phase behaviour in sulfuric acid of the block copolymers with pure PPTA, and a PPTA-oligomer of theoretically the same length as the PPTA blocks in the copolymer, it could be made clear that the flexible chains in the copolymer are indeed oriented¹. If flow is applied to these polymers solutions the overall orientation can be enhanced².

In principle the coupling of flexible segments to a rigid homopolymer could result in two important advantages compared to the pure rigid polymer. First, due to the combination of the rigid blocks providing stiffness and the flexible blocks providing elasticity it was expected that this type of polymers would display improved fracture energy and second the stability of the lyotropic phase can be considerably enlarged and allows processing from higher concentrations.

Fibers have been spun from liquid crystalline solutions in sulfuric acid, which show impressive modulus³. However up to now, the fiber's strength and the toughness are still relatively moderate compared with PPTA. But improvements can be expected by optimising the process conditions, which were chosen far away from the ultimate limits.

One should take into consideration that both the individual blocks and the overall block copolymer have a broad distribution of molecular weights. In this thesis the influence of the polydispersity of the blocks on the properties has not been dealt with. However it will of course be interesting to study this into more detail, since the polydispersity of the blocks will certainly influence the phase separation of the blocks,

and therefore also might have significant effect on the overall mechanical properties. For this purpose monodisperse blocks should be synthesized. However, this will be rather tedious since it requires a multiple steps procedure with repetitive protection-deprotection and purification processes in each step. Another problem that will occur is that by increasing the length of the aramid oligomer its solubility and melt-ability will decrease rapidly. This will complicate the subsequent reaction steps and will therefore limit the final length of the aramid block that can be obtained in the copolymer.

7.2 Scientific Outlook

Applications of rod-coil block copolyamides can be considered in fields where general engineering polymers like eg. polyamides and polyesters fail. Rod-coil block copolymer fibers considered here show a significant improvement in Young's modulus and heat-resistance in comparison to aliphatic polyamide fibers and a comparable strength and toughness, with further room for improvement.

Polyamide block copolymers comprised of blocks of different rigidity have already been suggested for the purpose to fulfil the concept of molecular composites⁴⁻¹³ frequently, but can also be considered for applications in fiber-reinforced composites, i.e. a block copolymer fiber-reinforced polymer composite. The copolymer may also be considered as the matrix material in e.g. an all aramid composite (PPTA-fiber/PPTA-PA block copolymer), which can be prepared via a pultrusion process or by impregnating the fibers with a copolymer solution in sulfuric acid and subsequently coagulating the composite to the solid state.

The block copolymer may finally be considered as an adhesion promoter between aramid fibers and aliphatic polyamides or other matrix polymers. For this purpose Martin et al.¹⁴ have coated PPTA fibers with a rod-coil block copolyamide, by impregnating the PPTA fibers with a solution of a block copolymer of polybenzamide and a random PA 6/6,6-copolymer in sulfuric acid, and showed that the coated PPTA fibers displayed an improved adhesion with a variety of matrix polymers.

7.3 References

- (1) Chapter 3; this thesis
- (2) Chapter 5; this thesis
- (3) Chapter 6; this thesis
- (4) Takayanagi, M.; Ogata, T.; Morikawa, M.; Kai, T. *J. Macromol. Sci., Phys.* **1980**, *B17*, 591-615.
- (5) Asrar, J.; Preston, J.; Ciferri, A.; Krigbaum, W. R. *J. Polym. Sci.: Pol. Chem. Ed.* **1982**, *20*, 373-381.
- (6) Preston, J.; Krigbaum, W. R.; Kotek, R. *J. Pol. Sci.: Pol. Chem. Ed.* **1982**, *20*, 3241-3249.
- (7) Martin, R.; Götz, W.; Vollmert, B. *Angew. Makromol. Chem.* **1985**, *132*, 91-109.
- (8) Mathias, L. J.; Moore, D. R.; Smith, C. A. *J. Polym. Sci., Part A: Pol. Chem.* **1987**, *25*, 2699-2709.
- (9) Krigbaum, W. R.; Preston, J.; Ciferri, A.; Zhang, S. F. *J. Polym. Sci., Part A: Polym. Chem.* **1987**, *25*, 653-667.
- (10) Marek Jr., M.; Stehlicek, J.; Duskocilova, D. *Eur. Pol. J.* **1995**, *31*, 363-368.
- (11) Wang, H.-H.; Lin, M.-F. *J. Appl. Pol. Sci.* **1998**, *68*, 1031-1043.
- (12) Wang, H.-H. *J. Appl. Pol. Sci.* **2001**, *80*, 2167-2175.
- (13) Xu, J. R.; Zhang, Y.; Zhang, Q. L. *Polymer* **2001**, *42*, 2689-2693.
- (14) Martin, R.; Götz, W.; Vollmert, B. *Angew. Makromol. Chem.* **1985**, *1985*, 121-140.

Summary

The objective of this thesis is to investigate block copolymers comprised of alternating rigid and flexible block for self-reinforcing materials. The incentive for this work was the expectation that the rigid segments would phase separate on a microscopic scale, and would form nematic domains, which will cause an enhanced orientation of the flexible segments leading to coil stretching. As a result the coils in the copolymer will be stiffer compared to unstretched coils, and the mechanical properties will be better than expected from the pure flexible polymer, therefore the term “self-reinforcement”.

For this purpose a block copolymer was chosen that is comprised of alternating rigid poly(*p*-phenylene terephthalamide) (PPTA) blocks and flexible coil polyamide 6,6 (nylon 6,6) blocks. In Chapter 2 of this thesis the synthesis of the copolymers and the characterization is described. A model is developed that combined the intrinsic viscosity relations of the homopolymers and the mean-square end-to-end distance of the copolymer to estimate the molecular weights of the copolymers. In Chapter 3 of this thesis the phase behaviour of the copolymers in sulfuric acid is studied. It is shown that if the aramid content in the copolymers is at least 50 mol% the polymers are able to show a lyotropic liquid crystalline phase. By comparing the phase behaviour of the copolymers with normal (high MW) PPTA and a PPTA oligomer with the same length as the PPTA blocks in the copolymer it can be shown easily that the flexible coils are indeed stretched. It is also shown that the phase behaviour can be described well with a modified Maier-Saupe model. From this model the persistence lengths of the copolymers (which describes its rigidity) are estimated and are found to be significantly higher than predicted by the weighted average of the individual homopolymers, what confirms that the flexible chain segments are indeed significantly stretched by the mesophase.

In Chapter 5 the orientational order and mechanical properties of a series of copolymers films, and in Chapter 6 the orientational order and mechanical properties of a series of fibers, with an aramid content of 50 mol%, are described. The order parameters are obtained from WAXS (wide-angle X-ray scattering) experiments. These polymers show interesting mechanical properties, e.g. block copolymer fibers display a high initial modulus, almost comparable to normal PPTA prepared under similar conditions in sulfuric acid. The obtained strength of the copolymers are up to now not so impressive although improvements of the properties might be expected

by adjusting some of spinning parameters (e.g. spinning from a higher polymer concentration in sulfuric acid).

The polymers described in this thesis show interesting properties and might be considered in applications such as high performance fibers or in aramid composites.

Samenvatting

De doelstelling van het onderzoek beschreven in dit proefschrift is het bestuderen van blok copolymeren bestaande uit alternerende rigide en flexibele segmenten om te kunnen worden toegepast als zelf-versterkende materialen. Het idee achter dit onderzoek was de verwachting dat de rigide segmenten in het copolymeer zouden fasescheiden en nematische domeinen zouden vormen. Deze domeinen zullen er vervolgens voor zorgen dat ook de flexibele segmenten worden georiënteerd. Dientengevolge zullen de georiënteerde flexibele segmenten stijver zijn in vergelijking met het standard ongeoriënteerde flexibele polymeer en de mechanische eigenschappen beter, vandaar de term “zelf-versterkend”.

Om dit principe te bestuderen is een blok copolymer geselecteerd dat bestaat uit alternerende rigide poly(*p*-phenylene terephthalamide) (PPTA) en flexibele polyamide 6,6 (nylon 6,6) blokken. In hoofdstuk 2 van dit proefschrift is de synthese en de karakterisering van de polymeren beschreven. Een model is ontwikkeld om vanuit de intrinsieke viscositeiten van de standard homopolymeren en de kwadratische eindpuntsafstand van het copolymeer een afschatting te kunnen maken van de molecuul gewichten van de blok copolymeren. In hoofdstuk 3 van dit proefschrift is het fasegedrag van de blok copolymeren in zwavelzuur bestudeerd. Wanneer het aramide gehalte in het copolymer ten minste 50 mol% bedraagt tonen geconcentreerde polymeer oplossingen vloeibaar kristallijn gedrag. Door het fasegedrag van de copolymeren te vergelijken met het gedrag van standaard PPTA met een hoog moleculair gewicht en een PPTA-oligomeer, van gelijke lengte als de PPTA blokken in het copolymer, kan eenvoudig worden aangetoond dat de flexibele blokken inderdaad georiënteerd zijn. Verder is aangetoond dat het fasegedrag zelf goed beschreven kan worden d.m.v. een gemodificeerd Maier-Saupe model. Met dit model kan tevens de persistentielengte van de copolymeren worden bepaald en deze blijken aanzienlijk hoger te zijn dan wanneer ze worden berekend uit het gewogen gemiddelde van de homopolymeren, wat ook weer een aanwijzing is dat in de vloeibaar kristallijne fase de flexibele ketens georiënteerd zijn. In de hoofdstuk 5 zijn de oriëntatie en de mechanische eigenschappen van een serie polymere films en in hoofdstuk 6 de oriëntatie van een serie vezels, met een PPTA gehalte van 50 mol%, beschreven. De oriëntatie parameters zijn bepaald d.m.v. WAXS (wide-angle X-ray scattering) experimenten. De polymeren vertonen veelbelovende mechanische eigenschappen, bijvoorbeeld de initiële modulus van de copolymeren zijn nagenoeg gelijk aan standaard PPTA als ze zijn gefabriceerd onder gelijke condities. De mechanische sterkte van de vezels zijn tot op dit moment nog niet zo indrukwekkend,

echter verbeteringen mogen worden verwacht als de vezels worden gemaakt vanuit een meer geconcentreerde oplossing.

Al met al vertonen de polymeren beschreven in dit proefschrift interessante eigenschappen en kunnen mogelijk worden toegepast als hoge temperatuurbestendige vezels of bijvoorbeeld in aramide composieten.

Curriculum Vitae

Christiaan de Ruijter werd geboren op 26 januari 1974 te Vlaardingen. Na eerst de MAVO en HAVO te hebben doorlopen behaalde hij in 1990 uiteindelijk het VWO diploma aan het CSG Blaise Pascal te Spijkenisse. Nog in dat zelfde jaar begon hij aan de studie Scheikundige Technologie aan de Technische Universiteit te Delft waar hij in 1997 de ingenieurstitel behaalde. Het afstudeerproject werd aan de universiteit gedaan, in de groep PME (Polymeer Engineering & Materials) onder begeleiding van Prof. Sjaak Elmendorp.

In oktober 2001 begon hij, eveneens bij de PME groep, aan een promotieonderzoek om het gedrag van vloeibaar kristallijne blok copolymeren te bestuderen waarvan de resultaten zijn beschreven in dit boekje. De dagelijkse begeleiding gedurende dit onderzoek bestond uit Dr. Eduardo Mendes, Dr. Wolter Jager en Prof. Dr. Stephen Picken. Na afronding van zijn proefschrift is hij begonnen als post-doctoraal onderzoeker aan de faculteit lucht- en ruimtevaarttechniek in de vakgroep FAM (Fundamentals of Advanced Materials) van de TU Delft. In samenwerking met Teijin Twaron bestudeerde hij de invloed van een thermotrope matrix op de ballistische en composiet eigenschappen van aramide vezels.

Dankwoord

In eerste plaats wil ik mijn promotor Stephen Picken bedanken, zonder jou enthousiaste begeleiding zou het proefschrift er in ieder geval niet in deze vorm gekomen zijn. Tevens wil ik de dagelijkse begeleiders Eduardo Mendes en Wolter Jager bedanken voor hun bijdrage aan dit proefschrift.

Verder heb ik gedurende mijn promotie de mogelijkheid gehad om samen te werken met een aantal medewerkers van Teijin Twaron. Dank ben ik daarbij verschuldigd aan Hanneke Boerstool, Monique Meeusen en Wido Nijenhuis voor de begeleiding van de vezelspin experimenten, Niek Tops en Hans Quaijtaal voor de mechanische tests en Johan Bos voor het uitwisselen van kennis op gebied van de polymeer chemie.

Jan Groenewold, Plamen Malchev en Liangbin Li wil ik bedanken voor de waardevolle discussies die veelal betrekking hadden tot de polymeer fysica en Theo Dingemans voor de essentiële hulp m.b.t. de synthese van de polymeren. Ben Norder wil ik bedanken voor alle TGA en DSC experimenten.

Voorts wil natuurlijk alle nog niet genoemde collega's en oud collega's bedanken voor de gezellige sfeer zoals daar zijn Arek, Seb, Zeynep, Max, Plamen, Ceren, Daniel, Wilco, Haley, Otto, Telma, Stefan, Marcel, Artemi, Piet, Karin, Tonny, Fem, Sjaak en Jan van Turnhout. Een speciaal bedankje voor de bewoners van kamer 0.301 alwaar ik regelmatig kwam binnengestormd voor wat afleiding van de dagelijkse beslommingen. Een special bedankje voor Gerard. Werd hij in proefschriften uit het verleden nog bestempeld als een tweede vader, ik zie hem meer als die vervelende oom die met zijn gebbetjes toch altijd maar weer een glimlach op het gezicht kon toveren. Nog een special bedankje voor Louise, ruim drie jaar lang mijn kamergenote.

Tot slot wil ik familie en vrienden bedanken er is ten slotte meer in het leven dan een promotie.

